NUREG/CR-6837, Vol. 1

The Battelle Integrity of Nuclear Piping (BINP) Program Final Report

Summary and Implications of Results

U.S. Nuclear Regulatory Commission
Office of Nuclear Regulatory Research
Washington, DC 20555-0001

AVAILABILITY OF REFERENCE MATERIALS IN NRC PUBLICATIONS

NRC Reference Material

As of November 1999, you may electronically access NUREG-series publications and other NRC records at NRC's Public Electronic Reading Room at http://www.nrc.gov/reading-rm.html. Publicly released records include, to name a few, NUREG-series publications; *Federal Register* notices; applicant, licensee, and vendor documents and correspondence; NRC correspondence and internal memoranda; bulletins and information notices; inspection and investigative reports; licensee event reports; and Commission papers and their attachments.

NRC publications in the NUREG series, NRC regulations, and *Title 10, Energy*, in the Code of *Federal Regulations* may also be purchased from one of these two sources.

1. The Superintendent of Documents
   U.S. Government Printing Office
   Mail Stop SSOP
   Washington, DC 20402–0001
   Internet: bookstore.gpo.gov
   Telephone: 202-512-1800
   Fax: 202-512-2250
2. The National Technical Information Service
   Springfield, VA 22161–0002
   www.ntis.gov
   1–800–553–6847 or, locally, 703–605–6000

A single copy of each NRC draft report for comment is available free, to the extent of supply, upon written request as follows:
Address: Office of the Chief Information Officer,
Reproduction and Distribution
Services Section
U.S. Nuclear Regulatory Commission
Washington, DC 20555-0001
E-mail: DISTRIBUTION@nrc.gov
Facsimile: 301–415–2289

Some publications in the NUREG series that are posted at NRC's Web site address http://www.nrc.gov/reading-rm/doc-collections/nuregs are updated periodically and may differ from the last printed version. Although references to material found on a Web site bear the date the material was accessed, the material available on the date cited may subsequently be removed from the site.

Non-NRC Reference Material

Documents available from public and special technical libraries include all open literature items, such as books, journal articles, and transactions, *Federal Register* notices, Federal and State legislation, and congressional reports. Such documents as theses, dissertations, foreign reports and translations, and non-NRC conference proceedings may be purchased from their sponsoring organization.

Copies of industry codes and standards used in a substantive manner in the NRC regulatory process are maintained at—
The NRC Technical Library
Two White Flint North
11545 Rockville Pike
Rockville, MD 20852–2738

These standards are available in the library for reference use by the public. Codes and standards are usually copyrighted and may be purchased from the originating organization or, if they are American National Standards, from—
American National Standards Institute
11 West 42nd Street
New York, NY 10036–8002
www.ansi.org
212–642–4900

Legally binding regulatory requirements are stated only in laws; NRC regulations; licenses, including technical specifications; or orders, not in NUREG-series publications. The views expressed in contractor-prepared publications in this series are not necessarily those of the NRC.

The NUREG series comprises (1) technical and administrative reports and books prepared by the staff (NUREG–XXXX) or agency contractors (NUREG/CR–XXXX), (2) proceedings of conferences (NUREG/CP–XXXX), (3) reports resulting from international agreements (NUREG/IA–XXXX), (4) brochures (NUREG/BR–XXXX), and (5) compilations of legal decisions and orders of the Commission and Atomic and Safety Licensing Boards and of Directors' decisions under Section 2.206 of NRC's regulations (NUREG–0750).

DISCLAIMER: This report was prepared as an account of work sponsored by an agency of the U.S. Government. Neither the U.S. Government nor any agency thereof, nor any employee, makes any warranty, expressed or implied, or assumes any legal liability or responsibility for any third party's use, or the results of such use, of any information, apparatus, product, or process disclosed in this publication, or represents that its use by such third party would not infringe privately owned rights.

NUREG/CR-6837, Vol. 1

The Battelle Integrity of Nuclear Piping (BINP) Program Final Report

Summary and Implications of Results

Manuscript Completed: September 2003
Date Published: June 2005

Prepared by
P.Scott[1], R.Olson[1], J.Bockbrader[1], M.Wilson[1], B.Gruen[1], R.Morbitzer[1], Y.Yang[1], C.Williams[1], F.Brust[1], L.Fredette[1], N.Ghadiali[1]

G.Wilkowski[2], D.Rudland[2], Z.Feng[2], R.Wolterman[2]

[1]Battelle
505 King Avenue
Columbus, OH 43201

Subcontractor:
[2]Engineering Mechanics Corporation of Columbus
3518 Riverside Drive
Suite 202
Columbus, OH 43221-1735

C. Greene, NRC Project Manager

Prepared for
Division of Engineering Technology
Office of Nuclear Regulatory Research
U.S. Nuclear Regulatory Commission
Washington, DC 20555-0001
NRC Job Code W6775

ABSTRACT

Over the past 15 to 20 years significant research has been conducted to further the understanding of the fracture behavior of piping systems in commercial nuclear power plants. While the results from these prior programs have advanced the state-of-the-art understanding, a number of key technical issues remained to be resolved.

The BINP program was developed to address what were perceived to be the most critical of these unresolved issues. The program was structured as a series of independent tasks, each focused on one of these issues.

After the research was completed, it was found that many of these issues did not have as significant effect on leak-before-break or in-service flaw evaluation criteria as was originally thought. However, one of the areas where significant benefit can be realized for both LBB and in-service flaw evaluations is by using nonlinear stress analysis instead of elastic analysis in the flaw assessments. The additional margin gained by accounting for the energy dissipated by plastic deformation can be significant.

Another important advance was the preliminary development of the technical basis for a flaw evaluation criteria for Class 2, 3, and balance of plant piping.

FOREWORD

Since 1965, the U.S. Nuclear Regulatory Commission (NRC) has been involved in research on various aspects of pipe fracture in nuclear power plant piping systems. The most recent programs are the Degraded Piping Program, Short Cracks in Piping and Piping Welds Program, and two International Piping Integrity Research Group programs. These programs have developed and validated "state-of-the-art" structural analysis methods and data for nuclear piping systems.

This report describes the results of the Battelle Integrity of Nuclear Piping (BINP) program, which was performed by Battelle Columbus Laboratories. The objective of the BINP program was to address the most important unresolved technical issues from the earlier research programs. The BINP program was initiated as an international program to enable fiscal leveraging and an expanded scope of work. Technical direction for the program was provided by a Technical Advisory Group composed of representatives from the funding organizations.

The BINP program was divided into eight independent tasks, each of which examined one of the unresolved technical issues. These eight tasks included both experimental and analytical efforts. The two pipe-system experiments examined the effects of secondary stresses (such as thermal expansion) and cyclic loading (such as during a seismic event) on the load-carrying capacity of flawed piping. For these experiments, the pipe system had large flaws or cracks. The remaining six tasks were "best-estimate" analyses to examine the effects of other factors, such as pipe system boundary conditions, and weld residual stresses on the behavior of flawed pipes. Many of these analyses involved the use of finite element modeling techniques. One of these analytical tasks was to examine the actual margins that may exist in flawed pipe evaluations as a result of non-linear behavior. While the magnitude of these margins would vary on a case-by-case basis, the results of this task show that a potential for significant margins does exist.

In addition to developing a technical basis for more advanced inservice flaw evaluation procedures for use with Class 1 piping, as defined by the American Society of Mechanical Engineers (ASME), the BINP program considered the development of flaw evaluation procedures for ASME Class 2 and 3 piping and balance-of-plant piping.

This research supports the NRC's goal to improve the effectiveness and realism of the agency's regulatory actions.

Charles J. Miller for

Carl Paperiello, Director
Office of Nuclear Regulatory Research
U.S. Nuclear Regulatory Commission

Table of Contents

ABSTRACT iii

FOREWORD v

List of Figures ix

List of Tables x

EXECUTIVE SUMMARY xiii

ACKNOWLEDGMENTS xix

NOMENCLATURE xxi

PREVIOUS REPORTS IN SERIES xxv

1. INTRODUCTION 1

1.1 References 2

2. IMPLICATIONS OF RESULTS 3

2.1 Implications of Results on Leak-Before-Break Analyses 3

2.1.1 Role of Secondary Stresses on Pipe Fracture in LBB Evaluations 3

2.1.2 Impact of Actual Margins for LBB Evaluations 7

2.1.3 Effect of the Restraint of Pressure Induced Bending on the Crack-Opening Displacements (COD) for LBB Evaluations 9

2.1.4 Effect of Weld Residual Stresses on COD Predictions for LBB Evaluations 11

2.1.5 Development of a J-estimation Scheme for Through-wall Cracks in Elbows that could be used in the Stability Analysis of a LBB Evaluation 18

2.2 Implications of Results on In-Service Flaw Evaluations 20

2.2.1 Role of Secondary Stresses on In-Service Flaw Evaluation Procedures 22

2.2.2 Impact of Using Actual Margins from Plant Piping Analyses for In-Service Flaw Evaluations 22

2.2.3 Development of Flaw Evaluation Criteria for Class 2, 3, and BOP Piping 22

2.2.3.1 Effect of R/t Ratios on the Fracture Behavior of Class 2, 3, and BOP Piping 23

2.2.3.2 Effect of Lower Operating Temperatures on the Fracture Behavior Class 2, 3, and BOP Piping Systems 30

2.3 References 33

3. EXAMPLE TEST CASES 35

3.1 Example Test Cases Illustrating the Effects of the Key Results from this Program on LBB Analyses 35

3.1.1 Role of Secondary Stresses on LBB 35

3.1.2 Effect of Actual Margins on LBB 37

3.1.3 Effect of Restraint of Pressure Induced Bending on LBB 41

3.1.4 Effect of Differences in J and COD Predictions between the GE/EPRI Method for Straight Pipe and the Elbow TWC Solutions 43

3.1.5 Effect of Weld Residual Stresses on the Postulated Leakage Crack Size for a Leak-Before-Break Assessment 45

3.2 Example Test Cases Illustrating the Effects of the Key Results from this Program on In-Service Flaw Evaluations 47

3.2.1 Role of Secondary Stresses on In-Service Flaw Evaluation Criteria 47

3.2.2 Effect of Actual Margins on In-Service Flaw Evaluation Criteria 47

3.3 Example Test Cases Illustrating the Application of the Newly Developed Flaw Evaluation Criteria for Class 2, 3, and Balance of Plant (BOP) Piping Systems 50

3.3.1 Differences Between the Existing ASME Section XI Appendix H F-functions and the F-functions Developed in the BINP Program 50

3.3.2 Effect of R/t ratio on Elastic-Plastic J-Estimation Scheme (SC.TNP) Analyses 52

3.3.3 Effect of Transition Temperature on Fracture Initiation Behavior of Ferritic Class 2, 3, and BOP Piping 52

3.4 References 59

4. CONCLUSIONS AND RECOMMENDATIONS FROM THE BINP PROGRAM .. 61

4.1 Conclusions 61

4.1.1 Task 1: Secondary Stresses 61

4.1.2 Task 2: Alternative Seismic Load History 62

4.1.3 Task 3: Actual Margins 62

4.1.4 Task 4: Restraint of Pressure- Induced Bending 63

4.1.5 Task 7: Development of a Flaw Evaluation Criteria for Class 2, 3, and Balance-of-Plant (BOP) Piping 63

4.1.5.1 Effect of R/t Ratio 64

4.1.5.2 Transition Temperature Effects 64

4.1.6 Task 8a: Development of Fracture Criteria for Through-Wall Cracks in Elbows 65

4.1.7 Task 8b: Analysis of the V. C. Summer Bimetal Weld Case for Primary Water Stress Corrosion Cracking (PWSCC) 66

4.1.8 Task 9: Weld Residual Stress Effects on COD Predictions for LBB Analyses 67

4.2 Recommendations 68

4.2.1 Potential Recommendations with Respect to Leak-Before-Break Procedures 68

4.2.2 Potential Recommendations with Regards to In-Service Flaw Evaluation Criteria 69

4.2.3 Recommendations for Future Work 69

4.3 References 70

List of Figures

Figure 2.1 Comparison of the results from the IPIRG-1 pipe-system experiments with companion quasi-static, four-point bend experiments demonstrating how global secondary stresses, such as thermal expansion and seismic anchor motion stresses, contribute to fracture 6

Figure 2.2 Comparison of moment-time plots for IPIRG-1 Experiment 1.3-5 and BINP Task 1 experiment 7

Figure 2.3 GE/EPRI tension equation modification for the case of $\theta = \pi/4$, R/t = 10, and 15 mm (0.59 each) thick pipe 14

Figure 2.4 Ratio of circumferentially through-wall-cracked pipe-to-elbow moments for constant applied J values versus the ASME B_2 stress index for the elbow 21

Figure 2.5 Ratio of axially through-wall-cracked pipe-to-elbow moments for constant applied J values versus the ASME B_2 stress index for the elbow 21

Figure 2.6 Plot of the ratio of the experimental stress to the predicted NSC stress as a function of pipe R/t ratio for pipes expected to fail under limit-load conditions 24

Figure 2.7 Comparison of new Class 2, 3, and BOP F-functions and F-functions in ASME Section XI Appendix H for a crack aspect ratio (c/a) of 16 and a pipe with an R/t ratio of 40 for internal circumferential cracks subject to pure bending. 25

Figure 2.8 Comparison of J versus moment results for various SC.TNP analyses with finite element results for the case of no pressure, $\theta/\pi = 0.25$, a/ t= 0.5 and R/t = 40 27

Figure 2.9 Toughness anisotropy of ASTM A106 Grade B pipe 28

Figure 2.10 Comparison of applied J versus moment curves from the original SC.TNP (Lw = t) and modified SC.TNP (Lw = C1*t) analyses for 28-inch diameter pipes with R/t ratios of 5 and 60 and cracks 25 percent of the pipe circumference long and 50 percent of the pipe wall thickness deep 29

Figure 2.11 Relationship between DWTT and Charpy 85% shear area transition temperatures (SATT) as function of Charpy specimen thickness 32

Figure 3.1 Shear area versus temperature from full-thickness Charpy test data for A106B pipe taken from PIFRAC database 55

Figure 3.2 Relationship between DWTT and Charpy 85% shear area transition temperatures (SATT) as function of Charpy specimen thickness 56

Figure 3.3 Axial through-wall-cracked pipe and DWTT data showing the temperature shift from the FITT to the FPTT for linepipe steel 57

Figure 3.4 Axial through-wall-cracked pipe and DWTT data showing the temperature shift from the FITT $_{(TWC)}$ to the FPTT for linepipe steel 57

Figure 3.5 Results comparing transition temperatures of bend-bar specimens and fixed-grip SEN(T) specimen 58

List of Tables

Table 2.1 Critical values of remote axial tension membrane stress that need to be exceeded to allow for crack opening with weld residual stress* 13

Table 2.2 Critical values of remote bending stresses ($\sigma_B^{\infty}{}_{Critical}$) for moment loading 13

Table 2.3 C_T values for tension loading 14

Table 2.4 C_B values for moment loading 15

Table 2.5 I_{OD} values 15

Table 2.6 I_{ID} values 16

Table 2.7 V_1 values for bending from Tables 4.3 and 4.8 of Reference 2.14 17

Table 2.8 Surface regression coefficients for C1 in Equation 2.18 27

Table 3.1 Example problem illustrating the role of secondary stresses on LBB 36

Table 3.2 Example problem illustrating effect of actual margins on LBB 38

Table 3.3 Example problem illustrating effect of restraint of pressure-induced bending on LBB 42

Table 3.4 Example problem illustrating the differences in J and COD predictions between the GE/EPRI method for straight pipe and the elbow through-wall-crack solutions developed as part of this program 44

Table 3.5 Example problem illustrating the effect of weld residual stresses on LBB 46

Table 3.6 Example problem illustrating the role of secondary stresses on in-service flaw evaluation criteria 48

Table 3.7 Example problem illustrating the effect of actual margins on in-service flaw evaluation criteria 49

Table 3.8 Example problem illustrating the differences between the existing F-functions from ASME Section XI Appendix H and the newly-developed F-functions from the BINP program 51

Table 3.9 Example problem illustrating the differences in maximum moment-carrying capacity between the SC.TNP1 analysis (Lw = t) and revised SC.TNP analysis (Lw = C1*t) for different R/t ratios 53

EXECUTIVE SUMMARY

Over the past 15 to 20 years, significant research has been conducted to further the understanding of the fracture behavior of piping and piping systems in commercial nuclear power plants. While the results of these research programs have significantly advanced the state-of-the-art in the area of piping fracture mechanics, a number of key technical issues remained to be resolved in order to develop the necessary technical basis for codifying these results through the rulemaking process or in international standards.

The Battelle Integrity of Nuclear Piping (BINP) program was developed to address what was perceived to be the most critical of these issues.

The program was structured as a series of independent tasks, each focused one of these outstanding technical issues. The impetus behind these tasks was developing or advancing the technical basis for either in-service flaw evaluation or leak-before-break (LBB) assessments. While the impact of many of these issues was found to be relatively minor (15 to 20 percent), a few major issues were found that could have a significant impact on either LBB or in-service flaw assessments.

The major issues are:

- Effect of actual margins when accounting for plasticity in the piping system,
- Effect of crack morphology parameters on LBB analysis,
- Effect of secondary stresses on LBB and in-service flaw evaluation criteria, and
- Effect of weld repair methods on the residual stress fields and the resultant subcritical crack initiation/growth behavior.

The issues which were found to be of lesser importance are:

- Effect of seismic loading on the load-carrying capacity of cracked pipe systems,
- Effect of restraint of pressure induced bending on the crack-opening displacements (COD) for LBB analyses, and
- Effect of weld residual stresses on the COD for LBB analyses.

In addition to addressing these separate effects, the BINP program also began the process of developing the technical basis for new flaw evaluation criteria for Class 2, 3, and Balance of Plant piping.

Effect of Actual Margins - During the IPIRG programs it was hypothesized that there may be some previously unaccounted-for margin in the LBB and in-service flaw evaluation criteria as a result of conducting elastic analysis to quantify a nonlinear problem. It was thought that plasticity in the piping system (remote from the crack section) and plasticity associated with the crack might absorb energy that would otherwise go into driving the crack. This effect had potentially the largest impact on either LBB or in-service flaw evaluations of any of the effects formally considered as part of this program. The

magnitude of this effect depends on a number of factors, including the magnitude of the load history, the stiffness and/or flexibility of the piping system and its associated boundary conditions, variability of the yield strength of piping segments/fittings in the pipe system, and the location under consideration. To illustrate the potential magnitude of this effect, the additional margin observed at certain locations along a surge line at 1 safe-shutdown earthquake (SSE) loading was on the order of a factor of 10 or more. This margin was due solely to the remote plasticity, and not to the presence of the crack. As part of this effort, it was shown that the nonlinearities associated with pipe yielding, remote from the crack, tended to have a more pronounced effect on the actual margins than the nonlinearities associated with the crack.

Effect of Crack Morphology Parameters on the Postulated Leakage Crack Size Analysis for LBB Analyses - As part of one of the example test cases considered during the course of this program, it was shown that the choice of the crack morphology parameters can have a significant effect on the postulated leakage crack size, and the resultant acceptability of LBB. When using the mean values for the crack morphology parameters for IGSCC cracks[1] from NUREG/CR-6004, it was found that for an actual surge line application (where the surge line joins to the pressurizer), the margin on crack size was less than 1.5, compared to the margin on crack size of 2.0 that is needed to satisfy the LBB approach in draft SRP 3.6.3. Conversely, when using the assumed crack morphology parameters from an actual LBB submittal [0.0078 mm (300 micro-inches) surface roughness and no turns], the margin on crack size was almost 3.0, well in excess of the value needed to satisfy LBB. This finding was supported by work from the USNRC's technical basis development for their planned Regulatory Guide for LBB.

Effect of Secondary Stresses - In this context, the term secondary stresses refers to the global thermal expansion or seismic anchor motion type displacement-controlled stresses, not the localized through-thickness weld residual stresses. As a result of the Task 1 experiment and related experiments from the IPIRG programs, it was concluded that:

Secondary stresses contribute just as much to the fracture process as do the primary membrane and primary bending stresses whenever the ratio of the failure stress to the yield stress ($\sigma_{failure}/\sigma_{yield}$) is less than 1.0. If $\sigma_{failure}/\sigma_{yield}$ is greater than 1.0, then secondary stresses may become less important in some nonlinear fashion. However, this nonlinear relationship is not defined at this time, and limited data currently exist from which this relationship may be defined.

As a result of this finding it could be concluded that the existing criteria in draft Standard Review Plan (SRP) 3.6.3 for LBB (Ref. 4.3) for addressing secondary stresses in LBB evaluations are probably adequate, at least for the case where the piping system under consideration is fabricated using lower toughness shielded-metal-arc or submerge-arc welds. For those cases, the secondary stresses are considered equally with the primary membrane and primary bending stresses. For piping systems fabricated

[1] These IGSCC crack morphology parameters are close to those for a PWSCC.

with higher toughness tungsten-inert gas (TIG) welds, the draft SRP procedures do not consider the secondary stresses. However, for these higher toughness situations, the failure stresses should be high enough that yielding remote from the crack location should be prevalent. In such applications, it has been argued that the contribution of secondary stresses may not be as significant. In those cases, an as yet undefined non-linear correction to the secondary stress contribution has been suggested to be needed. In addition, as applicants are seeking LBB relief for smaller and smaller diameter piping systems, the potential exists that the postulated leakage crack size (as a function of pipe circumference) may be large enough that the failure stress may be less than the yield strength, even for the case of postulated cracks in higher toughness TIG welds. In that case, the secondary stresses may need to be considered with the primary membrane and bending stresses, contrary to the existing criteria.

The existing flaw evaluation criteria in ASME Section XI for submerge-arc and shielded-metal-arc welds are adequate, especially in light of the excellent record that commercial nuclear piping systems have.

Effect of Weld Repair Methods on the Residual Stress Fields and the Resultant Subcritical Crack Initiation/ Growth Behavior - An analytical assessment was made, using the finite element method, of the weld residual stresses in the vicinity of the hot leg to reactor pressure vessel (RPV) nozzle bimetallic weld. The entire history of fabrication of the weld was included in the analysis, including the Inconel buttering, post weld heat treatment (PWHT), weld deposition, weld grind-out and repair, hydro-testing, service temperature heat-up, and finally service loads. The purpose of this assessment was to look at the effect of different weld repair procedures on the resultant weld residual stresses and their potential impact on primary water stress corrosion cracking (PWSCC). The key finding from this effort was that from a resultant residual stress and PWSCC perspective, the inside welding followed by outside welding repair process was the preferred method of repairing one of these welds. This finding was consistent whether the concern was for axial or circumferential crack growth.

Effect of Seismic Load History - As a result of the analysis of the alternative seismic load history pipe-system experiment conducted as part of this program, it was concluded that the combined effect of cyclic history and material composition (sulfur content) resulted in a 25 percent reduction in load-carrying capacity when compared with the results from the first simulated seismic experiment conducted in the Second IPIRG program. Of this reduction, about half (10 to 15%) was attributed to the more damaging cyclic history associated with the BINP seismic experiment and about half (10 to 15%) was attributed to the fact that the crack in the BINP experiment was in the higher sulfur, lower toughness heat of pipe material DP2-A8 while the crack in the IPIRG experiment was in the lower sulfur, higher toughness heat of DP2-A8. It should be noted, though, that this conclusion is based on data for a relatively high toughness material (stainless steel base metal) for which limit load conditions should prevail. Analysis indicated that for the case of a lower toughness material (cracks in carbon steels or stainless steel flux welds), in possibly a

larger diameter pipe, where EPFM conditions probably prevail, the effect on the load-carrying capacity due to the more damaging cyclic history may result in as much as a 30 to 40 percent reduction in the maximum load.

Effect of Restraint of Pressure Induced Bending - Near the end of the Second IPIRG program, an uncertainty analysis was conducted to identify the key issues, yet to be resolved, in the area of piping integrity. The most significant issue with regards to LBB analysis that was identified in this uncertainty analysis was that of restraint of pressure-induced bending. In that study, it was concluded that for small diameter pipe (on the order of 4-inch nominal diameter), the margin on LBB may be over a factor of ten less than anticipated when using traditional LBB analysis in which this effect is not considered. Thus, it was thought that this effect might be a key factor in future LBB applications, especially for small and intermediate diameter pipe. However, as a result of the analyses conducted as part the BINP program, it was shown that restraint of pressure induced bending has only a minor effect on LBB. The only times it could possibly play a significant role is for small diameter pipe, possibly operating at low operating stresses, or for steam lines, for which the leakage crack length is a large percent of the pipe circumference (approaching 50 percent of the pipe circumference).

Effect of Weld Residual Stresses on COD Analyses for LBB Assessments – A preliminary analysis conducted as part of the uncertainty study conducted at the end of the Second IPIRG program indicated that weld residual stress effects could have a potentially significant effect on the predicted crack-opening displacements (COD) needed for an LBB assessment. This effect was especially pronounced for thin-wall pipe operating at low stress levels. This preliminary analysis suggested that the through-wall residual stress field in welded pipe could cause the crack faces of a through-wall crack to rotate closed on the outside surface, thus restricting the flow of fluid through the crack, to a much greater degree than what might be predicted based on existing COD analyses. This restriction in flow would in turn cause the postulated leakage crack to be longer than anticipated for a prescribed leakage detection capability. Obviously, the longer-than-anticipated postulated leakage crack length would be detrimental to LBB. As part of this effort several corrections to the GE/EPRI method were made. As originally predicted, it was shown that the crack faces tend to rotate so that the crack on the outside surface opens less than on the inside surface. Furthermore, it was shown that there was a critical stress level that must be applied in order to overcome the crack closure on the outside surface, and thus open the crack. However, for most practical applications, the effect of weld residual stresses on the COD, by itself, was not a major contributing factor for LBB analyses, i.e., less than a 15 to 20 percent effect on the margin or crack size.

Development of Fracture Criteria for Through-wall Cracks in Elbows - An analysis methodology for predicting the applied J and the COD for a through-wall crack in an elbow was developed. This methodology was developed in support of the US NRC's initiative to formalize their LBB procedures through the publication of a new Regulatory Guide on LBB. In the end, this new analysis methodology for

circumferential through-wall-cracked elbows was probably not needed. The use of straight pipe solutions to predict the behavior of through-wall cracks in elbows is probably adequate. The differences in J and COD predictions between the new elbow through-wall crack analysis and existing straight pipe solutions (GE/EPRI) are minimal (less than 15 percent).

Development of a Flaw Evaluation Criteria for Class 2, 3, and Balance of Plant (BOP) Piping - The flaw evaluation criteria that currently exist in ASME Section XI for austenitic (Appendix C) and ferritic (Appendix H) piping are for Class 1 piping systems. No such criteria currently exist in the ASME code for Class 2, 3, and BOP piping. However, as inspection requirements for these piping systems increase, the need for such criteria is becoming more pressing.

There are two main differences between Class 1 piping and Class 2, 3, and BOP piping. The first is that Class 1 piping typically operates at higher pressures, and as such is typically fabricated from pipes with lower R/t ratios. The criteria in Section XI were typically developed for pipes with R/t ratios of 20 or less. Class 2, 3, and BOP piping, e.g., service water systems, can be fabricated from pipes with R/t ratios that approach or exceed 80. The second difference is that Class 2, 3, and BOP piping, which is typically fabricated from ferritic pipe, oftentimes operates at temperatures where there is a concern for transition temperature effects. Activities associated with this task were aimed at addressing each of these differences.

Effect of R/t Ratio - As part of this effort, a series of empirical equations was developed by curve fitting published finite element results of K-solutions and the associated F-functions. It was found that there is a rather significant effect of R/t ratio on the elastic F-functions for higher R/t ratio pipes (i.e., there was a significant difference between the ASME Section XI Appendix H equations and the new F-function equations for the higher R/t ratios.) The Appendix H solutions are supposedly only applicable to pipes with R/t ratios of 5 to 20. The agreement between the Appendix H equations and the new equations was fairly good in this regime, but as would be expected, the solutions diverged at higher R/t ratios. A major limitation associated with the new equations is that the FEA solutions which were used in the curve fitting process were limited to c/a values (half crack length divided by crack depth) of 32 or less. This limits the applicability of these new equations to relatively short flaws, especially for the higher R/t ratio pipes where these equations are most needed. For example, for a pipe with an R/t ratio of 50, the limit on flaw length for a 50 percent deep flaw is about 10 percent of the pipe circumference, i.e., $2\theta = 36$ degrees.

A second major activity associated with this task was the extension of one of the EPFM J-estimation schemes for surface cracked pipe to pipes with larger R/t ratios. The existing estimation schemes (e.g., SC.TNP1) were developed for pipes with R/t ratios of approximately 5 to 15. As part of this effort, the SC.TNP analysis was modified to make it more applicable to pipes with higher R/t ratios. The modification was made by adjusting the Lw term, which defines the distance from the crack plane at which the stress in the pipe approaches the uniform remote bending stress, i.e., the distance at which the effect of the crack

on the stress field diminishes. For the modified SC.TNP analysis, the Lw term was defined in terms of the pipe wall thickness as Lw = C1*t. The modified solution for J agrees much better with results from finite element analyses. The solutions developed as part of this program have only been developed for a single strain-hardening exponent (n = 5), but the methodology is currently being extended to account for different strain-hardening exponents as part of another US NRC program.

Transition Temperature Effects – The ASME Section XI Appendix H ferritic pipe flaw evaluation procedures require that a linear elastic (lower shelf) toughness value be used if the operating temperature is below 93°C (200°F). This can be a very limiting assumption. Consequently, a methodology for predicting the brittle fracture initiation transition temperature (FITT) of a surface crack in a ferritic pipe was developed. This methodology is based on knowing, or being able to estimate, the 85 percent shear area transition temperature from a set of Charpy specimens. Based on this analysis and the existing database of Charpy data for nuclear grade ferritic pipe, it appears that the probability of initiating a brittle fracture from a surface crack in a Class 2, 3 or BOP piping system, even down to 0°C (32°F), may be minimal. Consequently, the EPFM and limit-load analyses for Class 1 piping can probably be used with the corresponding strengths at the lower temperatures. (At temperatures below 150°C [300°F] there is no effect of dynamic strain aging, so that the toughness could be higher at the lower operating temperatures.)

ACKNOWLEDGMENTS

The BINP program was an international cooperative group program conducted at Battelle with assistance from staff at Engineering Mechanics Corporation of Columbus (Emc^2). There were a total of four member countries in the group. The member countries, and associated organizations, and their Technical Advisory Group (TAG) representatives were:

Japan
- CRIEPI Mr. Naoki Miura

Korea
- KINS Dr. Young-Hwan Choi
- KEPRI
- KOPEC

Taiwan
- INER Dr. L. C. Kang
- AEC-ROC
- Taiwan Power

United States
- US NRC Mr. Tanny Santos

In addition, Dr. Nilesh Chokshi and Dr. T. Y. Chang also served as TAG representatives for the US NRC during the course of this program. We would like to thank all of the individuals who participated in the two round-robin exercises undertaken as part of this effort. Their efforts laid the foundation for the work conducted as part of the pressure-induced bending task (Task 4) and the task aimed at developing a flaw evaluation criteria for Class 2, 3, and balance-of-plant piping (Task 7).

Others who deserve special mention are Mr. Robert Gertler, who was the lead technician for all of the pipe experiments conducted as part of this program, and Ms. Tracey Thomas, Ms. Donna Detillion, and Ms. Paula Morgan who were responsible for the final preparation of this document.

NOMENCLATURE

1. SYMBOLS

A	Crack size parameter
B_2	Stress index from ASME Section III
c	Half crack length
c_{crit}	Half length of critical crack
C	Factor which relates restraint length (L) to pipe stiffness (k)
C_B	Slope term for bending in the weld residual stress COD analysis
C_T	Slope term for tension loading in the weld residual stress COD analysis
C1	Correction factor for Lw parameter in revised SC.TNP analysis
E	Elastic modulus
F	Elastic F-function
F_B	Elastic F-function due to bending
F_T	Elastic F-function due to tension
h	An elbow parameter ($R_{el}t/R_m^2$)
h_1	Function in GE/EPRI method
h_2	Function in GE/EPRI method
I	Moment of inertia
I_{ID}	Intercept term for inside surface
I_{OD}	Intercept term for outside surface
J	J-integral fracture parameter
$J_{applied}$	Applied value of J
J^e	Elastic component of J
J_B^e	Elastic component of J due to bending
J_T^e	Elastic component of J due to tension
J^p	Plastic component of J
J-R	J-resistance
k	Pipe stiffness
K	Stress intensity factor
K_B	Bending component of the stress intensity factor
K_T	Tension component of the stress intensity factor
L	Restraint length
L_1	Short restraint length
L_2	Long restraint length
Lw	Distance parameter in SC.TNP analysis from the crack plane to the location where the stress in the pipe is no longer influenced by the crack
M	Margin associated with load combination method in LBB analysis
M	Moment
M_{elbow}	Moment in an elbow
M_{max}	Maximum moment
M_{pipe}	Moment in a pipe
M_x	Bending moment about x-axis
M_y	Bending moment about y-axis

n	Strain hardening exponent
p	Pressure
P	Applied load
P_b	Bending stress
P_e	Thermal expansion stress
P_m	Membrane stress
r_{COD}	Correction factor that accounts for restraint of pressure-induced bending on the crack-opening displacements
R	Pipe radius
R_{el}	Bend radius of an elbow
R_m	Mean radius
S_m	ASME Code Design Stress
S_1	Earthquake design magnitude in Japan
t	Wall thickness
t	Time
T	Temperature
V	Functions in GE/EPRI analysis for predicting COD
Z	ASME Section XI stress multipliers to account for low toughness
α	Curve fitting parameter in Ramberg-Osgood relationship
β	Stress inversion angle in Net-Section-Collapse analysis
δ	Crack opening displacement
δ_e	Elastic component of COD
δ_p	Plastic component of COD
δ_{ID}	COD on inside surface
δ_{OD}	COD on outside surface
δ_T	Total crack opening displacement
ε	Strain
ε^e	Elastic component of strain
ε^p	Plastic component of strain
ε_0	Reference strain
σ	Stress
σ_B	Bending stress
σ_f	Flow stress
σ_m	Membrane stress
σ_0	Reference stress
σ_T	Stress due to tension loads
σ_u	Ultimate strength
σ_y	Yield strength
σ^∞	Remote stress
$\sigma^\infty_{critical}$	Critical remote stress that must be overcome for cracks to be open when affected by weld residual stresses
θ	Half crack angle

2. ACRONYMS AND INITIALISMS

AEC-ROC	Atomic Energy Commission – Republic of China
ASME	American Society of Mechanical Engineers
ASTM	American Society for Testing and Materials
BINP	Battelle Integrity of Nuclear Piping
BOP	Balance of Plant
CEA	Commissariat A L'Energie Atomique (France)
COD	Crack-opening displacement
CRIEPI	Central Research Institute of Electric Power Industry (Japan)
C(T)	Compact (tension)
DPZP	Dimensionless plastic zone parameter
DTT	Dynamic tear test
DWTT	Drop weight tear test
Emc^2	Engineering Mechanics Corporation of Columbus
EPFM	Elastic plastic fracture mechanics
EPRI	Electric Power Research Institute
FEA	Finite element analysis
FITT	Fracture initiation transition temperature
FPTT	Fracture propagation transition temperature
GE	General Electric
IGSCC	Intergranular stress corrosion cracking
INER	Institute of Nuclear Energy Research (Taiwan)
IPIRG	International Piping Integrity Research Group
KEPRI	Korea Electric Power Research Institute
KINS	Korean Institute of Nuclear Safety
KOPEC	Korean Power Engineering Company
LBB	Leak-Before-Break
LEFM	Linear elastic fracture mechanics
MPC	Materials Property Council
NRC	Nuclear Regulatory Commission
NSC	Net-Section-Collapse
OD	Outside diameter
PICEP	PIpe Crack Evaluation Program (leak rate code)
PIFRAC	PIping FRACture mechanics material property database
PWHT	Post-weld heat treat
PWR	Pressurized water reactor
PWSCC	Primary-water stress-corrosion cracking
QS	Quasi-static
RPV	Reactor pressure vessel
SAM	Seismic anchor motion
SAW	Submerge-arc weld
SEN(T)	Single-edge notch (tension)
SF	Safety factor
SG	Steam generator
SIS	Safety injection system

SMAW	Shielded-metal-arc weld
SQUIRT	Seepage Quantification of Upsets In Reactor Tubes
SRP	Standard Review Plan
SSE	Safe shutdown earthquake
TAG	Technical Advisory Group
TIG	Tungsten-inert-gas weld
TWC	Through-wall crack
US	United States
USNRC	United States Nuclear Regulatory Commission

PREVIOUS REPORTS IN SERIES

Reports from the IPIRG-2 Program

"Summary of Results from the IPIRG-2 Round-Robin Analyses," NUREG/CR-6337, BMI-2186, January 1996.

"IPIRG-2 Task 1 – Pipe System Experiments With Circumferential Cracks in Straight-Pipe Locations," NUREG/CR-6389, BMI-2187, February 1997.

"The Effect of Cyclic and Dynamic Loads on Carbon Steel Pipe," NUREG/CR-6438, BMI-2188, February 1996.

"Design of the IPIRG-2 Simulated Seismic Forcing Function," NUREG/CR-6439, BMI-2189, February 1996.

"The Effect of Cyclic and Dynamic Loading on the Fracture Resistance of Nuclear Piping Steels," NUREG/CR-6440, BMI-2190, December 1996.

"Deterministic and Probabilistic Evaluations for Uncertainty in Pipe Fracture Parameters in Leak-Before-Break and In-Service Flaw Evaluations," NUREG/CR-6443, BMI-2191, June 1996.

"Fracture Behavior of Circumferentially Surface-Cracked Elbows," NUREG/CR-6444, BMI-2192, December 1996.

"Development of a J-Estimation Scheme for Internal Circumferential and Axial Surface Cracks in Elbows," NUREG/CR-6445, BMI-2193, June 1996.

"Fracture Toughness Evaluations of TP304 Stainless Steel Pipes," NUREG/CR-6446, BMI-2194, February 1997.

"The Second International Piping Integrity Research Group (IPIRG-2) Program," Final Report, October 1991 – April 1996, NUREG/CR-6452, BMI-2195, March 1997.

"State-of-the-Art Report on Piping Fracture Mechanics," NUREG/CR-6540, BMI-2196, January 1998.

Reports from the IPIRG-1 Program

"Evaluation and Refinement of Leak-Rate Estimation Models," NUREG/CR-5128, BMI-2164, Revision 1, June 1994.

"Loading Rate Effects on Strength and Fracture Toughness of Pipe Steels Used in Task 1 of the IPIRG Program," Topical Report, NUREG/CR-6098, BMI-2175, October 1993.

"Stability of Cracked Pipe Under Inertial Stresses," NUREG/CR-6233, BMI-2177, Volume 1, August 1994.

"Stability of Cracked Pipe Under Seismic/Dynamic Displacement-Controlled Stresses," NUREG/CR-6233, BMI-2177, Vol. 2, June 1997.

"Cracked Stability in a Representative Piping System Under Combined Inertial and Seismic/Dynamic Displacement-Controlled Stresses," NUREG/CR-6233, BMI-2177, Vol. 3, June 1997.

"International Piping Integrity Research Group (IPIRG) Program," NUREG/CR-6233, BMI-2177, Vol. 4, June 1997.

Previous Related Documents from NRC's Short Cracks in Piping and Piping Welds Program

"Short Cracks in Piping and Piping Welds," First Semiannual Report, NUREG/CR-4599, BMI-2173, Vol. 1, No. 1, March 1991.

"Short Cracks in Piping and Piping Welds," Second Semiannual Report, NUREG/CR-4599, BMI-2173, Vol. 1, No. 2, April 1992.

"Short Cracks in Piping and Piping Welds," Third Semiannual Report, NUREG/CR-4599, BMI-2173, Vol. 2, No. 1, September 1992.

"Short Cracks in Piping and Piping Welds," Fourth Semiannual Report, NUREG/CR-4599, BMI-2173, Vol. 2, No. 2, February 1993.

"Short Cracks in Piping and Piping Welds," Fifth Semiannual Report, NUREG/CR-4599, BMI-2173, Vol. 3, No. 1, October 1993.

"Short Cracks in Piping and Piping Welds," Sixth Semiannual Report, NUREG/CR-4599, BMI-2173, Vol. 3, No. 2, March 1994.

"Short Cracks in Piping and Piping Welds," Progress Report, NUREG/CR-4599, BMI-2173, Vol. 4, No. 1, April 1995.

"Assessment of Short Through-Wall Circumferential Cracks in Pipes," NUREG/CR-6235, BMI-2178, April 1995.

"Fracture Behavior of Short Circumferential Short-Surface-Cracked Pipe," NUREG/CR-6298, BMI-2183, November 1995.

"Fracture Evaluations of Fusion Line Cracks in Nuclear Pipe Bimetallic Welds," NUREG/CR-6297, BMI-2182, April 1995.

"Effect of Dynamic Strain Aging on the Strength and Toughness of Nuclear Ferritic Piping at LWR Temperatures," NUREG/CR-6226, BMI-2176, October 1994.

"Effects of Toughness Anisotropy and Combined Loading on Fracture Behavior of Ferritic Nuclear Pipe," NUREG/CR-6299, BMI-2184, April 1995.

"Refinement and Evaluation of Crack-Opening Analyses for Circumferential Through-Wall Cracks in Pipes," NUREG/CR-6300, April 1995.

"Probabilistic Pipe Fracture Evaluations for Leak-Rate Detection Applications," NUREG/CR-6004, BMI-2174, April 1995.

"Stainless Steel Submerged Arc Weld Fusion Line Toughness," NUREG/CR-6251, BMI-2180, April 1995.

"Validity Limits in J-Resistance Curve Determination: Volume 1: An Assessment of the J_M Parameter," NUREG/CR-6264, BMI-2181, Vol. 1, February 1995.

"Validity Limits in J-Resistance Curve Determinations: Volume 2: A Computational Approach to Ductile Crack Growth Under Large-Scale Yielding Condition," NUREG/CR-6264, BMI-2181, Vol. 2, February 1995.

Previous Related Documents from NRC's Degraded Piping Program - Phase I Reports

"The Development of a Plan for the Assessment of Degraded Nuclear Piping by Experimentation and Tearing Instability Fracture Mechanics Analysis," NUREG/CR-3142, Vols. 1 and 2, June 1983.

Previous Related Documents from NRC's Degraded Piping Program - Phase II Reports

"Degraded Piping Program - Phase II," Semiannual Report, NUREG/CR-4082, BMI-2120, Vol. 1, Oct. 1984.

"Degraded Piping Program - Phase II," Semiannual Report, NUREG/CR-4082, BMI-2120, Vol. 2, June 1985.

"Degraded Piping Program - Phase II," Semiannual Report, NUREG/CR-4082, BMI-2120, Vol. 3, March 1986.

"Degraded Piping Program - Phase II," Semiannual Report, NUREG/CR-4082, BMI-2120, Vol. 4, July 1986.

"Degraded Piping Program - Phase II," Semiannual Report, NUREG/CR-4082, BMI-2120, Vol. 5, Dec. 1986.

"Degraded Piping Program - Phase II," Semiannual Report, NUREG/CR-4082, BMI-2120, Vol. 6, April 1988.

"Degraded Piping Program - Phase II," Semiannual Report, NUREG/CR-4082, BMI-2120, Vol. 7, March 1989.

"Degraded Piping Program - Phase II," Semiannual Report, NUREG/CR-4082, BMI-2120, Vol. 8, March 1989.

"NRC Leak-Before-Break (LBB.NRC) Analysis Method for Circumferentially Through-Wall Cracked Pipes Under Axial Plus Bending Loads," Topical Report, NUREG/CR-4572, BMI-2134, March 1986.

"Elastic-Plastic Finite Element Analysis of Crack Growth in Large Compact Tension and Circumferentially Through-Wall-Cracked Pipe Specimen--Results of the First Battelle/NRC Analysis Round Robin," Topical Report, NUREG/CR-4573, BMI-2135, September 1986.

"An Experimental and Analytical Assessment of Circumferential Through-Wall Cracked Pipes Under Pure Bending," Topical Report, NUREG/CR-4574, BMI-2136, June 1986.

"Predictions of J-R Curves With Large Crack Growth From Small Specimen Data," Topical Report, NUREG/CR-4575, BMI-2137, September 1986.

"An Assessment of Circumferentially Complex-Cracked Pipe Subjected to Bending," Topical Report, NUREG/CR-4687, BMI-2142, September 1986.

"Analysis of Cracks in Stainless Steel TIG Welds," Topical Report, NUREG/CR-4806, BMI-2144, November 1986.

"Approximate Methods for Fracture Analyses of Through-Wall Cracked Pipes," Topical Report, NUREG/CR-4853, BMI-2145, January 1987.

"Assessment of Design Basis for Load-Carrying Capacity of Weld-Overlay Repair," Topical Report, NUREG/CR-4877, BMI-2150, February 1987.

"Analysis of Experiments on Stainless Steel Flux Welds," Topical Report, NUREG/CR-4878, BMI-2151, February 1987.

"Experimental and Analytical Assessment of Circumferentially Surface-Cracked Pipes Under Bending," Topical Report, NUREG/CR-4872, BMI-2149, April 1987.

Other Related Program Reports

"Validation of Analysis Methods for Assessing Flawed Piping Subjected to Dynamic Loading," NUREG/CR-6234, ANL-94/22, BMI-2178, August 1994.

"Development of Technical Basis for Leak-Before-Break Evaluation Procedures," NUREG/CR-6765, May 2002.

1. INTRODUCTION

Over the past 15 to 20 years, significant research has been conducted to further the understanding of the fracture behavior of piping and piping systems in commercial nuclear power plants. While the results of these research programs have significantly advanced the state-of-the-art in the area of piping fracture mechanics, a number of key technical issues remained to be resolved in order to develop the necessary technical basis for codifying these results through the rulemaking process. These unresolved issues were first identified near the end of the Second International Piping Integrity Research Group program (IPIRG-2) in a report entitled "Deterministic and Probabilistic Evaluations for Uncertainty in Pipe Fracture Parameters in Leak-Before-Break and In-Service Flaw Evaluations," Ref. 1.1. These issues were then further prioritized through a series of piping review meetings, sponsored by the USNRC, aimed at prioritizing these issues in light of shrinking research budgets.

The Battelle Integrity of Nuclear Piping (BINP) program was developed to address what were perceived to be the most critical outstanding issues. The program was structured as a multi-client, cooperative program, similar to the structure of the IPIRG programs. The four organizations that funded this program and ultimately provided direction for its conduct are:

- Central Research Institute of Electric Power Industry (CRIEPI) in Japan,
- Institute of Nuclear Energy Research (INER) in Taiwan that led a consortium of organizations from Taiwan, including the Atomic Energy Commission-Republic of China (AEC-ROC) and Taiwan Power Company,
- Korean Institute of Nuclear Safety (KINS) that led a consortium of organizations from Korea, including Korean Electric Power Research Institute (KEPRI) and Korean Power Engineering Company (KOPEC), and
- Nuclear Regulatory Commission in the United States.

The program was structured as a series of independent tasks, each focused on addressing one of the outstanding technical issues identified in Reference 1.1 and/or the NRC piping review committee meetings. The impetus behind these tasks was developing or advancing the technical basis for either in-service flaw evaluation or leak-before-break (LBB) assessments. The tasks ultimately funded as part of this program were:

- Task 1 – Experimental Assessment of the Effects of Secondary Stresses on Pipe Fracture Behavior
- Task 2 – Pipe-System Experiment with an Alternative Seismic Input Function
- Task 3 – Assessment of Actual Margins in Plant Piping
- Task 4 – Assessment of Pipe-System Boundary Condition Effects on Leak-Before-Break Analysis
- Task 7 – Development of Flaw Evaluation Criteria for Class 2, 3, and Balance-of-Plant Piping
- Task 8 – Resolution of Issues of Interest to Selected Members
  - Subtask 8.1 – Development of a J-estimation Scheme for Through-Wall Cracks in Elbows
  - Subtask 8.2 – Evaluation of the Hot-Leg Piping to Reactor Pressure

Vessel Nozzle Bimetallic Weld Joint Integrity for the V. C. Summer Nuclear Power Plant

- Task 9 – Effect of Weld Residual Stresses on Crack-Opening-Displacement (COD) Predictions for Leak-Before-Break Analyses

In addition, two round-robin analyses were conducted as part of this program during which the program participants provided independent solutions to the problems. These solutions then in turn provided a part of the basis for two of the technical tasks conducted as part of BINP. The two round-robin analyses were:

- First round robin on the effect of the restraint of piping system boundary conditions on crack-opening displacement (COD) predictions for LBB analyses. The results from this round robin fed into Task 4.
- Second round robin on the effect of pipe radius to thickness (R/t) ratio on elastic-plastic fracture mechanics (EPFM) surface-cracked pipe J-estimation schemes. The results from this round robin fed into Task 7.

This final report for the BINP program is structured as a two volume report. Volume 1 provides a summary and implications of the results from both a leak-before-break and in-service flaw evaluation perspective. Volume 2 is a series of detailed appendices documenting the detailed results from the various tasks.

1.1 References

1.1 Ghadiali, N., Rahman, S., Choi, Y. H., and Wilkowski, G., "Deterministic and Probabilistic Evaluations for Uncertainty in Pipe Fracture Parameters in Leak-Before-Break and In-Service Flaw Evaluations," NUREG/CR-6443, June 1996.

2. IMPLICATIONS OF RESULTS

The impetus behind the various technical tasks undertaken as part of the BINP program was the advancement of the technical basis for either leak-before-break (LBB) or in-service flaw evaluation assessments. In this section of this report the implications of the results from the various technical tasks on these two subjects will be discussed. First, the implications related to LBB assessments will be discussed, and then those related to in-service flaw evaluations.

2.1 Implications of Results on Leak-Before-Break Analyses

A number of the technical tasks conducted as part of this program had potential implications with regards to LBB analyses. These included:

- Task 1 – Role of Secondary Stresses on Pipe Fracture
- Task 3 – Assessment of Actual Margins in a Plant Piping Analyses
- Task 4 – Effect of Restraint of Pressure Induced Bending on the Crack-Opening Displacement (COD) Analyses for LBB Assessments
- Task 8 – Development of a J-estimation Scheme for Through-Wall Cracks in Elbows
- Task 9 – Effect of Weld Residual Stresses on COD Predictions for LBB Analyses

In the sections that follow, each effect will be discussed separately. In the next section of this report (Section 3) a series of sample test case problems will be presented to illustrate the impact that these effects might have.

2.1.1 Role of Secondary Stresses on Pipe Fracture in LBB Evaluations

The crack stability analysis for austenitic steel piping in the existing LBB evaluation procedures in the USNRC draft Standard Review Plan (SRP) Section 3.6.3 (Ref. 2.1) is based on a modified limit-load analysis. Traditional limit-load analysis is modified by the inclusion of a stress multiplier (Z) in the crack-driving-force term to account for cracks in lower toughness shielded-metal arc and submerge-arc welds (SMAW and SAW) or in ferritic steel base metal. In addition, for these lower toughness materials, the combined thermal expansion stress at normal operating conditions (P_e) is included with the primary membrane and bending stress terms in the crack-driving force side of the stability analysis equation, i.e., the left-hand side of Equation 2.1.

$$M(P_m + P_b + P_e)Z = \frac{2\sigma_f}{\pi}(2\sin(\beta) - \sin(\theta)) \tag{2.1}$$

where,

M = the margin associated with the load combination method selected for the analysis (i.e., absolute or algebraic sum),
σ_f = flow stress,
P_m = the combined membrane stress, including pressure, deadweight and seismic components,
P_b = the combined primary bending stress,
P_e = the combined thermal expansion stress at normal operating conditions,
θ = half angle in radians of the postulated circumferential through-wall flaw,
β = stress inversion angle, i.e., angle in radians from the point 180 degrees removed from the crack centerline to the neutral axis of the pipe when accounting for the presence of the through-wall crack, and

Z = stress multiplier to account for the fact that the crack is located in a lower toughness material.

For higher toughness tungsten inert gas (TIG) welds and austenitic wrought base metals, the crack-driving force term in the LBB evaluation procedures in draft SRP 3.6.3 does not include either the thermal expansion stresses or the stress multiplier term (Z). The crack-driving force term (left-hand side of Equation 2.1) in draft SRP 3.6.3 for austenitic wrought base metals and TIG welds is reduced to:

$$M(P_m + P_b) \qquad (2.2)$$

The inclusion of the thermal expansion stresses in the LBB evaluation procedures for postulated cracks in SMAW and SAW is consistent with wording in NUREG-1061 Volume 3 (Ref. 2.2) which states,

> "The fracture mechanics analyses described in subsequent sections of this report should include thermal expansion stresses, which are conservatively included as primary stresses. The Task Group further believes that other secondary stresses (e.g., through-the-thickness stresses) do not contribute significantly to crack driving potential and, in view of the conservative treatment of thermal expansion stresses, can be neglected."

This philosophy for the treatment of thermal expansion stresses is also similar to that used in the ASME Section XI flaw evaluation criteria for cracks found in SMAW and SAW in austenitic piping in Appendix C of ASME Section XI[2]. The exception is that when the thermal expansion stresses in Appendix C are included for cracks in SMAW and SAW, they are included with a safety factor of 1.0 whereas the primary membrane and bending stresses are included with the full safety factors of 2.77 for normal operating conditions and 1.39 for emergency and faulted conditions. The crack-driving force term in Appendix C for SMAW and SAW is:

$$SF(P_m + P_b + P_e / SF)Z \qquad (2.3)$$

Comparing Equation 2.3 with the left-hand side of Equation 2.1, one can see that the crack-driving force terms for LBB and the in-service flaw evaluation are similar, with the exception that the LBB criteria includes the thermal-expansion stress term with the full safety factor whereas the flaw evaluation criteria from ASME Section XI Appendix C for flaws in lower toughness austenitic flux welds includes the thermal expansion stresses with a safety factor of 1.0. For cracks in higher toughness austenitic wrought base metals and TIG welds, the crack-driving force term in Appendix C (see Equation 2.4) is consistent with that in draft Standard Review Plan (SRP) Section 3.6.3 (see Equation 2.2).

$$SF(P_m + P_b) \qquad (2.4)$$

As a further point of reference, the British R6 approach (Ref. 2.3) also addresses the issue of primary versus secondary stresses. The R6 procedures classify primary stresses as those stresses that arise from loads that contribute to plastic collapse and secondary stresses as those stresses that arise from loads that do not contribute to plastic collapse. The R6 procedures provide further clarification on the issue by saying:

> "The classification of stresses into these two types is a matter of some judgment. Primary stresses are produced by applied external loads such as pressure,

[2] Further discussion of the impact of secondary stresses on pipe flaw evaluation criteria is reserved for Section 2.2 of this report.

deadweight or interaction from other components. Thermal or other displacement-induced stresses must often be classified as primary stresses at the region of the defect if there is significant elastic follow-up. These stresses will not, in general, be self equilibrating.

Secondary stresses are generally produced as a result of internal mismatch caused by, for example, thermal gradients and welding processes. These stresses will be self equilibrating, i.e., the net force and bending moment will be zero.

Thermal and residual welding stresses which are self-equilibrating in the whole structure may be not self-equilibrating on the section containing the flaw. Such stresses are not necessarily classifiable as secondary stresses. If in doubt about the stress category primary stresses should be assumed."

Based on the above discussion there appears to be a level of uncertainty as to how to treat thermal expansion stresses in a LBB evaluation, or for that matter in in-service flaw evaluations, i.e., are they included, and if so, what safety factor should be applied. This uncertainty was first addressed during the analysis of a series of pipe-system experiments from the First International Piping Integrity Research Group (IPIRG) program (Ref. 2.4). The results from the IPIRG pipe-system experiments indicated that for large surface cracks, where the failure stresses are below the yield strength of the uncracked pipe, the displacement-induced thermal expansion and seismic anchor motion (SAM) stresses contributed just as much to the fracture process as did the primary stresses, see Figure 2.1. (Similar analysis of the experimental results from the through-wall-cracked pipe-system and quasi-static bend experiments from the Second IPIRG program yielded a similar conclusion as did finite element analysis of a through-wall-cracked pipe system, conducted as part of the Margin Assessment task of this program (Task 3)).

Figure 2.1 shows a plot of the maximum experimental stress normalized by the Net-Section-Collapse (NSC) stress for five quasi-static bend and five pipe-system experiments conducted as part of the IPIRG (Ref. 2.4) and related programs (Refs. 2.5 and 2.6). The crack sizes in each of these experiments were relatively large, such that the failure moments were low enough that plasticity was restricted to the crack section, especially in light of the fact that the bulk of the piping system (excluding the test specimen) was fabricated from higher strength carbon steel pipe. In Figure 2.1, the maximum experimental stresses have been normalized by the NSC stress to account for slight differences in pipe size and crack size. For each experiment, the maximum stress has been broken down into its various stress components, i.e., primary membrane, primary bending, seismic anchor motion, and thermal expansion. (For the quasi-static bend companion experiments, the only stress components applicable are primary membrane and primary bending [quasi-static bending].) From Figure 2.1, it can be seen that if the thermal expansion and seismic anchor motion stresses are ignored in the stress terms for the pipe-system experiments, then the normalized failure stresses for the pipe-system experiments would only be 40 to 60 percent of the normalized failure stresses for the quasi-static bend experiments. This suggests that these displacement-induced stresses do contribute to fracture, at least for the case of large surface cracks where plasticity is limited to the cracked section.

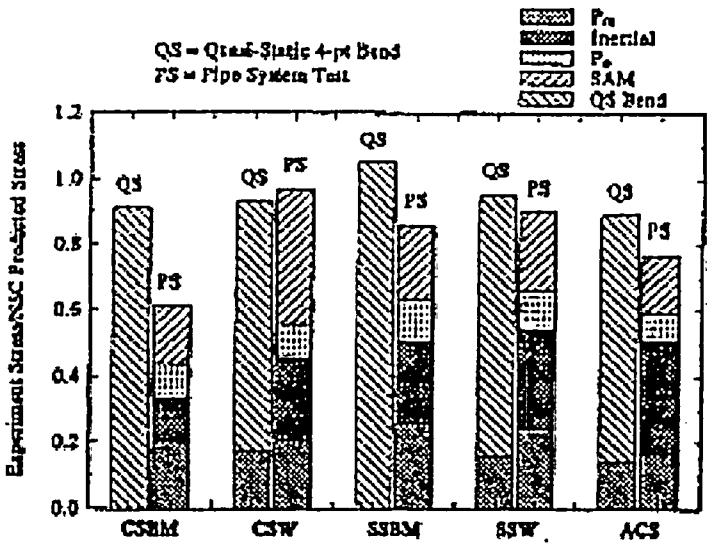

Figure 2.1 Comparison of the results from the IPIRG-1 pipe-system experiments with companion quasi-static, four-point bend experiments demonstrating how global secondary stresses, such as thermal expansion and seismic anchor motion stresses, contribute to fracture

This phenomenon was studied further as part of Task 1 of this program. This task involved a stainless steel SAW pipe-system experiment in which the actuator was intentionally offset at the start of the test to simulate a larger thermal expansion stress component. (Details of this Task 1 experiment are provided in Appendix A of this report.) From this experiment there are a couple of points of note which support the findings from the IPIRG-1 program. First, the maximum moment from this experiment was about the same as that for a companion stainless steel weld experiment (with nominal thermal expansion) from IPIRG-1, see Figure 2.2. Second, the crack actually initiated while initially offsetting the actuator to simulate the larger thermal expansion stress. Both of these findings support the contention that the thermal expansion stresses (displacement-induced stresses) are not less detrimental than the primary membrane and bending stresses, at least for these test conditions for which the stresses at failure for the uncracked pipe were less than the yield strength.

For such conditions (i.e., limited yielding), there is the potential for elastic follow-up. Section III of the ASME Code recognizes this potential in its local overstrain criteria in paragraph NC-3672.6(b). This paragraph implies that global secondary stresses, such as thermal expansion and seismic anchor motion stresses, can act as primary stresses under certain conditions, such as when the weaker or higher stressed portions of the piping system are subjected to strain concentrations due to elastic follow-up of the stiffer or lower stressed portions of the piping system. One obvious example of this is the IPIRG pipe system in which a large crack was introduced. Consequently, the resultant stresses for the uncracked pipe sections were less than the yield strength at the time of failure of the cracked section. The implication is that the safety factor for

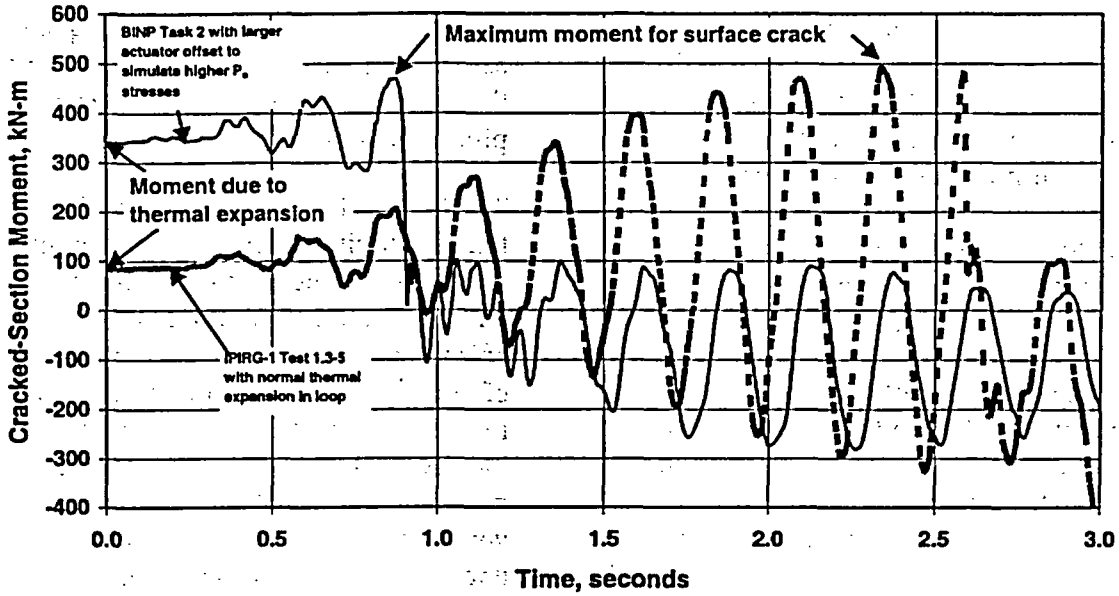

Figure 2.2 Comparison of moment-time plots for IPIRG-1 Experiment 1.3-5 and BINP Task 1 experiment

the displacement-induced stresses may be a function of the ratio of the failure stress to yield strength. If the failure/yield stress ratio is less than 1.0, then the displacement-induced thermal expansion and seismic anchor motion stresses should be treated as primary stresses for fracture. If the opposite holds true (that is, if the failure/yield strength ratio is greater than 1.0), then these displacement-induced (secondary) stresses may become less important with some nonlinear function.

At this time, however, no experimental data are known to exist for which the failure stresses were less than the yield strength of the uncracked pipe. In light of this lack of data, quantifying this nonlinear function would be difficult at best. Consequently, the most defensible course of action would be to leave the criteria in draft SRP 3.6.3 as is and to consider the thermal expansion stresses equal with the primary bending and membrane stresses, at least for the case of postulated cracks in lower toughness SMAW and SAW.

2.1.2 Impact of Actual Margins for LBB Evaluations

Battelle and Emc^2 recently completed a study for the US NRC in which they developed the technical basis for a new Regulatory Guide on leak-before-break (LBB), Ref. 2.7. That effort proposes a tiered approach to LBB. The first tier of analysis (Level 1) was designed to be the simplest of the three levels and to provide a conservative assessment of LBB acceptability, and yet still be of sufficient accuracy that piping systems that readily pass the existing draft SRP 3.6.3 criteria (e.g., main coolant loop piping) can pass this Level 1 criteria. The Level 1 approach was structured such that one did not need to use sophisticated leak rate codes in the analysis, but merely a series of simple empirically-derived algebraic expressions or closed-form solutions from which one could estimate the

postulated leakage crack size. In addition, instead of having to use more sophisticated J-estimation scheme analyses to calculate the allowable stresses for the postulated crack size, the Level 1 fracture stability analysis was based on the simple ASME Section XI limit-load type analysis, modified as necessary by the ASME Section XI Z-factors to account for the postulated crack being located in a lower-toughness stainless steel flux weld.

The next level of complexity for LBB assessments will be the Level 2 methodology. The Level 2 methodology is similar in scope to the existing draft SRP 3.6.3 methodology except that it incorporates many of the enhancements that have resulted from research over the last 15 years. Two of these enhancements, i.e., the effect of restraint of pressure-induced bending on the crack-opening displacements (COD) for LBB analyses and the effect of weld residual stresses on the CODs for LBB analyses, will be discussed next. It is envisioned that this level of assessment (Level 2) would be used in the vast majority of future LBB applications.

The final level of assessment (Level 3) is the most complex of the three levels of deterministic analyses, requiring the greatest amount of information/data for its application. In all likelihood, this level of analysis would only be used for those cases where LBB cannot be demonstrated using the simpler Level 1 or 2 methods. This level of analysis will involve a very detailed deterministic analysis, including nonlinear stress analyses and possibly incorporating nonlinear behavior of the cracked section. The nonlinear stress analysis will be used to take advantage of the inherent margins that exist when one invokes an elastic analysis on a nonlinear problem. By incorporating plasticity into the modeling, energy that would have otherwise gone into driving the crack will be absorbed in plastically deforming the surrounding uncracked pipe material. As part of Task 3 of this program a quantitative assessment was made as to the magnitude of these actual margins for representative piping systems.

The bottom line from this Task 3 effort is that the additional margin one might realize by using nonlinear analysis, instead of linear analysis, could be significant. Of all the effects studied as part of this program, this effect appears to have the potential of making the most impact on either LBB or in-service flaw evaluations. Additional margins on the order of 2 to 3 are not unrealistic when one considers plasticity in the uncracked pipe sections. In the example problem considered in Section 3, an additional margin of approximately 2.5 was realized by conducting a nonlinear uncracked pipe analysis in lieu of an elastic uncracked pipe analysis. For this example test case, the additional margin was over 10 when the combined effect of remote piping system plasticity and plasticity due to the crack was considered. Furthermore, detailed finite element analyses conducted as part of this program showed that the additional margin observed at certain locations along a surge line at one safe-shutdown earthquake (SSE) loading was on the order of 10 or more. This margin was due solely to the remote plasticity and not the presence of the crack. This effect had by far the biggest impact of any of the topics considered directly as part of this program[3]. Thus, if

[3] Another effect that was also found to have a pronounced impact on LBB considerations was the choice of the crack morphology parameters used in the leak-rate analysis. While not directly considered as part of the BINP program, it was indirectly considered as part of the assessment of the impact of restraint of pressure-induced bending on LBB in one of the example problems in Section 3 of this report. Furthermore, it was considered in detail in a related US NRC program conducted at Battelle and Emc[2] (Ref. 2.7). As part of the example considered in

one finds oneself in a situation where one is having a hard time demonstrating LBB for a particular application, one logical source of relief may be found by invoking a Level 3 type LBB analysis, and conducting a non-linear stress analysis of the piping system under consideration. The calculated moments and forces from that stress analysis are compatible with those in an elastic-plastic fracture mechanic analysis.

2.1.3 Effect of the Restraint of Pressure Induced Bending on the Crack-Opening Displacements (COD) for LBB Evaluations

One of the technical areas of concern in the existing procedures in draft SRP 3.6.3 for LBB evaluations is the prediction of the crack-opening displacement needed for estimating the postulated leakage crack size for a prescribed leakage detection capability. Two specific concerns in this regard that were identified near the end of the Second IPIRG program (Ref. 2.9) are the effect of the restraint of pressure-induced bending and the effect of weld residual stresses on the COD predictions for LBB evaluations. In this section, the impact that restraint of pressure-induced bending has on the COD predictions, and subsequently the LBB assessment, will be discussed. In the section that follows, the impact of weld residual stresses will be discussed.

As part of Task 4 of this program, the effect of restraint of pressure-induced bending on the crack-opening displacements (COD) for LBB evaluations was considered. Typical COD analyses used in past LBB submittals calculated the COD across the center of the crack for a pipe under bending and axial tension (from pressure and other loads), but all these models assumed the pipe was an end-capped condition with free rotation conditions at the ends. Real pipe systems have rotation restraints at their terminal ends, which will reduce certain COD contributions. The COD contribution of concern is that from the axial membrane loads and how they induce a bending contribution to the COD due to the eccentricity created from the neutral axis shift of the crack plane. Note that although this is referred to as "restraint of pressure-induced bending", it is actually restraint of bending from any axial membrane stress component, including seismic, thermal expansion dead-weight etc.

From the Task 4 efforts, it was found that the COD for the case where the piping system was restrained (COD_{res}) was related to the COD for an unrestrained pipe (COD_{unres}) by a factor r_{COD}, i.e.,

$$COD_{res} = r_{COD} COD_{unres} \qquad (2.5)$$

The factor r_{COD}, which is 1.0 or less, was found to be a function of the crack size (as a percent of the pipe circumference) and the restraint length (normalized by the pipe diameter, i.e., L/D). Basically, the longer the normalized crack length ($2c/\pi D$), the greater the effect of restraint. In practice the longer normalized crack lengths ($2c/\pi D$) tended to be associated with smaller diameter pipe since the actual crack lengths (2c) for a prescribed leakage detection capability are nearly independent of pipe diameter. Steam lines would similarly tend to have longer cracks than subcooled water lines for a given leak rate. In a similar vein, the closer the section under evaluation was to a restraint, i.e., the smaller the L/D, the greater the effect of restraint. This effect of

Section 3, it was shown that the choice of the crack morphology parameters can have a significant impact (factor of 2) on the postulated leakage crack size. This finding is supported by findings from a recent paper by Rudland, et. al. (Ref. 2.8). This effect, along with the effect of actual margins currently under discussion, have by far the greatest impact on LBB of any of the issues raised in recent years.

restraint can thus be expected to be biggest for applications where the pipe diameter is small and the restraint length is short or close to a terminal end.

Two separate analyses were developed as part of this task. One was for the case where the restraint was fairly symmetric, i.e., the restraint lengths on either side of the section under consideration were about the same, i.e., $L_1/D = L_2/D$. Practically speaking, there are not many applications where this occurs. The more common application is where the restraint is asymmetric, and the two restraint lengths on each side of the section under consideration are not the same, i.e., $L_1/D < L_2/D$. For this set of conditions, an entirely different set of equations was developed for predicting the r_{COD} value than for the symmetric case. However, the set of equations developed for the asymmetric case were only developed for a single set of pipe R/t ratios, i.e., R/t = 10. The symmetric equations that were developed were independent of R/t.

Furthermore, as part of this effort, it was shown that the restraint length was a function of the stiffness ($k = M/\theta$) of the piping system at the location under consideration. An empirical analysis was developed where the restraint length was related to the pipe stiffness through a constant (C), which is a function of the second moment of inertia (I) of the pipe cross section. Unfortunately, this empirical relationship was only valid for pipes with moments of inertia greater than 10^{-4} m^4 (240 $inch^4$), which equates to pipes 10-inch diameter, Schedule 80 and greater.

In order to assess the magnitude of this effect on applications of potential interest from an LBB perspective, a finite element model of a three-loop Westinghouse primary piping system was analyzed. The model included the hot leg, cold leg, cross-over leg, surge line, and one of the safety-injection systems, as well as the major hardware components associated with this system, e.g., reactor pressure vessel, steam generator, reactor coolant pump, and pressurizer. Analyses were conducted at 18 potentially LBB sensitive locations along the various piping systems. The location thought to be of possible greatest concern was where the surge line joined to the pressurizer, because it involves relatively small diameter pipe (14-inch versus approximately 30-inch) and high restraint. From an ANSYS finite element analysis of the piping system, it was found that the short restraint length (L_1/D) was 0.14, i.e., 14 percent of the pipe diameter, indicative of a highly restrained location. However, due to the length and relative flexibility of the surge line, the long restraint length was 29 times the pipe diameter ($L_2/D = 29$).

To see the effect of this restraint condition on an LBB evaluation, one must first calculate the COD and crack length for the case of an unrestrained pipe. Using the Windows® version of SQUIRT (Version 1.1) and assuming crack morphology parameters for an IGSCC crack, one can estimate the crack length and COD for the unrestrained case using the loads and thermo-hydraulic conditions for normal operations, and the prescribed leakage detection capability of the plant under consideration, in this case 1.9 lpm (0.5 gpm). The resultant leakage crack size was found to be on the order of 20 percent of the pipe circumference. Using the equations developed as part of this effort for the asymmetric case (even though the R/t ratio for this application is closer to 5 than 10), one sees that the effect of restraint on the crack-opening displacement, and thus the corresponding postulated leakage crack length, is less than 1 percent. (If the longer restraint length had been closer to 5 times the pipe diameter than 29 times, then the effect would have been on the order of 20 to 25 percent.) Thus, this

analysis (even though it may not be technically valid due to R/t constraints) tends to show that piping systems of this size and flexibility are probably not significantly impacted by the effect of restraint of pressure-induced bending. If one wanted to consider a smaller diameter piping system, such as a 6-inch diameter safety injection system (SIS) line, with an associated longer normalized leakage crack length, then this effect may be more pronounced, but to do so would violate the relationship between restraint length (L/D) and pipe stiffness (k) developed as part of this effort. Some other means of quantifying the restraint lengths to use in this analysis would have to be developed.

The bottom line is that unless the piping system is very small diameter (such that the leakage crack length is a large percent of the pipe circumference), this effect is probably a second order effect at best, and can probably be safely ignored. To apply it to smaller diameter pipe, where the effect may be more pronounced, additional effort is required to develop the appropriate relationship to define the restraint lengths.

2.1.4 Effect of Weld Residual Stresses on COD Predictions for LBB Evaluations

If cracks develop in and around welds, as is most often the case, weld-induced residual stresses in and around the girth weld may cause the crack to be closed (or to be open less than anticipated) even though traditional COD analyses would suggest otherwise. Earlier studies have shown that pipe welding produces high residual stresses with a sharp stress gradient through the thickness (Ref. 2.10). For thicker pipe, this stress gradient is typically tension-compression-tension through the thickness. For thinner wall pipe, this stress gradient is typically tension to compression through the thickness from the inside surface out. Thus, for thinner pipe these weld residual stresses tend to open the crack on the inside surface and close the crack on the outside surface. As a result of these through thickness stress gradients, the crack-opening displacements are effectively less than what one would predict based on traditional COD analyses methods, such as those developed at General Electric for the Electric Power Research Institute, i.e., the GE/EPRI method (Ref. 2.11). As a result of the smaller effective COD (at least on the outside surface), the crack length for a prescribed leak-rate detection capability will be longer than predicted based on thermal hydraulic models, such as SQUIRT (Ref. 2.12) or PICEP (Ref. 2.13). This longer postulated through-wall-crack length reduces the actual margin if the effects of the weld residual stresses are not properly considered.

As part of this effort, correction factors to the GE/EPRI equations to account for the effects of the weld residual stresses on the crack-opening displacements were developed. (Details of this development process are presented in Appendix H.) The basic GE/EPRI expression for COD, as shown in Equation 2.6, specifies that the crack-opening displacement (δ) is a function of the applied remote stress (σ^{∞}), the half crack length (a), and a non-dimensional function from the GE/EPRI methodology (V_1), which is a function of the normalized crack depth (a/t) and the R/t ratio of the pipe.

$$\delta = \frac{4\sigma^{\infty} a}{E} V_1\left(\frac{a}{t}, \frac{R}{t}\right) \qquad (2.6)$$

Analyses undertaken as part of Task 9 of the BINP program showed that there is a critical stress ($\sigma^{\infty}_{critical}$) that is a function of the normalized crack depth (a/t), R/t ratio of the pipe, and wall thickness of the pipe (t). If the remote applied stress (σ^{∞}) was below this critical stress value, then the crack on

the outside surface of the pipe would remain closed. Values for these critical stress values for tension and bending loading are provided in Tables 2.1 and 2.2. (The shaded areas in Table 2.1 represent those cases where the crack would be predicted to be closed at the normal operating pressure of a pressurized water reactor (PWR), 15.5 MPa (2,250 psi).) If the remote applied stress was above this critical stress value, then the COD, corrected for weld residual stress effects, was found to be a function of the basic GE/EPRI value, corrected by a slope term, C, and an intercept term I, that are functions of a/t, R/t, and t, see Equation 2.7.

$$\delta = \frac{4\sigma^{\infty} a}{E} V_1\left(\frac{a}{t},\frac{R}{t}\right) C\left(\frac{a}{t},\frac{R}{t},t\right) + aI\left(\frac{a}{t},\frac{R}{t},t\right) \tag{2.7}$$

Figure 2.3 shows a comparison plot of the basic GE/EPRI COD values with the weld residual stress corrected values for the case of a quarter circumference long through-wall crack ($\theta = \pi/4$), R/t ratio of 10, and pipe wall thickness of 15.0 mm 0.59 inches) for remote tensile loading. As evident in Figure 2.3, two separate intercept terms, I, are needed, one for the inside pipe surface and one for the outside pipe surface. Tabulated values for C for remote tension and bending (C_T and C_B) and I for both the inside and outside pipe surfaces (I_{OD} and I_{ID}) are provided in Tables 2.3 through 2.6. Certain thermal hydraulics models, like SQUIRT, allow the user to input COD values for both the inside and outside pipe surface. Values for the basic GE/EPRI V_1 functions for tension and bending are provided in Reference 2.11 and Table 2.7.

Table 2.1 Critical values of remote axial tension membrane stress that need to be exceeded to allow for crack opening with weld residual stress*

		Critical Remote Tension Stress, MPa (ksi)			
		Thickness mm, (in.)			
R / t	θ/π	7.5 (0.295)	15.0 (0.59)	22.5 (0.886)	30.0 (1.181)
5	1/16	133.0, (19.3)	105.0, (15.2)	44.0, (6.39)	31.5, (4.56)
5	1/8	134.6, (19.5)	48.5, (7.03)	25.0, (3.63)	20.6, (2.99)
5	1/4	83.7, (12.1)	28.7, (4.17)	14.7, (2.14)	10.8, (1.57)
5	1/2	21.2, (3.7)	9.61, (1.39)	3.98, (0.58)	0.00
10	1/16	84.7, (12.3)	35.7, (5.17)	22.0, (3.18)	13.0, (1.89)
10	1/8	52.5, (7.62)	24.7, (3.58)	13.4, (1.94)	9.45, (1.37)
10	1/4	33.4, (4.85)	16.7, (2.42)	8.65, (1.25)	5.06, (0.73)
10	1/2	11.3, (1.64)	4.50, (0.65)	2.42, (0.35)	0.00
20	1/16	28.7, (4.16)	6.54, (0.45)	9.35, (1.36)	5.29, (0.77)
20	1/8	21.7, (3.15)	3.82, (0.55)	5.78, (0.84)	0.43, (0.06)
20	1/4	16.1, (2.33)	2.08, (0.30)	3.50, (0.51)	2.18, (0.32)
20	1/2	4.83, (0.70)	0.65, (0.09)	1.00, (0.15)	0.00

*Grayed cells indicate that the crack would remain closed at at an operating pressure of 15.5 MPa (2,250 psi)

Table 2.2 Critical values of remote bending stresses ($\sigma_B^{\infty}{}_{Critical}$) for moment loading

		Critical Remote Bending Stress, MPa (ksi)			
		Thickness mm, (in.)			
R / t	θ/π	7.5, (0.295)	15.0, (0.59)	22.5, (0.886)	30.0, (1.181)
5	1/16	231.4, (33.6)	127.6, (18.5)	44.5, (6.45)	36.3, (5.26)
5	1/8	191.0, (27.7)	54.9, (7.96)	29.2, (4.23)	23.8, (3.45)
5	1/4	77.2, (11.2)	57.8, (8.39)	19.9, (2.89)	14.6, (2.12)
5	1/2	41.3, (5.99)	26.8, (3.88)	8.62, (1.25)	2.57, (0.37)
10	1/16	96.3, (14.0)	37.6, (5.45)	23.0 (3.34)	13.9, (2.02)
10	1/8	51.6, (7.49)	25.5, (3.70)	14.2, (2.06)	9.93, (1.44)
10	1/4	54.3, (7.88)	20.3, (2.94)	10.3, (1.50)	6.42, (0.93)
10	1/2	31.8, (4.60)	10.8, (1.57)	5.36, (0.78)	2.43, (0.35)
20	1/16	31.7, (4.60)	12.9, (1.87)	9.45, (1.37)	5.72, (0.83)
20	1/8	24.0, (3.48)	9.65, (1.40)	6.00, (0.87)	4.85, (0.70)
20	1/4	22.7, (3.29)	7.58, (1.10)	4.46, (0.65)	3.63, (0.53)
20	1/2	17.6, (2.55)	5.51, (0.80)	3.12, (0.45)	2.83, (0.41)

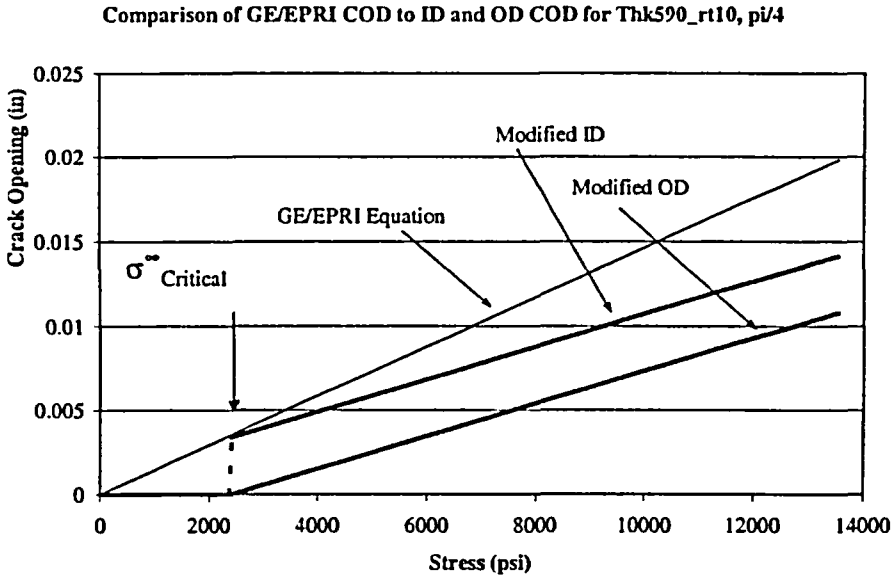

Figure 2.3 GE/EPRI tension equation modification for the case of θ= π/4 R/t = 10, and 15 mm (0.59 each) thick pipe

Table 2.3 C_T values for tension loading

		Thickness, mm (inch)			
		7.5 (0.295)	15.0 (0.59)	22.5 (0.886)	30.0 (1.181)
R/t	θ/π	C_T			
5	1/16	0.869	1.007	0.789	0.813
5	1/8	0.906	0.959	0.861	0.899
5	1/4	0.731	0.744	0.722	0.726
5	1/2	0.852	0.862	0.827	0.868
10	1/16	0.883	0.769	0.806	0.817
10	1/8	0.918	0.825	0.803	0.847
10	1/4	0.650	0.651	0.617	0.661
10	1/2	0.762	0.758	0.709	0.767
20	1/16	0.786	1.517	0.769	0.801
20	1/8	0.766	1.795	0.720	0.765
20	1/4	0.572	1.526	0.515	0.587
20	1/2	0.806	1.524	0.638	0.810

Table 2.4 C_B values for moment loading

		Thickness, mm (inch)			
		7.5 (0.295)	15.0 (0.59)	22.5 (0.886)	30.0 (1.181)
R/t	θ/π	C_B			
5	1/16	0.397	0.711	0.586	0.608
5	1/8	0.874	0.672	0.662	0.676
5	1/4	0.480	0.574	0.549	0.573
5	1/2	0.369	0.446	0.410	0.441
10	1/16	0.699	0.706	0.651	0.695
10	1/8	0.641	0.703	0.660	0.686
10	1/4	0.501	0.541	0.489	0.520
10	1/2	0.258	0.276	0.253	0.266
20	1/16	0.763	0.758	0.749	0.776
20	1/8	0.677	0.700	0.661	0.698
20	1/4	0.376	0.384	0.355	0.382
20	1/2	0.105	0.106	0.101	0.105

Table 2.5 I_{OD} values

		Thickness, mm (inch)			
		7.5 (0.295)	15.0 (0.59)	22.5 (0.886)	30.0 (1.181)
R/t	θ/π	I_{OD}			
5	1/16	-0.00256	-0.00240	-0.00074	0.00038
5	1/8	-0.00288	-0.00119	-0.00053	0.00049
5	1/4	-0.00271	-0.00086	-0.00040	0.00050
5	1/2	-0.00295	-0.00112	-0.00042	0.00055
10	1/16	-0.00172	-0.00060	-0.00037	0.00019
10	1/8	-0.00132	-0.00055	-0.00028	0.00026
10	1/4	-0.00103	-0.00051	-0.00024	0.00027
10	1/2	-0.00147	-0.00058	-0.00028	0.00033
20	1/16	-0.00051	-0.00022	-0.00016	0.00009
20	1/8	-0.00051	-0.00021	-0.00012	0.00012
20	1/4	-0.00055	-0.00019	-0.00010	0.00014
20	1/2	-0.00086	-0.00024	-0.00013	0.00021

Table 2.6 I_{ID} values

		Thickness, mm (inch)			
		7.5 (0.295)	15.0 (0.59)	22.5 (0.886)	30.0 (1.186)
R/t	θ/π	I_{ID}			
5	1/16	0.00214	0.00016	0.00028	-0.00050
5	1/8	0.00207	0.00082	0.00039	-0.00038
5	1/4	0.00139	0.00073	0.00027	-0.00025
5	1/2	-0.00012	-0.00001	0.00001	0.00004
10	1/16	0.00071	0.00019	0.00020	-0.00022
10	1/8	0.00082	0.00029	0.00026	-0.00019
10	1/4	0.00076	0.00022	0.00018	-0.00013
10	1/2	-0.00014	-0.00004	0.00001	0.00002
20	1/16	0.00033	0.00004	0.00007	-0.00009
20	1/8	0.00038	0.00008	0.00009	-0.00009
20	1/4	0.00028	0.00007	0.00007	-0.00007
20	1/2	-0.00017	-0.00003	-0.00001	0.00004

Table 2.7 V_1 values for bending from Tables 4.3 and 4.8 of Reference 2.14

R/t	θ/π			
	1/16	1/8	1/4	1/2
5	1.234	1.388	2.008	5.331
10	1.206	1.480	2.379	7.165
20	1.111	1.482	3.079	11.585

For the combined load case of tension plus bending, the expression in Equation 2.8 should be used. For the COD on the outside surface (δ_{OD}), the outside surface intercept value (I_{OD}) is used. For the COD on the inside surface (δ_{ID}), the inside surface intercept value (I_{ID}) is used.

$$\delta_{OD,ID} = \frac{4a}{E}\left[\sigma_T V_T\left(\frac{a}{t},\frac{R}{t}\right)C_T\left(\frac{a}{t},\frac{R}{t}\right)+\sigma_B V_B\left(\frac{a}{t},\frac{R}{t}\right)C_B\left(\frac{a}{t},\frac{R}{t}\right)\right]+aI_{OD,ID}\left(\frac{a}{t},\frac{R}{t},t\right) \qquad (2.8)$$

The end result of this work is a more robust crack-opening displacement analysis that accounts for the effects that weld residual stresses have on the COD, and in turn the postulated through-wall-crack length. Ignoring this effect will lead to a nonconservative assessment of the length of the postulated through-wall crack, and thus a nonconservative LBB assessment. A quantitative assessment of the impact of this effect will be made in Section 3 of this report when a series of example problems are presented.

At this time, this modified-COD analysis that accounts for weld residual stresses has been incorporated into a new version of the SQUIRT code. The incorporation of this modified methodology was made as part of a separate ongoing US NRC sponsored program at Battelle and Emc[2]. In the SQUIRT4 module[4] of this new version of SQUIRT, the user has the option of either using the original GE/EPRI COD expressions or the revised expressions for COD that account for weld residual stresses.

In addition to developing these correction factors to account for the effects of weld residual stresses on the COD values for uniform welds (nominally the same residual stress field around the entire pipe circumference), the effect of weld starts and weld stops on the COD values was examined. From 3-dimensional finite element analyses, the key finding from this effort was that the cracks in the vicinity of the start-stop are more open than those placed 180 degrees away from the start-stop region, where the effects of start-stops should be the smallest. As a result, ignoring the effects of start-stops will lead to a conservative estimate of the postulated through-wall-crack length from an LBB perspective. This is because the postulated through-wall-crack length is back-calculated from an assumed crack-opening area for a prescribed leak rate. This area is based on the COD and the crack

[4] The SQUIRT4 module is the module that allows for the determination of a postulated through-wall-crack length for a prescribed leak rate for a given set of load and pipe geometry/material conditions.

length. Thus, if the crack is more open in the region of the start-stop than would be predicted by ignoring the start-stop effects, then the postulated through-wall-crack length would actually be shorter in the start-stop region than would be predicted from an analysis that ignores the start-stop effects. Thus, ignoring the start-stop effects would be conservative. Of note is that only one pipe geometry and size was evaluated in this analysis. Therefore, the results should be viewed more qualitatively than quantitatively. A range of pipe sizes and radius-to-thickness ratios should be studied to obtain a better understanding of the start-stop effects for a wider range of situations.

2.1.5 Development of a J-estimation Scheme for Through-wall Cracks in Elbows that could be used in the Stability Analysis of a LBB Evaluation

In the past, leak-before-break (LBB) assessments of piping systems have typically not specifically addressed the issue of pipe fittings, such as elbows and tee joints. One reason is the lack of a predictive COD analysis or a fracture stability criterion for through-wall cracks in such geometries. Most of the available COD and fracture stability criteria are for cracks in straight pipe. In the past, if one wanted to consider a crack in an elbow, about the only means available was finite element analyses. As part of the Second IPIRG program, a surface-crack J-estimation scheme for elbows was developed (Ref. 2.15). This methodology used simple influence functions, based on ASME Section III stress indices, along with existing straight-pipe solutions, to predict the fracture response of a surface-cracked elbow. The use of these stress indices, along with existing straight-pipe J-estimation methods, showed promise in predicting the fracture response of surface-cracked elbows.

However, in order to make an LBB assessment of an elbow (or other pipe fitting), a through-wall-crack solution is needed. As part of Task 8 of the BINP program, such an estimation scheme was developed. (See Appendix F for the details of this development process.) Both axial flank cracks and circumferential cracks along the intrados and extrados were considered. Solutions were compiled for pure pressure, pure bending, and combined pressure and bending. Ultimately, it was hoped that this estimation scheme could be used to validate a methodology in which simple influence functions, such as the ASME stress indices, could be used in conjunction with straight-pipe through-wall-crack solutions to predict the crack-opening displacement and the fracture behavior of cracked elbows.

Elastic-plastic estimation schemes used to estimate either the crack-opening displacements (δ) or the crack-driving force (using the J-integral parameter) are based on the concept of proportional loading. If a cracked body is loaded in a proportional manner, such that the constitutive response is adequately modeled via deformation theory plasticity, then Illyushin has shown that the deformations, stresses, and energies (e.g., J-integral) are proportional to a load parameter, material parameters, and geometric quantities.

The estimation of J is typically written as:

$$J = J^e + J^p \qquad (2.9)$$

where,

J = total estimated value of J,
J^e = the elastic component of J, and
J^p = the plastic component of J.

In the past, it has been observed that developing elastic-plastic estimation schemes using the separate elastic and plastic com-

ponents provides a reasonable estimate for engineering purposes. Typically, the constitutive material response is assumed to follow the Ramberg-Osgood relationship where,

$$\frac{\varepsilon}{\varepsilon_0} = \frac{\sigma}{\sigma_0} + \alpha\left(\frac{\sigma}{\sigma_0}\right)^n \qquad (2.10)$$

where,

σ_0 = the reference stress,
ϵ_0 = the reference strain (σ_0/E),
n = the strain hardening exponent, and
α = a material constant.

The estimation scheme for crack-opening displacement (δ) is written as:

$$\delta_T = \delta_e + \delta_p \qquad (2.11)$$

where,

δ_T = total crack-opening displacement,
δ_e = elastic component of the crack-opening displacement, and
δ_p = plastic component of the crack-opening displacement.

The elbow analysis was developed following this basic approach and was structured in the motif of the GE/EPRI J-estimation scheme analysis for through-wall cracks in straight pipe. A series of influence functions based on curve-fit analyses of finite element results were developed. These functions are tabulated in Appendix F. These influence functions (F-functions for the elastic component of J, V_1 for the elastic component of COD, h_1 for the plastic component of J, and h_2 for the plastic component of COD), are functions of the crack geometry, crack size, R/t ratio, strain-hardening exponent (n), and applied load. With these functions, the elastic and plastic components of J and COD can be readily calculated using a series of algebraic expressions, i.e.,

$$J^e = J_T^e + J_B^e = \frac{\left(F_T\sigma_T\sqrt{\pi a}\right)^2}{E} + \frac{\left(F_B\sigma_B\sqrt{\pi a}\right)^2}{E} \qquad (2.12)$$

$$\delta_e = \delta_T^e + \delta_B^e = \frac{4\sigma_T a}{E}V_1(t) + \frac{4\sigma_B a}{E}V_1(B) \qquad (2.13)$$

$$J^p = \alpha\sigma_0\varepsilon_0 a(1-\theta/\pi)h_1\left(P/P_0'\right)^{n+1} \qquad (2.14)$$

$$\delta^p = \alpha\varepsilon_0 a h_2\left(P/P_0'\right)^n \qquad (2.15)$$

The subscripts T and B in Equations 2.12 and 2.13 refer to the contribution to J and COD from the tension and bending loads, respectively.

As part of this effort a limited number of finite element solutions were developed and a J-estimation scheme with h-function fits through these solutions was derived. However, the complexity of this methodology and the limited scope of solutions developed limited the applicability of this approach. As such, it was desirable to see if a simplified solution based on the ASME stress indices could be developed from these basic results that would be applicable over a wider range of through-wall cracks in elbows. The goal was to see if this simplified approach could be crafted in the motif of the simplified surface-crack solution developed for surface cracks in elbows as part of the Second IPIRG program (Ref. 2.15). This involved comparing the elbow results to those for a circumferential through-wall crack in a straight pipe of the same dimensions and with the same material properties. The straight-pipe J-estimation schemes considered were the GE/EPRI method (Ref. 2.11) and the LBB.ENG2 method (Ref. 2.14).

From Reference 2.15 it was found that for surface cracks that the ratio of the straight pipe to elbow moment values at the same J value was constant as the J value increased for applied J values generally greater than 100 kJ/m^2 (570 in-lbs/in^2), which is near the lower bound of the toughness range for most nuclear piping materials, except perhaps some aged cast stainless steels. In Reference 2.15, these constant ratios of straight pipe to elbow moment values were plotted against the ASME Section III stress indices for elbows, e.g., the B_2[5] stress index for primary bending. What was found was that the M_{pipe}/M_{elbow} values increased in a linear fashion with B_2, but were generally less than B_2, i.e.,

$$M_{pipe}/M_{elbow} < B_2 \qquad (2.16)$$

Consequently, a conservative assessment of the moment-carrying capacity of a surface-cracked elbow could be made by dividing the straight-pipe solution (e.g., SC.TNP1 solution) by the ASME B_2 stress index.

A similar analysis approach was followed for though-wall-cracked elbows. As part of this analysis, it was found that for circumferential through-wall cracks in elbows, the ratio M_{pipe}/M_{elbow} was essentially 1.0, independent of the B_2 stress index, see Figure 2.4. What this implies is that one can use a straight-pipe solution (either GE/EPRI or LBB.ENG2) to predict the fracture stability behavior (moment-carrying capacity) of a circumferential through-wall crack in an elbow. For axial flank cracks, the ratio of M_{pipe} to M_{elbow} increased as the stress index B_2 increased, but was generally less than B_2, see Figure 2.5. Consequently, a conservative approach would be to use the straight-pipe solution, but divide the straight-pipe moment solution (from either GE/EPRI or LBB.ENG2) by the elbow B_2 index in order to predict the moment capacity of an axial crack along the flank of an elbow. This approach for predicting the fracture behavior of through-wall-cracked elbows could be readily incorporated into the new Regulatory Guide for LBB the NRC is currently formulating.

To make an assessment of crack-opening displacements (COD), however, one must rely more on the full J-estimation scheme as outlined in Appendix F. No such assessment for COD was made in this effort. Caution should be used in trying to apply this same approach for the COD values in that the COD should be for elastic loading where the constant moment ratio that occurs under plastic loading does not exist. It should be noted that some linear-elastic fracture mechanics (LEFM) COD solutions do exist in the open literature (Ref. 2.16).

2.2 Implications of Results on In-Service Flaw Evaluations

A number of the technical tasks conducted as part of this program had implications with regards to in-service flaw evaluations. These included:

- Task 1 – Role of Secondary Stresses on Pipe Fracture
- Task 3 – Assessment of Actual Margins in a Plant Piping Analyses
- Task 7 – Development of Flaw Evaluation Criteria for Class 2, 3, and Balance of Plant (BOP) Piping

In the sections that follow each of these effects will be discussed separately.

---

[5] Article NB-3683.7 of Section III of the ASME Code defines the B_2 stress index for an elbow as

$B_2 = 1.3h^{2/3}$; $B_2 \geq 1.0$

where,

$h = tR_{el}/R_m^2$,
t = wall thickness,
R_{el} = radius of curvature of the elbow, and
R_m = mean radius of the elbow cross section.

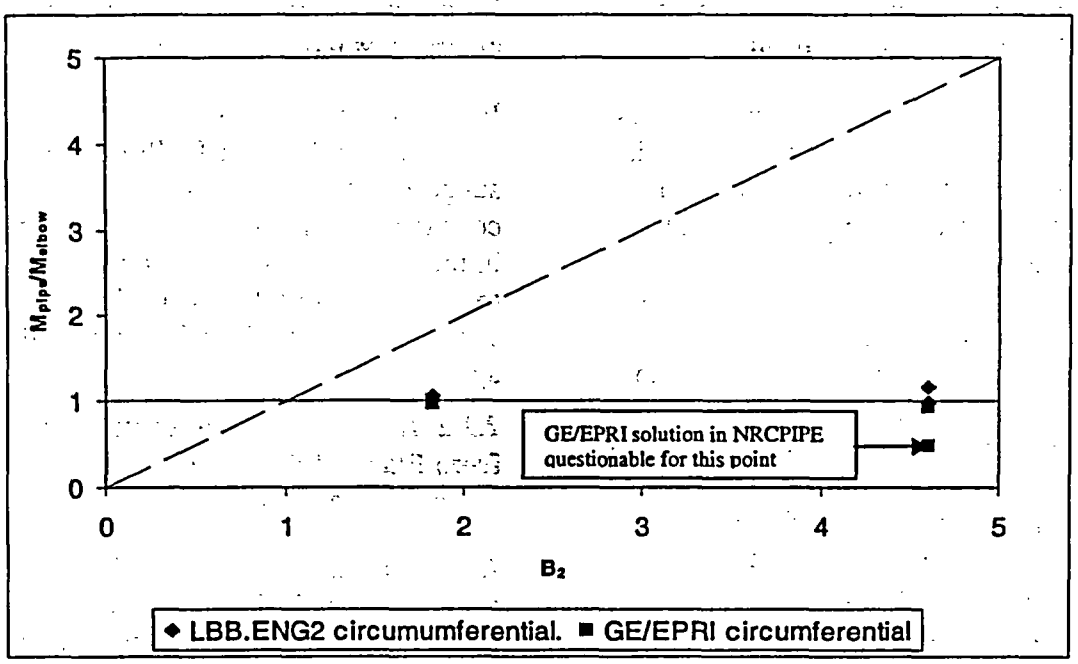

Figure 2.4 Ratio of circumferentially through-wall-cracked pipe-to-elbow moments for constant applied J values versus the ASME B_2 stress index for the elbow

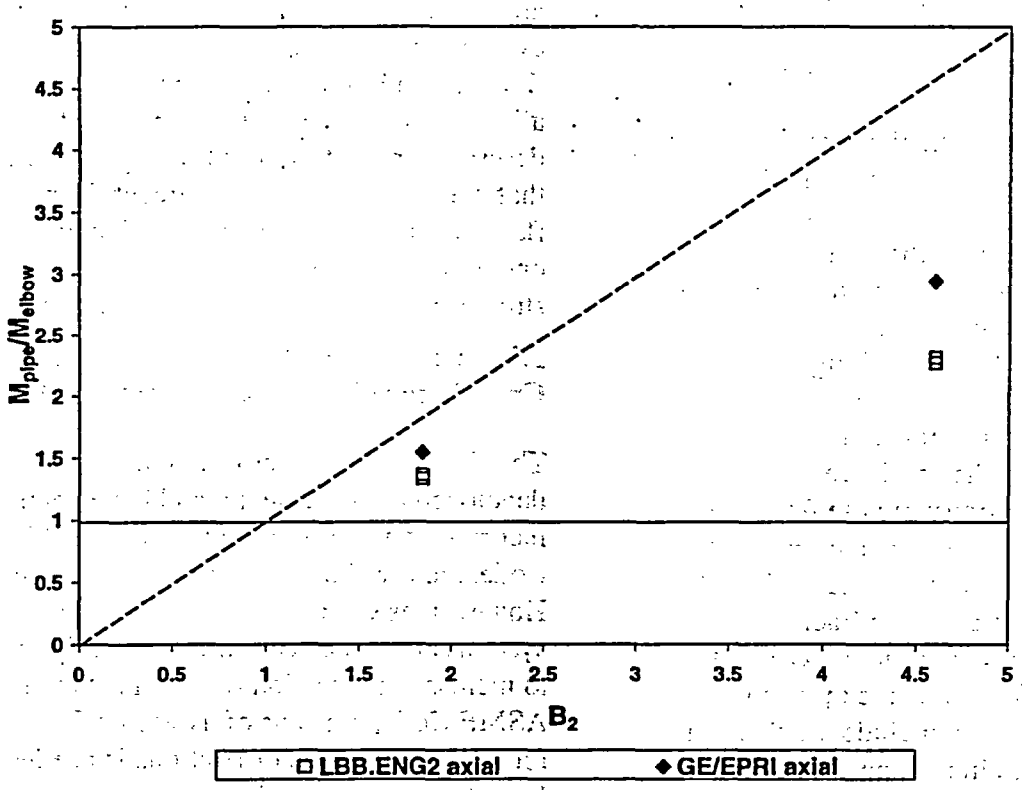

Figure 2.5 Ratio of axially through-wall-cracked pipe-to-elbow moments for constant applied J values versus the ASME B_2 stress index for the elbow

2.2.1 Role of Secondary Stresses on In-Service Flaw Evaluation Procedures

The issue of how to treat secondary stresses for in-service flaw evaluation procedures is the same as for leak-before-break (LBB) analyses. Currently existing experimental data indicate that global secondary stresses (i.e., displacement-induced stresses), such as thermal expansion and seismic anchor-motion stresses, contribute just as much to pipe fracture as do primary membrane and bending stresses. There is the question as to whether this statement is universally true, i.e., does it apply to the case where the neighboring uncracked pipe is plastically deformed. If such is the case, then some would argue that these displacement-induced secondary stresses may not play as significant a role in the fracture process as the primary membrane and bending stresses. Some have suggested, in cases such as this, that the displacement-induced secondary stresses should be combined with the primary stresses in some nonlinear fashion.

Such may have been the thought process of the authors of the ASME Section XI flaw evaluation criteria for Class 1 piping. Essentially they ignore thermal expansion type stresses altogether in both Appendix C for austenitic piping and Appendix H for ferritic piping for the case of higher toughness materials where limit-load conditions exist. For these conditions, the stresses necessary to drive the crack are probably sufficient that plasticity remote from the crack section may be extensive. For lower toughness materials (such as SMAW and SAW), where elastic-plastic fracture mechanics (EPFM) conditions exist and plasticity away from the crack plane is probably limited, they include the thermal expansion stresses in the applied stress term, but only with a safety factor of 1.0. For the primary membrane and bending stresses, they include the full safety factors of 2.77 for normal operating conditions and 1.39 for emergency and faulted conditions.

In light of the fact that the results from this program and the prior IPIRG programs suggest that secondary stresses be considered with more vigor than they have in the past, one means of doing so would be to have the safety factor for thermal expansion stresses be a function of the applied stress level.

2.2.2 Impact of Using Actual Margins from Plant Piping Analyses for In-Service Flaw Evaluations

As was the case for LBB applications, using a nonlinear analysis instead of an elastic analysis to define the stresses in the piping system can have a significant effect on the allowable flaw size from an in-service flaw evaluation perspective. The additional margins on moment from the LBB perspective are equally available in an in-service flaw evaluation. These additional margins can then in turn have a significant effect on the allowable flaw size. An example test case described in Section 3 of this report showed that one could allow a 60 percent deeper flaw to exist (for the same flaw length) when one used a nonlinear analysis to define the stresses instead of a linear elastic analysis.

2.2.3 Development of Flaw Evaluation Criteria for Class 2, 3, and BOP Piping

The flaw-evaluation criteria that have been developed over the years, and have been incorporated in Section XI of the ASME Code, are for Class 1 piping systems only. However, as Class 2, 3, and BOP piping systems are inspected more frequently due to increased inspection requirements in the ASME Code, a means of assessing flaws found through these inspections is needed. In addition, as plants age, flaws are more likely to become a potential problem. It is also of note that some Class 2, 3, and BOP

piping systems may be more important than their Class 1 counterparts relative to plant risk analyses from a core-damage frequency perspective.

As such, the objective of Task 7 was to develop data and analysis procedures in support of establishing flaw evaluation procedures for Class 2, 3, and BOP piping. (For a more detailed description of this development effort, the reader is referred to Appendix E.) This initial development of a technical basis for a flaw evaluation criteria for Class 2, 3, and BOP piping addressed two main issues not particularly relevant to Class 1 piping. One is the fact that Class 2, 3, and BOP piping systems typically operate at lower operating pressures, and as such are often fabricated from pipe with higher R/t ratios than those used in Class 1 piping systems. The second is the fact that these piping systems often operate at lower temperatures than the Class 1 systems, and as such, may be susceptible to transition temperature effects if fabricated from ferritic pipe.

2.2.3.1 Effect of R/t Ratios on the Fracture Behavior of Class 2, 3, and BOP Piping

As part of this effort, the effect of the pipe R/t ratio on the fracture behavior of Class 2, 3, and BOP piping in both the linear elastic (LEFM) regime as well as the elastic-plastic (EPFM) regime was investigated. In addition, previously it was shown that the R/t ratio had an effect on the load-carrying capacity of cracked pipe under limit-load conditions (Ref. 2.5 and 2.17). Figure 2.6 shows a plot of the ratio of the experimental stress to the predicted Net-Section-Collapse (Ref. 2.18) stress (NSC) as a function of R/t ratio for a series of experiments that were predicted to fail under limit-load conditions based on the Dimensionless-Plastic-Zone-Parameter (DPZP) screening criterion (Ref. 2.19). As can be seen from Figure 2.6, the higher the R/t ratio, the lower the experimental stress when compared with the predicted limit-load stress, i.e., NSC stress. It has been hypothesized that this reduction in load-carrying capacity stems from the pipe cross section ovalizing more for the thinner, higher R/t ratio pipes. As part of this program, additional data were to have been generated for a pipe section with a higher R/t ratio than those in Figure 2.6. However, preliminary analysis suggested that to conduct such an experiment would require a significant internal pipe pressure be simultaneously applied with the bending moment to preclude the pipe section from buckling on the compressive side of the pipe. This internal pipe pressure would not only minimize the potential for buckling, but it would also limit the amount of ovalization occurring, thus complicating any post-test analysis through the addition of another variable in the analysis, i.e., pressure. As such it was decided to forego the conduct of the one planned high R/t ratio, limit-load pipe experiment and to redirect the resources from that effort to other related efforts in this flaw-evaluation criteria development process. In the sections that follow, the effect of R/t ratio on the elastic F-functions and elastic-plastic J-estimation scheme analyses will be presented.

Effect of R/t Ratio on the Elastic F-functions – As part of this effort, the fracture behavior of flawed piping operating in the linear-elastic fracture mechanics (LEFM) regime was investigated. The crack-driving force under LEFM conditions is typically expressed in terms of the stress intensity factor (K), where the expression for K is:

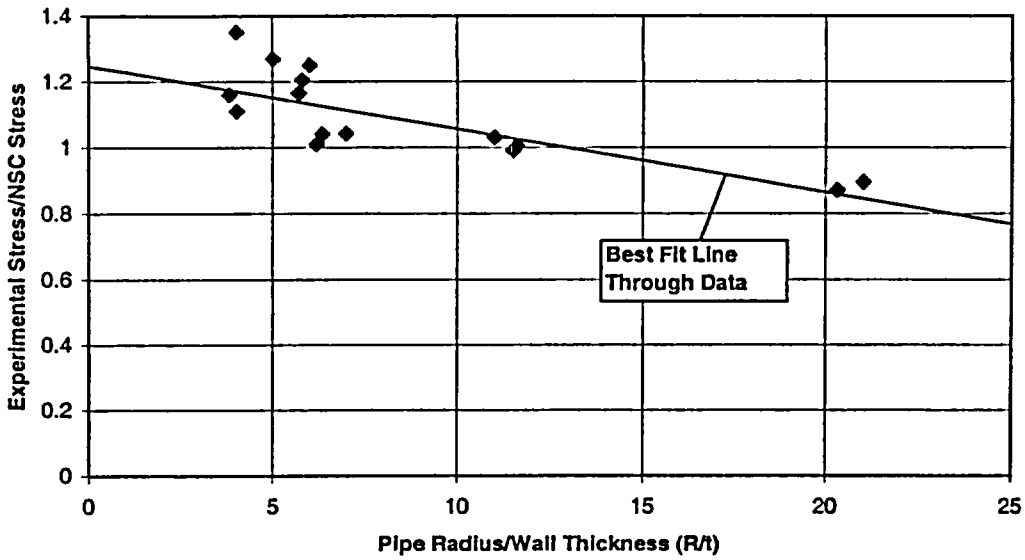

Figure 2.6 Plot of the ratio of the experimental stress to the predicted NSC stress as a function of pipe R/t ratio for pipes expected to fail under limit-load conditions

$$K = F\sigma\sqrt{\pi a} \qquad (2.17)$$

where,

K = stress intensity factor,
F = elastic F-function
σ = remote applied stress, and
a = crack size.

Currently, for Class 1 ferritic piping, Section XI, Appendix H limits the applicability of the F-functions they report to pipes with R/t ratios of less than 15. While this limitation is acceptable for Class 1 ferritic piping, it is much too restrictive for Class 2, 3, and BOP piping, which typically are fabricated from thinner wall pipes with much larger R/t ratios. In order to address this limitation, researchers working for The Materials Property Council (MPC) in the United States (Ref. 2.20) and researchers at CEA in France (Ref. 2.21) have developed an extensive database of numerical solutions for F using the finite element method for a variety of pipe and circumferential surface flaw geometries (flaw depth (a/t) and flaw length [c/a or θ/π]), pipe R/t ratios, and crack locations and loading conditions (i.e., internal flaw loaded in tension, internal flaw loaded in bending, external flaw loaded in tension, and external flaw loaded in bending). As part of this effort in the BINP program, these tabulated numerical results were curve fit to a series of mathematical expressions, with the goal of including these mathematical expressions into a code useable expression. The detailed mathematical expressions, with the applicable coefficients developed from the curve-fitting operations, are provided in Appendix E. Algebraic expressions of F as a function of flaw depth (a/t), flaw length (c/a or θ/π), and pipe R/t ratio were developed for internal and external circumferential flaws loaded in both tension and bending.

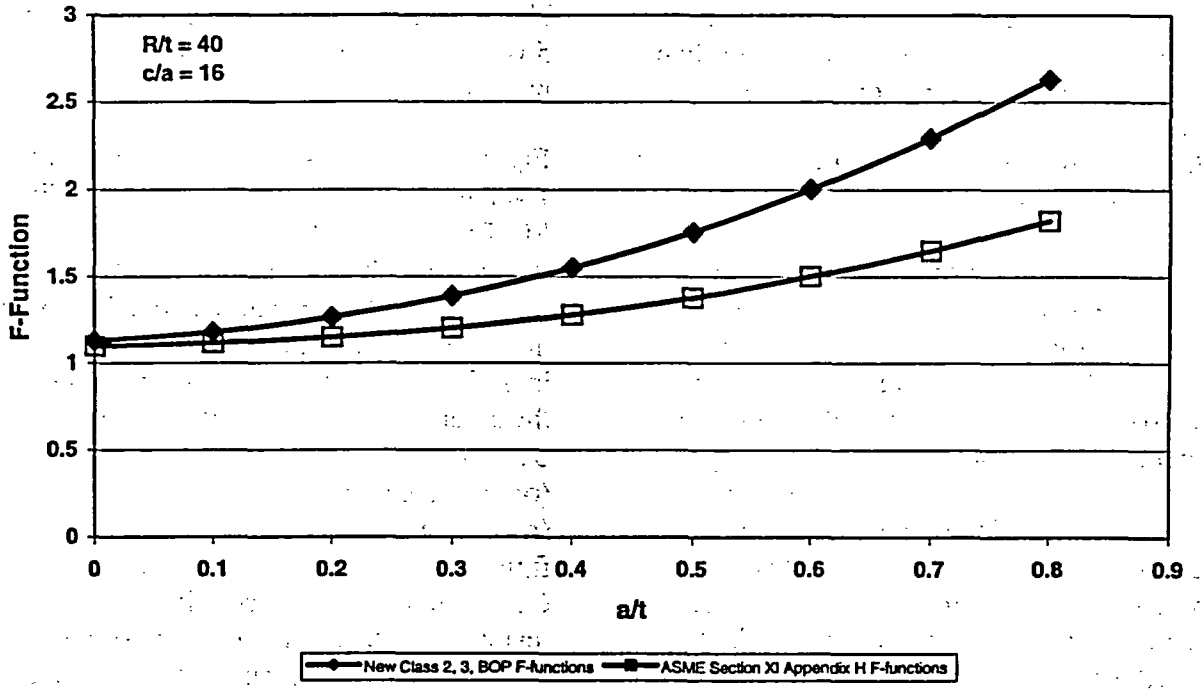

Figure 2.7 Comparison of new Class 2, 3, and BOP F-functions and F-functions in ASME Section XI Appendix H for a crack aspect ratio (c/a) of 16 and a pipe with an R/t ratio of 40 for internal circumferential cracks subject to pure bending.

Figure 2.7 shows a comparison between the existing ASME Section XI Appendix H F-functions and the newly developed F-functions from this effort as a function of crack depth for the case of an internal crack loaded in bending for a normalized crack length (c/a) of 16 and for a pipe with an R/t ratio of 40. As can be seen from this example, for the flaw depth less than the workmanship standards (a/t < ~0.1), the difference in the F-function is near zero, however, as the crack depth (a/t) increases, the difference becomes much more substantial. For a very deep crack (75 percent through the thickness), the difference is nearly 45 percent. Consequently using the existing F-functions in Section XI to predict the behavior of flaws in Class 2, 3, or BOP piping with much higher R/t ratios would result in a significant underprediction of the crack-driving force, resulting in a nonconservative in-service flaw-evaluation assessment, at least for this set of conditions.

Effect of R/t Ratio on Elastic-Plastic Fracture Mechanics (EPFM) J-estimation Scheme Analyses – This effort involved the development of analyses to evaluate circumferential surface flaws in nuclear pipe with pipe radius-to-thickness (R/t) ratios greater than 15 that operate in the EPFM regime. The effort used finite element analyses to assess the crack-driving force for higher R/t ratio pipe. This was done for internal circumferential surface-flawed pipe for pure bending or bending with a hoop stress equal to S_m for typical austenitic and ferritic pipe steels. These finite element results were then compared with existing J-estimation schemes available in the NRCPIPES computer code. The objective was to determine whether a correction factor could readily be applied to one of the estimation schemes currently available in NRCPIPES to obtain a

more accurate estimation of the applied J (i.e., crack driving force) versus moment behavior for higher values of R/t, rather than to develop a new J-estimation scheme procedure that would require a separate option to be programmed into the NRCPIPES code.

It was found that it was probably best to incorporate a correction factor into the SC.TNP methodology. SC.TNP already allows for the use of a weighting function (Lw) to obtain better agreement with finite element analyses for particular geometry and material inputs. Lw is the distance down the length of the pipe away from the crack plane where the stresses first equal the remote stress in the pipe, i.e., the effect of the crack on the stresses is diminished. A detailed matrix of analyses was conducted in which this correction factor (Lw = C1*t, where t is the pipe wall thickness) was systematically varied such that the J values from the estimation scheme were within 10 percent of the finite element results for the range of J_{Ic} values representative of nuclear grade piping materials. Regression analysis of the results from these analyses produced a relationship of the form shown in Equation 2.18.

$$C1 = a_1 * \exp^{-0.5 \cdot \left[\left(\frac{\frac{a}{t} - x_0}{b} \right)^2 + \left(\frac{\left(\frac{R_m}{t} - y_0 \right)}{c} \right)^2 \right]} \qquad (2.18)$$

The coefficients prescribed for Equation 2.18 (a_1, x_0, y_0, b, and c), which are provided in Table 2.8, were developed for the case where the strain-hardening exponent (n) was 5. Hence, Equation 2.18 using these coefficients is only valid for this case, n = 5. Additional analyses are being developed as part of another USNRC program being conducted at Battelle and Emc^2 where this expression and related coefficients are being updated to be applicable to a wider range of values of the strain-hardening exponent (n). Nevertheless, a strain-hardening exponent of 5 is typical of ferritic and austenitic base metals.

Figure 2.8 shows a comparison plot of the J versus moment results from the modified SC.TNP analysis (Lw = C1*t; open circles in figure) with FEA results (closed circles) for the case of a/t = 0.5, $\theta/\pi = 0.25$, no internal pipe pressure, and R/t = 40. Also included in Figure 2.8 for comparison are the J versus moment results from the SC.TNP1 (closed squares) and SC.TNP2 (open squares) analyses, where Lw = t and (n-1)*t, respectively. As can be seen in this figure, the modified SC.TNP analysis (Lw = C1*t) agrees nearly perfectly with the FEA results. The SC.TNP2 analysis slightly underpredicts J for a given moment value, while the SC.TNP1 analysis significantly underpredicts J. Although the SC.TNP1 method does not match the finite element results very well, it is the best of all the J-estimation schemes in predicting the experimental results, at least from a load/moment perspective (Ref. 2.17). This has been attributed in part to a compensating error from using fracture toughness data from the L-C orientation in analyzing a crack growing in the L-R orientation. Figure 2.9 shows some data for A106 Grade B pipe material in which the toughness, measured in terms of Charpy Energy, in the L-R direction (Curve D from Specimen D) is significantly higher than the toughness in the L-C direction (Curve C from Specimen C). Thus, the error in using the lower applied J from the SC.TNP1 analysis (Lw = t) is offset by the error of using fracture toughness data from a lower toughness orientation, i.e., the L-C direction. Also, the difference in constraint between the fracture toughness specimens and the surface-cracked pipe may contribute to the difference in moment predictions.

Table 2.8 Surface regression coefficients for C1 in Equation 2.18

Coefficient	$\theta/\pi = 0.25$ $P_i = 0$	$\theta/\pi = 0.50$ $P_i = 0$	$\theta/\pi = 0.25$ $P_i = f(S_m)$	$\theta/\pi = 0.50$ $P_i = f(S_m)$
a_1	18.89	5.021	25.16	3.692
b	0.1936	0.1999	0.1981	0.2317
c	29.01	36.44	31.76	46.55
x_0	0.7528	0.6656	0.6871	0.6013
y_0	59.29	58.03	63.30	61.76
R^2	0.9934	0.9841	0.9885	0.9018

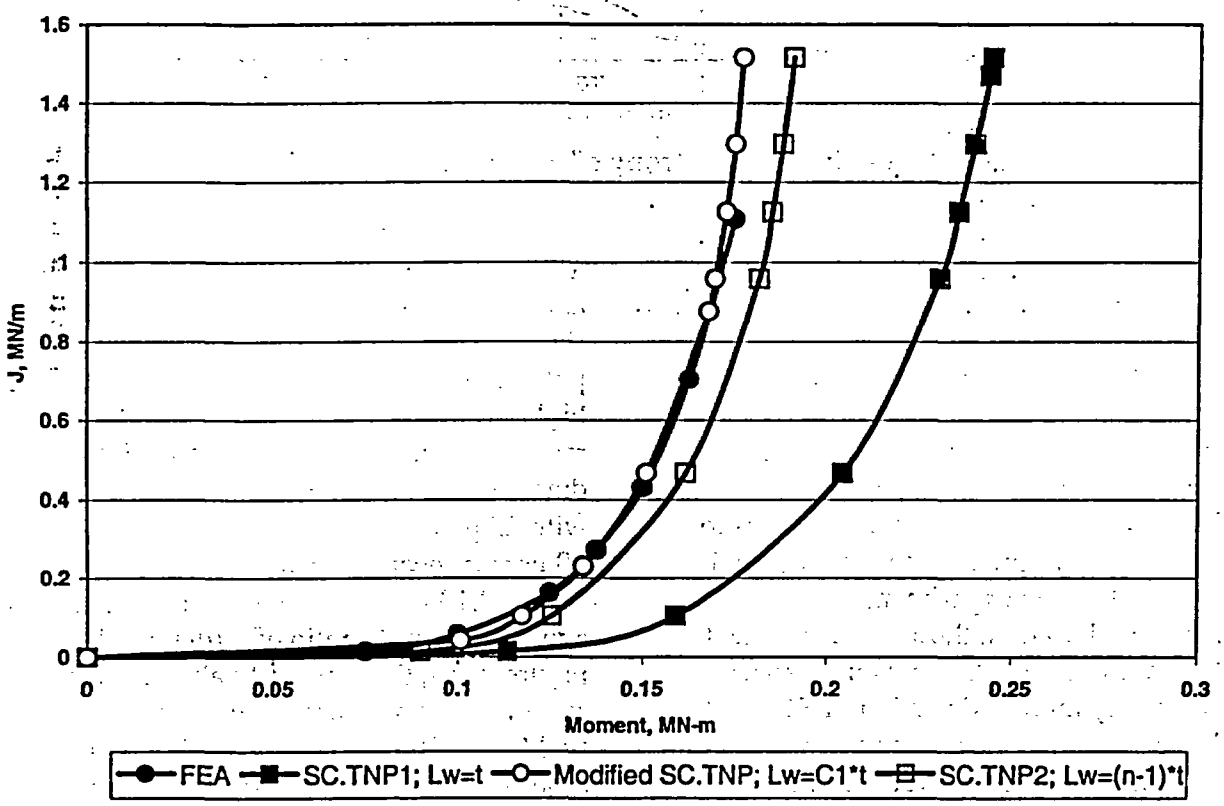

Figure 2.8 Comparison of J versus moment results for various SC.TNP analyses with finite element results for the case of no pressure, $\theta/\pi = 0.25$, a/ t= 0.5 and R/t = 40

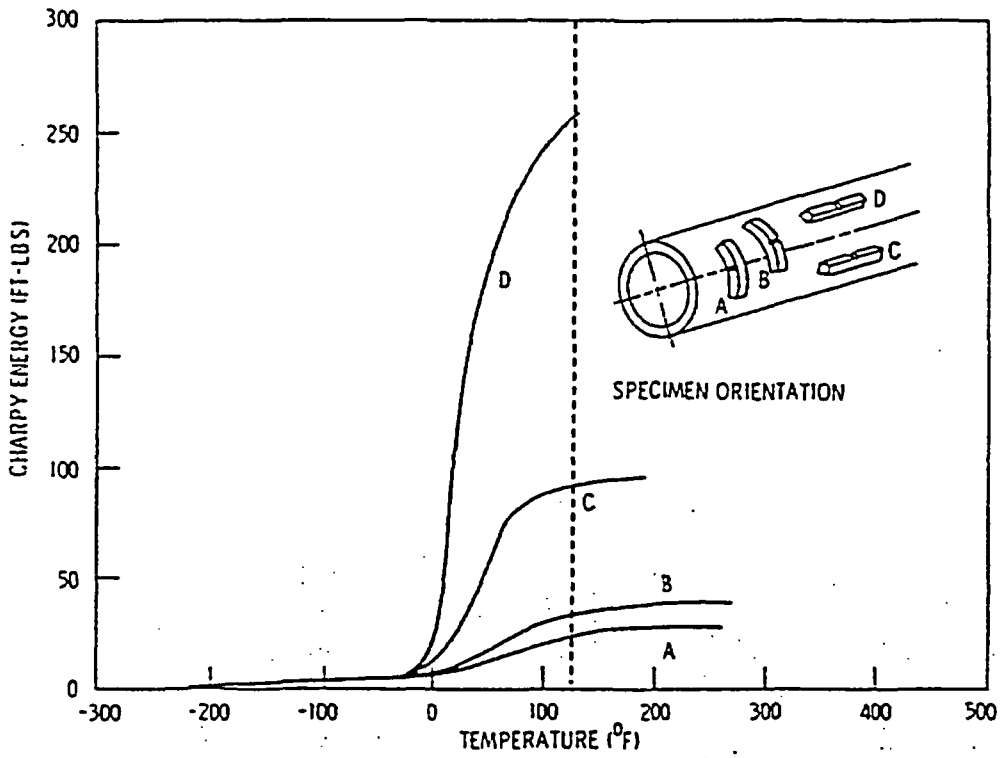

Figure 2.9 Toughness anisotropy of ASTM A106 Grade B pipe

(This difference in toughness and constraint between specimens was another topic of investigation and will be discussed further in the next section of this report.) The SC.TNP1 method does a poor job of matching the FEA applied J values and a good job of matching the experimental results, while the SC.TNP2 method tends to significantly underpredict the experimental loads from the pipe experiments. Furthermore, based on the J versus moment results from Figure 2.8, one would expect that the newly modified version of SC.TNP would do so to an ever greater extent. Consequently, for a flaw evaluation criteria one would need to address the discrepancies with the modified SC.TNP approach in load predictions due to toughness orientation and constraint effects, or accept the inherent conservatism of using the modified SC.TNP analysis as a fracture criterion.

The advantage of the modified SC.TNP analysis from a Class 2, 3, and BOP piping flaw evaluation criteria perspective is its potentially greater applicability to pipes with higher R/t ratios. Figure 2.10 shows the results of analyses of unpressurized 28-inch diameter pipes with R/t ratios of 5 and 60 with 25 percent long ($\theta/\pi = 0.25$) by 50 percent deep ($a/t = 0.5$) cracks. From Figure 2.10 it can be seen that for the case of a pipe with an R/t ratio of 5 (diamonds in Figure 2.10), the applied J value (for the same applied moment[6] value) for the modified SC.TNP analysis (Lw = C1*t) is 1.55 times the applied J value from the original SC.TNP analysis (Lw = t).

[6] The applied moment value chosen for this assessment was the maximum moment from the modified SC.TNP analysis.

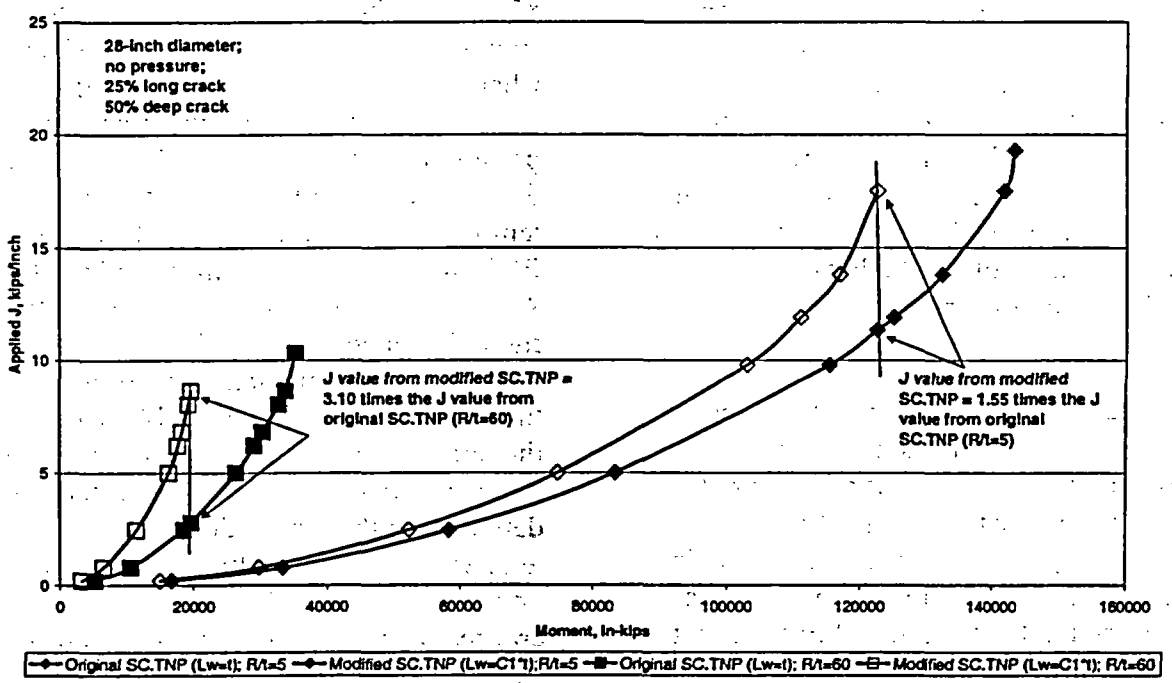

Figure 2.10 Comparison of applied J versus moment curves from the original SC.TNP (Lw = t) and modified SC.TNP (Lw = C1*t) analyses for 28-inch diameter pipes with R/t ratios of 5 and 60 and cracks 25 percent of the pipe circumference long and 50 percent of the pipe wall thickness deep

For the case of a pipe with an R/t ratio of 60 (squares in Figure 2.10), the applied J value for the modified SC.TNP analysis is 3.1 times the applied J value from the original SC.TNP analysis.

The implication is that the original SC.TNP analysis (SC.TNP1; Lw = t) may overpredict (i.e., nonconservatively predict) the actual moment-carrying capacity of a cracked pipe section for very high R/t ratio pipe. The rationale for this assertion is the following:

- The $J_{applied}$ from the original SC.TNP analysis is less than the $J_{applied}$ from the modified SC.TNP analysis (and thus the FEA) since it has been shown that the $J_{applied}$ values for the modified SC.TNP analysis and FEA agree so well for all values of R/t considered.
- The original SC.TNP analysis does a good job (typically within 10 percent) of predicting the maximum loads from full-scale surface-cracked pipe experiments for the case where the R/t ratio is less than 15. This observation has been attributed to the lower values of $J_{applied}$ for the SC.TNP analyses being offset by the use of fracture toughness data from the lower toughness L-C orientation, and possible constraint effects. Thus, considering Figure 2.10, for the case where the R/t ratio is 5, the lower $J_{applied}$ value from the original SC.TNP analysis (with respect to FEA) is being offset by a corresponding increase (55 percent) in fracture toughness in the L-R orientation when compared with the L-C orientation.
- If the effect of orientation on toughness remains roughly constant (55 percent

increase in L-R orientation when compared with the L-C orientation), then as the R/t ratio increases, and the $J_{applied}$ value from the modified SC.TNP analysis (and FEA) becomes greater with respect to the $J_{applied}$ values from the original SC.TNP analysis, then the use of the lower toughness L-C data may no longer totally offset the lower $J_{applied}$ values from the original SC.TNP analysis.

Consequently, one might expect that the original SC.TNP analysis may begin to overpredict (i.e., nonconservatively predict from a flaw evaluation perspective) the moment-carrying capacity of a cracked pipe section for the case of high R/t ratio pipes such as used in Class 2, 3, and BOP piping systems. Furthermore, this overprediction may be significant considering the fact that the modified SC.TNP applied J value, with respect to the original SC.TNP applied J value, for the higher R/t ratio case was twice the relative applied J values for the lower R/t ratio case. Consequently, for high R/t ratio pipes, such as those often used in Class 2, 3, and BOP applications, the original SC.TNP analysis (SC.TNP1; Lw = t) may not be adequate. Based on the logic presented above, it may significantly overpredict (maybe by as much as a factor of two) the actual moment-carrying capacity of the cracked-pipe section. Thus, one must use a more robust analysis, such as the modified SC.TNP analysis (Lw = C1*t), as a flaw evaluation criterion for these classes of piping.

2.2.3.2 Effect of Lower Operating Temperatures on the Fracture Behavior Class 2, 3, and BOP Piping Systems

As part of this effort a methodology was developed and subsequently verified in which one could predict the lowest temperature where ductile initiation occurs for a surface-cracked ferritic pipe from the 85 percent shear area transition temperature from Charpy impact tests. Obviously, if Charpy data exists for the actual piping material under consideration, that would be preferred. However, in the absence of actual data, A106 Grade B shear area versus temperature data was extracted from the PIFRAC (Ref. 2.22) database and plotted in Appendix E (see Figure E.44). From that figure it can be seen that the mean value of the 85 percent shear area transition temperature is approximately 65°C (149°F) while the upper-bound Charpy transition temperature is about 75°C (167°F). The steps in determining the lowest ductile initiation temperature or the fracture initiation transition temperature (FITT) for a surface-cracked pipe from the Charpy 85 percent shear area transition temperature are as follows:

- First the fracture propagation transition temperature (FPTT) for a full-thickness drop-weight-tear test (DWTT) specimen can be estimated as a function of the pipe wall thickness using a relationship such as found in Figure 2.11. The FPTT is the lowest temperature where a crack dynamically propagates as a ductile fracture, rather than a brittle crack. From this figure it can be seen that the thicker the pipe, the higher the full-size FPTT with respect to the Charpy 85 percent shear area transition temperature.
- Next, knowing the FPTT for the full-thickness specimen, one can estimate the fracture initiation transition temperature (FITT) for a through-wall-cracked pipe using a relationship such as is shown in Figures E.34 and E.35. These figures show that the FITT for the through-wall-cracked pipe is 33 to 50°C (60 to 90°F) lower than the full-size FPTT from a drop weight tear test specimen. Taking the conservative approach, one would

assume that the FITT is 33°C (60°F) lower than the FPTT for a DWTT specimen.

- Finally, one could use the relationship shown in the upper figure in Figure E.40 to estimate the shift in FITT between a through-wall-cracked pipe and a surface-cracked pipe. As can be seen in this figure, this shift is a function of the crack depth (a/t ratio). For deep cracks (greater than 50 percent of the pipe wall thickness), this shift in transition temperature is approximately 31°C (55°F), i.e., the FITT for the surface crack is approximately 31°C (55°F) lower than the FITT for a through-wall crack. For shallower flaws, this shift increases. For flaws less than 20 percent of the pipe wall thickness, the FITT for a surface crack is 56°C (100°F) or more less than the FITT for a through-wall crack. Again, from a conservative perspective, one would probably want to consider the case of a deep crack where this shift in transition temperature is the smallest.

In one of the example test cases in Section 3 of this report, an assessment as to the FITT for a surface-cracked pipe is made. For this test case, worse case assumptions as to transition temperature shifts are made. In addition, the upper bound 85 percent shear area transition temperature for L-C oriented Charpy specimens from Figure E.44 is assumed. Based on these conservative assumptions, the predicted FITT for a surface flaw 50 percent of the wall thickness deep in a 12.7 mm (0.5 inch) thick pipe is approximately 4°C (39°F). Consequently, if it is a piping system drawing service water from a lake in the middle of winter, then there is a chance of initiating a brittle fracture from a surface flaw. However, if all of these conservative assumptions do not fall in line, then the likelihood of initiating a brittle fracture from a surface crack is remote.

Note, the one element of this assessment for this test case that may not be generically conservative is the choice of the pipe wall thickness, see Figure 2.11. If the actual piping system under consideration is greater than 12.7 mm (0.5 inches) thick, then the shift in fracture propagation transition temperature (FPTT) between the full size DWTT specimen and the Charpy specimen will be greater than the -7°C (-13°F) shift for the 12.7 mm (0.5 inch) thick pipe. For a 19.1 mm (0.75 inch) thick pipe, this shift in transition temperature is +6°C (+10°F) such that the FITT for the surface-cracked pipe would be 17°C (62°F) following the same logic as before. The likelihood of a piping system operating at this temperature is obviously greater than having one operate at 4°C (39°F). However, since many Class 2, 3, and BOP piping systems operate at lower pressures, as well as lower temperatures, the chances are that these piping systems will be fabricated from thinner, rather than thicker, pipe. What is needed is a survey to assess what wall thicknesses these Class 2, 3, and BOP piping systems are fabricated from and what temperatures they operate at. Then, an assessment could be made as to whether the initiation of a brittle fracture from a surface crack in one of these piping systems is a credible event.

The above discussion is based entirely on data developed for cracks in base metals. The question that naturally arises is what effect would cracks in welds, and the associated weld residual stresses, have on this overall assessment. The concern is that the weld residual stresses may increase the constraint conditions and cause the transition temperature to be higher relative to the Charpy data. It was hoped that if additional members had joined this program, then funding would have been available to make such an assessment.

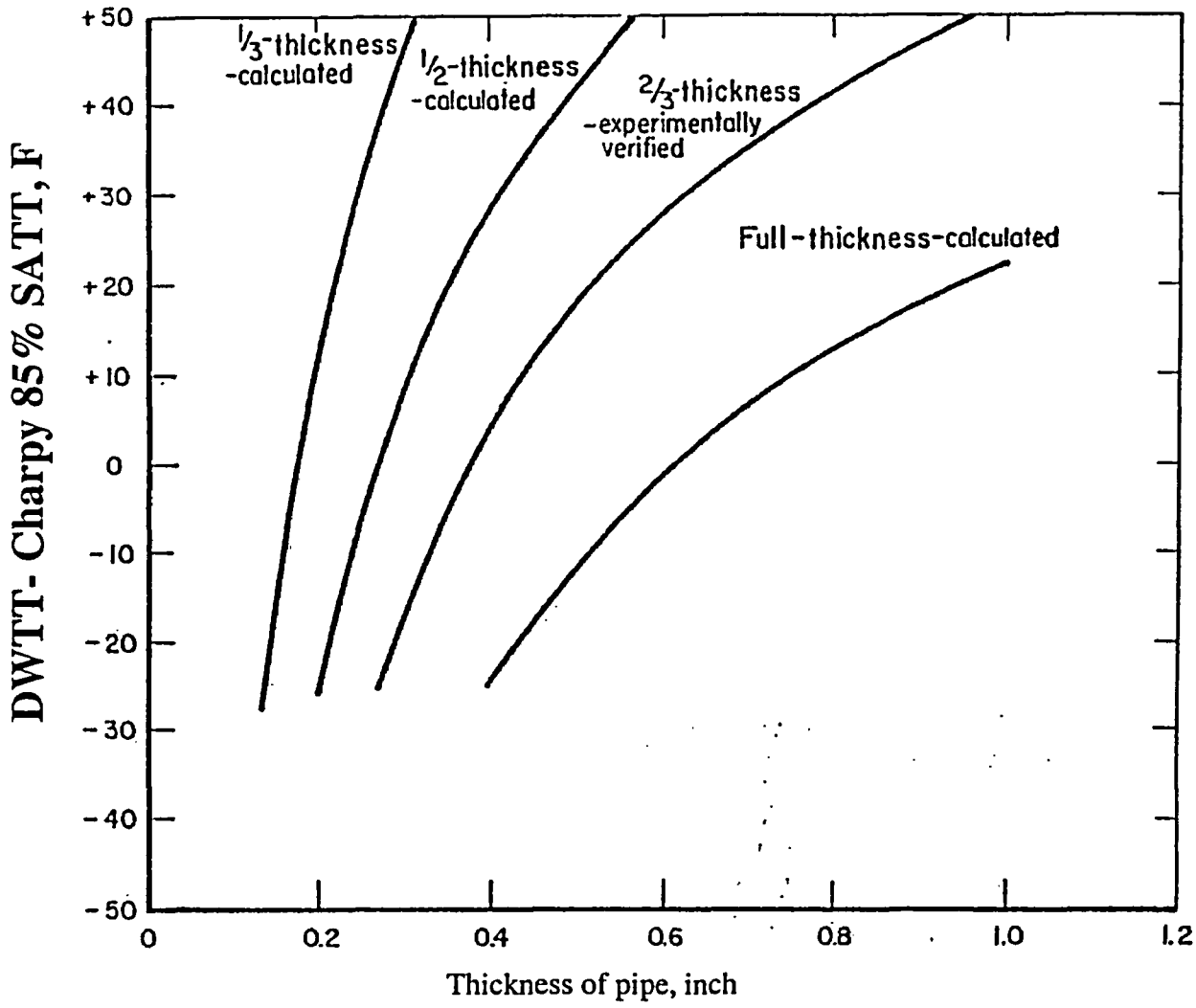

Figure 2.11 Relationship between DWTT and Charpy 85% shear area transition temperatures (SATT) as function of Charpy specimen thickness

However, without these additional members, funding for these full-scale pipe tests with cracks in the vicinity of welds was not available.

Another consideration is what role do dynamic loading rates have on this assessment. All of the data developed to date, as part of this program, has been developed at quasi-static loading rates. It has been speculated that the transition temperature may increase at dynamic loading rates.

2.3 References

2.1 "Leak-Before-Break Evaluation Procedures," draft Standard Review Plan 3.6.3, August 1987.

2.2 "Report of the U.S. Nuclear Regulatory Commission Piping Review Committee. Evaluation of Potential for Pipe Breaks," NUREG-1061, Vol. 3, November 1984.

2.3 Milne, I., and others, "Assessment of the Integrity of Structures Containing Defects, CEGB Report R/H/R6 – Revision 3," January 1987.

2.4 Scott, P., and others, "Crack Stability in a Representative Piping System Under Combined Inertial and Seismic/ Displacement-Controlled Stresses," NUREG/CR-6233, Vol. 3, June 1997.

2.5 Wilkowski, G. M., and others, "Degraded Piping Program – Phase II, Summary of Technical Results and Their Significance to Leak-Before-Break and In-Service Flaw Acceptance Criteria, March 1984 – January 1989," NUREG/CR-4082, Vol. 8, March 1989.

2.6 Kanninen, M. F., and others, "Instability Predictions for Circumferentially Cracked Type-304 Stainless Steel Pipes Under Dynamic Loading," EPRI Report NP-2347, April 1982.

2.7 Scott, P., Olson, R., and Wilkowski, G., "Development of Technical Basis for Leak-Before-Break Evaluation Procedures," NUREG/CR-6765, May 2002.

2.8 Rudland, D. L., Wilkowski, G., and Scott, P., "Effects of Crack Morphology Parameters on Leak-Rate Calculations in LBB Evaluations," *International Journal of Pressure Vessels and Piping*, Vol. 79, pp. 99-102, 2002.

2.9 Ghadiali, N., and others, "Deterministic and Probabilistic Evaluations for Uncertainty in Pipe Fracture Parameters in Leak-Before-Break and In-Service Flaw Evaluations," NUREG/CR-6443, June 1996.

2.10 Rahman, S., and others, "Summary of Results from the IPIRG-2 Round-Robin Analyses," NUREG/CR-6337, February 1996.

2.11 Kumar, V., and others, "An Engineering Approach for Elastic-Plastic Fracture Analysis," EPRI Report NP-1931, July 1981.

2.12 Paul, D. D., and others, "Evaluation and Refinement of Leak-Rate Estimation Models," NUREG/CR-5128, Rev. 1, June 1994.

2.13 Norris, D., and others, "PICEP: Pipe Crack Evaluation Program," EPRI Report NP-3596-SR, 1984.

2.14 Brust, F. W., and others, "Assessment of Short Through-Wall Circumferential Cracks in Pipes," NUREG/CR-6235, April 1995.

2.15 Kilinski, T., and others, "Fracture Behavior of Circumferentially Surface-Cracked Elbows," NUREG/CR-6444, December 1996.

2.16 Kozluk, M.J., and others, "Linear-Elastic Solutions for Long Radius Piping Elbows with Curvilinear Through-Wall Cracks," PVP Vol. 143, June 1998.

2.17 Krishnaswamy, P., and others, "Fracture Behavior of Short Circumferentially Surface-Cracked Pipe," NUREG/CR-6298, November 1995.

2.18 Kanninen, M. F., and others, "Mechanical Fracture Predictions for Sensitized Stainless Steel Piping with Circumferential Cracks," Final Report, EPRI NP-192, September 1976.

2.19 Wilksowski, G. M., and Scott, P. M., "A Statistical Based Circumferentially Cracked Pipe Fracture Mechanics Analysis for Design or Code Implementation," *Nuclear Engineering and Design*, Vol. 111, pp. 173-187, 1989.

2.20 Anderson, T. L., "Stress Intensity Solutions for Surface Cracks and Buried Cracks in Cylinders, Spheres, and Flat Plates," prepared for The Materials Property Council, Inc., March 2000.

2.21 Chapuliot, S., and Lacire M. H., "Stress Intensity Factors for External Circumferential Cracks in Tubes Over a Wide Range of Radius Over Thickness Ratios," PVP Vol. 388, 1999.

2.22 Hiser, A. L., and others, "A User's Guide to the NRC Piping Fracture Mechanics Database (PIFRAC)," NUREG/CR-4894, May 1987.

3. EXAMPLE TEST CASES

This section of the report presents a series of example test cases illustrating the effects of the key results from this program on both leak-before-break (LBB) and in-service flaw evaluation criteria. Where available, the input parameters for these test cases will be taken from data supplied to Battelle by the US NRC from actual plant piping system LBB applications. If no such data exist, then example data will be made up to illustrate the effect being discussed.

3.1 Example Test Cases Illustrating the Effects of the Key Results from this Program on LBB Analyses

Tables 3.1 through 3.5 summarize five example test cases that illustrate the effects of the key results from this program on LBB analyses. Included in this table is the purpose or objective of each test case, the input parameters invoked, and the key findings from each test case. Note that each test case is a series of multiple example problems whereby the key findings are gleamed by comparing the results from these individual problems.

3.1.1 Role of Secondary Stresses on LBB

In Test Case 1 (Table 3.1), the role of secondary stresses on LBB was examined. The data used in this test case came from an actual LBB submittal supplied to Battelle by the US NRC. The submittal was for a 12-inch nominal diameter safety injection system (SIS) line. The piping system was fabricated from 12-inch diameter, Schedule 160 (33.32 mm [1.312 inch] wall thickness) pipe. The internal pipe pressure was 16.0 MPa (2,327 psi) and the pipe temperature was 285°C (545°F). For the plant in question, the leak-rate detection limit capability was 1.9 lpm (0.5 gpm).

For the postulated leakage crack size analysis, mean value material data were used. In addition, the loads at normal operating conditions were summed algebraically. The postulated leakage crack size was calculated using the SQUIRT4 module in the SQUIRT leak-rate computer code (Windows® Version 1.1). The postulated leakage crack size was found to be 192 mm (7.54 inches), which is approximately 19 percent of the outside pipe circumference.

For the critical crack size analysis, two separate analysis cases were conducted. For Case 1a, the thermal expansion stresses (i.e., the secondary stresses) at normal operating conditions were included with the primary membrane and primary bending (i.e., seismic) stresses at the faulted conditions. This is the procedure specified in the existing draft Standard Review Plan (SRP) section on LBB (draft SRP 3.6.3). For Case 1b, the thermal-expansion stresses were not included with the primary membrane and bending stresses in the critical crack size analysis. For both cases, lower-bound material data were used in the critical crack size analysis. In addition, the GE/EPRI J-estimation scheme was used as the analysis methodology for these critical crack size analyses. For Case 1a (where the secondary stresses were included), the critical crack size was found to be 394 mm (15.53 inches). For Case 1b (where the secondary stresses were not included), the critical crack size was found to be 484 mm (19.05 inches). The resultant margin on crack size was 2.06 for Case 1a and 2.53 for Case 1b. Consequently, the effect on margin is about 23 percent.

Table 3.1 Example problem illustrating the role of secondary stresses on LBB

Purpose or Objective of Test Case	Input Parameters	Results and Conclusions
	Test Case 1 – Role of Secondary Stresses on LBB	
Case 1a – Include secondary stresses in both postulated leakage TWC analysis and critical crack size stability analysis (existing SRP 3.6.3 procedures)	Source of data: Actual plant LBB application for 12 inch diameter Safety Injection System (SIS) line - OD = 12.75 inches - t = 33.3 mm (1.312 inches) - Crack location in a TP316 stainless SMAW - Crack type - IGSCC - 16.0 MPa (2,327 psi) pressure - 285°C (545°F) temperature - 1.9 lpm (0.5 gpm) leakage detection system Mean value material data used for leak-rate analysis; lower-bound material data for instability analysis Algebraic sum of dead-weight, thermal, and pressure loads at normal operating conditions for leak-rate analysis; absolute sum of membrane and bending stresses at faulted conditions and thermal-expansion stresses at normal operating conditions for critical crack size stability analysis - Normal operating loads o Dead weight: M_y = -5.74 kN-m (-4,231 ft-lbs), M_z = -3.26 kN-m (-2,405 ft-lbs) o Thermal: M_y = 30.95 kN-m (-22,826 ft-lbs); M_z = 51.7 kN-m (38,127 ft-lbs) - SSE loads: M_y = 14.6 kN-m (10,799 ft-lbs); M_z = 12.3 kN-m (9,045 ft-lbs)	Postulated leakage crack size = 192 mm (7.54 inches) Critical crack size = 394 mm (15.53 inches), using GE/EPRI method Margin on crack size = 2.06
Case 1b – Include secondary stresses in postulated leakage TWC analysis but exclude thermal expansion stresses in critical crack size stability analysis	Same as above except thermal expansion stresses are not included in the critical crack size stability analysis	Postulated leakage crack size = 192 mm (7.54 inches) Critical crack size = 484 mm (19.05 inches), using GE/EPRI method Margin on crack size = 2.53

3.1.2 Effect of Actual Margins on LBB

In this set of example cases (Table 3.2), two separate series of three sets of comparative analyses were conducted. In each case, the piping system under consideration is the IPIRG pipe loop facility. This is a 16-inch nominal diameter, Schedule 100 piping system fabricated as an expansion loop. The load history used in all of these test cases was an increasing amplitude, single-frequency, sinusoidal-forcing function superimposed on an increasing ramp. The cyclic frequency was set at about 90 percent of the first natural frequency of the pipe loop. This was the same forcing function used in a number of the IPIRG-1 pipe-system experiments. The internal pipe pressure and temperature were representative of pressurized water reactor (PWR) conditions, i.e., 15.5 MPa (2,250 psi) and 288°C (550°F). The actual conditions replicated in this test case were the same as those for Experiment 1.3-3 from the First IPIRG program.

The postulated leakage crack size used in these analyses was based on TP304 stainless steel material data as used in Experiment 1.3-3. The applied moment value at the assumed normal operating conditions for the postulated leakage crack size analysis was established by assuming that the primary membrane (P_m) plus primary bending (P_b) stresses at normal operating conditions was equal to 0.73 S_m. For a 1.9 lpm (0.5 gpm) leakage detection system and applying a factor of safety of 10 on the leakage detection capability, the calculated leakage crack size (using a SQUIRT4 analysis) was 171 mm (6.73 inches), which is approximately 13.4 percent of the outside pipe circumference. This is based on using the default crack morphology parameters for an IGSCC crack in SQUIRT. This crack length does not include the safety factor of 2.0 on crack length currently specified in draft SRP 3.6.3.

In the analyses that follow the factor of safety of 2.0 on crack size was applied in some cases and was not in others.

In the first set of comparative analyses (Cases 2aNo and 2aWith), the additional margin due to using elastic analyses to analyze a nonlinear problem was estimated. This test case involved two separate uncracked piping system analyses, for which it was assumed that the entire piping system was fabricated from TP304 stainless steel pipe. In one case, elastic analysis was used. In the other case, plasticity due to pipe yielding was introduced into the piping-system analysis. The nonlinear plasticity analysis was conducted first. This time-history analyses were run until the moments at the postulated crack section reached a value equal to the maximum moment capacity of the postulated leakage cracks (i.e., 171 mm [6.73 inch] for Case 2aNo [no safety factor on crack size] and 342 mm (13.5 inches) for Case 2aWith (with a factor of safety of 2.0 on crack size]). The maximum moment values for these crack sizes, using the TP304 stainless steel material data from Experiment 1.3-3, were calculated, using the GE/EPRI analysis, to be 565 kN-m (5,000 in-kips) and 289 kN-m (2,560 in-kips) for the short (no safety factor) and long (with safety factor) crack cases, respectively. The time it took to reach these moment values in the nonlinear analyses were 3.93 and 1.39 seconds, respectively, for the short and long crack cases.

The uncracked elastic analyses were run next. The same displacement time history used in the nonlinear analyses was used in the elastic analyses as well. These elastic analyses were run for the same amount of time as it took to reach the maximum

Table 3.2 Example problem illustrating effect of actual margins on LBB

Purpose or Objective of Test Case	Input Parameters	Results and Conclusions
	Test Case 2 – Effect of Actual Margins on LBB	
Case 2a – Additional margin due to using elastic analyses to analyze nonlinear problem (uncracked pipe analysis)	IPIRG pipe loop geometry (IPIRG-1 Experiment 1.3-3) OD = 16.37 inches; t = 26.2 mm (1.031 inches); material TP304 stainless steel; P = 15.5 MPa (2,250 psi); T = 288°C (550°F) Normal operating moments for leakage crack size analysis based on primary membrane (P_m) plus primary bending (P_b) stresses at normal operating conditions equaling 0.73 S_m for TP304 stainless steel at 288°C (550°F), i.e., 117 MPa (16.95 ksi); M = 69.8 kN-m (618 in-kips) Postulated leakage TWC based on 1.9 lpm (0.5 gpm) leak detection system with safety factor of 10 on leakage detection capability; IGSCC crack morphology parameters used Faulted load history is based on IPIRG single-frequency load history – for both the nonlinear analysis and elastic analysis, the duration of the load history will be the same, equal to the time to achieve the maximum moment value for the postulated TWC during the nonlinear analysis (i.e., 565 kN-m [5,000 in-kips] for the case where the factor of safety of 2.0 on crack size was not applied [Case2aNo] and 289 kN-m [2,560 in-kips] for the case where it was applied [Case 2aWith].)	Postulated leakage crack size = 171 mm (6.73 inches); no safety factor on crack size (Case 2aNo) Time to reach M_{max} of 565 kN-m (5,000 in-kips) for nonlinear uncracked analysis = 3.93 seconds M_{max}(elastic uncracked analysis) at 3.93 seconds = 1,442 kN-m (12,760 in-kips) Additional Margin = M_{max}(elastic uncracked)/M_{max}(nonlinear uncracked) = 1,442/565 = 2.55 Postulated leakage crack size = 342 mm (13.5 inches); with safety factor of 2.0 on crack size (Case2aWith) Time to reach M_{max} of 289 kN-m (2,560 in-kips) for nonlinear uncracked analysis = 1.39 seconds M_{max}(elastic uncracked analysis) at 1.39 seconds = 291 kN-m (2,575 in-kips) Additional Margin = M_{max}(elastic uncracked)/M_{max}(nonlinear uncracked) = 291/289 = 1.01
Case 2b – Additional margin due to the nonlinear behavior of the TWC	Same as above, except the duration of the load history for both sets of analyses will be equal to the time to achieve the maximum moment value for the postulated TWC for the elastic TWC analysis	Postulated leakage crack size = 171 mm (6.73 inches); no safety factor on crack size (Case 2bNo) Time to reach M_{max} of 565 kN-m (5,000 in-kips) for elastic TWC analysis = 2.655 seconds M_{max}(elastic, uncracked analysis) at 2.655 secs = 756 kN-m (6,690 in-kips) Additional Margin = M_{max}(elastic uncracked)/M_{max}(elastic cracked) = 1.34

Table 3.2 Example problem illustrating effect of actual margins on LBB (cont.)

Purpose or Objective of Test Case	Input Parameters	Results and Conclusions
		Postulated leakage crack size = 342 mm (13.5 inches); with safety factor on crack size (Case 2bWith) Time to reach M_{max} of 289 kN-m (2,560 in-kips) for elastic TWC analysis = 2.15 seconds M_{max}(elastic, uncracked analysis) at 2.15 secs = 547 kN-m (4,840 in-kips) Additional Margin = M_{max}(elastic uncracked)/M_{max}(elastic cracked) = 1.89
Case 2c – Additional margin due to combined effect of the nonlinear behavior of the pipe and the nonlinear behavior of the TWC	Same as above, except the duration of the load history for both sets of analyses will be equal to the time to achieve the maximum moment value for the postulated TWC during the nonlinear TWC analysis	Postulated leakage crack size = 171 mm (6.73 inches); no safety factor on crack size (Case 2cNo) Time to reach M_{max} of 565 kN-m (5,000 in-kips) for nonlinear TWC analysis = >10 seconds M_{max}(elastic, uncracked analysis) at 10 secs = 5,790 kN-m (51,250 in-kips) Additional Margin = M_{max}(elastic uncracked)/M_{max}(nonlinear cracked) > 10.2 Postulated leakage crack size = 342 mm (13.5 inches); with safety factor on crack size (Case 2cWith) Time to reach M_{max} of 289 kN-m (2,560 in-kips) for nonlinear TWC analysis = 2.155 seconds M_{max}(elastic, uncracked analysis) at 2.155 secs = 551 kN-m (4,880 in-kips) Additional Margin = M_{max}(elastic uncracked)/M_{max}(nonlinear cracked) = 1.91

moment values in the uncracked nonlinear plasticity analyses, i.e., $t_{elastic} = t_{nonlinear\ at\ max\ moment}$. Due to the nonlinearities in the nonlinear analysis for the short crack case, i.e., yielding in the piping system, the moment at this time (3.93 seconds) for the elastic analysis (1,442 kN-m [12,760 inch-kips]) was a factor of 2.55 greater than the moment at this time for the nonlinear analysis (565 kN-m [5,000 inch-kips]). This factor is indicative of the additional margin one might realize as a result of accounting for the plasticity in the stress analysis of the uncracked pipe. Conversely, due to the longer length crack for the case where the factor of safety of 2.0 on crack length was applied (Case2aWith), the crack failed relatively early (1.39 versus 3.93 seconds) into the forcing function. As a result, the associated plasticity did not have time to build up such that the moments at 1.39 seconds for the nonlinear and elastic analyses were nearly the same, i.e., 291 kN-m (2,575 in-kips) for the elastic analysis versus 2.89 kN-m (2,560 in-kips) for the nonlinear analysis. Thus, for this case (Case 2aWith), there was essentially no benefit (i.e., additional margin) to be gained from invoking plasticity into the piping system stress analysis.

For the second set of comparative analyses (Cases 2bNo and 2bWith), the additional margin due to the nonlinear behavior of a through-wall crack is assessed. The same piping system, same postulated leakage through-wall cracks (short and long depending on whether the safety factor of 2.0 is applied), same forcing function, same material, and same operating conditions as assumed for Case 2a, were assumed here. The first analyses conducted as part of this test case were linear piping system analyses, but with nonlinear spring representations of the postulated leakage cracks introduced at the postulated crack location. These analyses were run until the maximum moment values at the crack location reached the maximum moment capacity of the postulated leakage crack sizes, i.e., 565 kN-m (5,000 in-kips) for the case where the safety factor of 2.0 on crack size was not applied and 289 kN-m (2,560 in-kips) for the case where it was. Next elastic, uncracked pipe analyses were run, using the same forcing function, out to the time necessary to achieve the maximum moment value in the previous elastic, TWC analyses, i.e., 2.655 and 2.15 seconds, for the short (no safety factor) and long (with safety factor) crack cases, respectively. The maximum moment values for these elastic, uncracked analyses (756 kN-m [6,690 in-kips and 547 kN-m [4,840 in-kips]) were compared with the corresponding results from the elastic, cracked analyses to assess the additional margin due to the presence of the crack, and its associated nonlinear behavior. The ratios of moments for the short (no safety factor) and long (with safety factor) crack cases were 1.34 and 1.89, respectively. These ratios are indicative of the additional margin one might realize by incorporating a nonlinear spring representation of the crack in the piping system analyses.

For the final set of comparative analyses (Cases 2cNo and 2cWith), the additional margin due to the combined effect of the nonlinear behavior of the pipe and the presence of the through-wall crack is assessed. The same piping system, same postulated leakage through-wall cracks (short and long depending on whether the safety factor of 2.0 is applied), same forcing function, same material, and same operating conditions as assumed for Cases 2a and 2b, were assumed here. The first analyses conducted as part of this test case were nonlinear piping system analyses, with non-linear spring representations of the postulated leakage cracks introduced at the

postulated crack location. These analyses were run until the maximum moment values at the crack location reached the maximum moment capacity of the postulated leakage crack sizes (i.e., 289 kN-m (2,560 in-kips), for the long (with safety factor) crack case. For the short crack case (no safety factor on crack size), the moment at the crack section never reached the predicted failure moment of 565 kN-m (5,000 in-kips) in the 10 seconds that the forcing function was applied. Next elastic, uncracked pipe analyses were run, using the same forcing function, out to the time necessary to achieve the maximum moment value in the previous nonlinear, TWC analysis, 2.155 seconds, for the long crack case. For the short crack case the forcing function for this elastic, uncracked analysis was run out to 10 seconds. The maximum moment values these elastic, uncracked analyses (551 kN-m [4,880 in-kips] and 5,790 kN-m [51,250 in-kips] for the long and short crack cases, respectively) were compared with the corresponding results from the nonlinear, cracked analyses to assess the additional margin due to the combined effect of the crack and the nonlinear piping system behavior. The ratios of moments for the short (no safety factor on crack size) and long (with safety factor on crack size) crack cases were 10.2 and 1.91, respectively. These ratios are indicative of the additional margin one might realize by the combined effect of incorporating a nonlinear spring representation of the crack in a nonlinear piping system analyses.

Of all the effects examined as part of this program (e.g., restraint of pressure-induced bending, weld residual stress effects, etc.), this has the biggest potential to impact LBB analyses.

3.1.3 Effect of Restraint of Pressure Induced Bending on LBB

In Test Case 3 (Table 3.3), the role of the restraint of pressure-induced bending on the crack-opening displacements and associated leakage through-wall-crack size for an LBB analysis was assessed. This assessment used actual data from an LBB submittal for a surge line in a PWR. The exact location under consideration was the weld joint where the surge line joined to the pressurizer. For this comparative analysis, a baseline analysis was first conducted in which the effect of restraint of pressure-induced bending was not considered. Using the SQUIRT4 module in the Windows® version of SQUIRT (Version 1.1), the leakage crack length and associated crack-opening displacement were calculated. For this unrestrained condition, the leakage crack length was 162 mm (6.37 inches) and the associated COD was 0.361 mm (0.0142 inches). (This is based on a 1.9 lpm (0.5 gpm) leakage detection system with a factor of safety of 10 on the leak rate.) Next, the equations in Appendix D were used to calculate the r_{cod} values for both the symmetric and asymmetric cases. For both cases, the restraint lengths (L/D) were first calculated from the rotational stiffness at the surge line/pressurizer weld joint using a finite element analysis of this surge line. Neither the symmetric nor the asymmetric analysis is totally valid for this case. This piping system at this weld joint is highly asymmetric, with the L_1/D value being 0.14 and the L_2/D value being 29, but the asymmetric analysis was developed for a specific R/t ratio, R/t = 10, and the R/t ratio of this piping system is 5. Since neither analysis method was truly precise, both were considered for illustrative purposes.

From Table 3.3 it can be seen that the effect of restraint of pressure-induced bending was minimal for both analyses methods. For

Table 3.3 Example problem illustrating effect of restraint of pressure-induced bending on LBB

Purpose or Objective of Test Case	Input Parameters	Results and Conclusions
Test Case 3 – Effect of Restraint of Pressure-Induced Bending on LBB		
Case 3a – Ignoring the effect of restraint of pressure-induced bending on the COD and crack length in an LBB analysis	Source of data: Actual plant LBB application for 14-inch diameter surge line - Crack location considered – at weld joint where surge line joins to bottom of pressurizer - OD = 14-inch; t = 31.6 mm (1.246 inch) - Crack type – IGSCC - Pressure = 16.0 MPa (2,327 psi); Temperature = 345°C (653°F) - 1.9 lpm (0.5 gpm) leakage detection system; leakage crack size based on 19 lpm (5.0 gpm) leak rate; safety factor of 10 on leak detection. Mean value used for both leak-rate and instability analysis Algebraic sum of loads at normal operating conditions used for leak rate analysis; absolute sum of loads used in instability analysis Moment at normal operating conditions = 225.5 kN-m (1,996 in-kips) Moment at SSE loading conditions = 267.3 kN-m (2,366 in-kips)	Crack length and COD assuming unrestrained conditions - 2c = 162 mm (6.37 inch) - δ = 0.361 mm (0.0142 inch) Critical crack size using draft SRP 3.6.3 procedures = 293.4 mm (11.55 inch) Margin on crack size = 1.81
Case 3b – Including the effect of restraint of pressure-induced bending on the COD and crack length in an LBB analysis	Same as above except for leakage crack size analysis, two conditions of restraint were assumed, i.e., symmetric (L/D = 7.85) and asymmetric (L_1/D = 0.14 and L_2/D = 29). [The effect of restraint was the same for both cases, i.e., $R_{COD,\,sym} = R_{COD,\,asym} = 0.985$.]	Crack length and COD assuming either symmetric or asymmetric restraint - 2c = 164 mm (6.46 inch) - δ = 0.355 mm (0.0140 inch) Critical crack size using draft SRP 3.6.3 procedures = 293.4 mm (11.55 inch) Margin on crack size = 1.79

both the symmetric and asymmetric analyses, the r_{cod} value was 0.985 which meant that the restrained COD value was very nearly the same as the unrestrained value. Since the restrained COD value is just slightly less than the unrestrained value, ([0.0355 mm 0.0140 inch]) versus 0.36 mm [0.0142 inch]), the leakage crack length is also only proportionately slightly longer. Using a trial and error approach for a SQUIRT2 analysis, it was found that the resultant 19 lpm (5.0 gpm) leakage crack length for this restrained COD value was 164 mm (6.46 inches), compared with 162 mm (6.37 inches) for the unrestrained case.

Thus, even for this case (i.e., where the piping system joins to a large pressure vessel), the effect of this restraint on pressure-induced bending is relatively minor.

As an extension to this analysis, the critical crack size was calculated using the procedures in draft SRP 3.6.3 (Ref. 3.1). The draft SRP 3.6.3 critical crack size procedures are essentially the modified Net-Section-Collapse procedures from ASME Section XI Appendix C (Ref. 3.2) where a Z-factor is incorporated in the analysis to account for the crack being in a lower toughness shielded-metal-arc weld (SMAW). As can be seen in Table 3.3, the critical crack length is 293.4 mm (11.55 inches). Thus, the margin on crack size is only 1.81 for the unrestrained case and 1.79 for the restrained case. These margins are slightly less than the 2.0 required for LBB. It appears that the reason this piping system was approved for LBB in the first place was that the applicant assumed a surface roughness of 0.0076 mm (300 micro-inch) and no turns for the crack morphology characteristics. This is significantly smoother than the crack morphology parameters for an IGSCC used in this example test case analysis. The mean value surface roughness and number of turns from NUREG/CR-6004 (Ref. 3.3) were used in this example test case analysis, i.e., global roughness = 0.080 mm (315 micro-inches), local roughness = 0.0047 mm (185 micro-inches), and 71.7 90-degree turns per inch. Using the applicants crack morphology parameters (0.0076 mm [300 micro-inch] surface roughness with no turns), and assuming a 1.9 lpm (0.5 gpm) leakage detection system and applying a factor of safety of 10 on leakage detection, it was found that the calculated leakage crack size was 99.8 mm (3.93 inches), almost a factor of two less than that found when using the mean value crack morphology parameters for an IGSCC crack from NUREG/CR-6004. This shows the significant impact the choice of crack morphology parameters can have on an LBB analysis. Similar findings were reported by Rudland in Reference 3.4.

3.1.4 Effect of Differences in J and COD Predictions between the GE/EPRI Method for Straight Pipe and the Elbow TWC Solutions

In Test Case 4 (Table 3.4), the effect of difference in the J and COD predictions between the GE/EPRI straight-pipe solutions and the elbow TWC solutions developed as part of Task 8 of this program were assessed. In Test Case 4a, the differences in the COD values between the straight-pipe and elbow solutions are shown. For this case, a 16-inch nominal-diameter pipe with a wall thickness of 37.0 mm (1.455 inches) was assumed. This wall thickness was chosen because it resulted in a pipe mean radius-to-thickness (R/t) ratio of 5, i.e., one of the R/t ratios for which V- and h-functions have been developed. The internal pipe pressure was 15.5 MPa (2,250 psi) and the applied moment value was 25.4 kN-m (225 in-kips). For a prescribed leak rate

Table 3.4 Example problem illustrating the differences in J and COD predictions between the GE/EPRI method for straight pipe and the elbow through-wall-crack solutions developed as part of this program

Purpose or Objective of Test Case	Input Parameters	Results and Conclusions
Test Case 4 – Difference in J and COD Predictions between GE/EPRI Method for Straight Pipe and Elbow TWC Solutions		
Test Case 4a – Difference in COD values between elbow solution and straight-pipe solution	Pipe and crack geometry: • OD = 16 inches, t = 37.0 mm (1.455 inches), $R_m/t = 5$ • Circumferential crack; $\theta = 45$ degrees (half crack length); (19 lpm [5 gpm] leakage crack for IGSCC) Loading: • Pressure = 15.5 MPa (2,250 psi), Applied moment = 25.4 kN-m (225 in-kips) Material data: • Yield = 179 MPa (26 ksi), Ultimate = 455 MPa (66 ksi), E = 176 GPa (25,500 ksi), $\alpha = 4$, $n = 5$ • J-R curve is lower bound J-R curve for stainless steel SMAW from Reference 3.5	COD_{pipe} = 0.171 mm (0.00673 inches), GE/EPRI COD_{elbow} = 0.236 mm (0.0.929 inches), using Equations in Appendix F) $2\theta_{elbow}$ (total crack length) = 65 degrees; assuming the leak rate is proportional to the crack-opening area
Test Case 4b – Difference in applied J between elbow solution and straight-pipe solution for crack stability analysis	Same as above except applied moment = 388 kN-m (3,440 in-kips), crack initiation moment using GE/EPRI method	J_{elbow} = 244 kJ/m^2 (1.394 kips/inch) J_{pipe} = 195 kJ/m^2 (1.111 kips/inch)

of 19 lpm (5 gpm), i.e., 1.9 lpm (0.5 gpm) leakage detection capability with a safety factor of 10, the resultant through-wall-crack length and COD values using the GE/EPRI straight-pipe solution (using a SQUIRT4 analysis) were 90 degrees and 0.171 mm (0.00673 inches), respectively. For a postulated circumferential through-wall crack along the extrados of an elbow for a similar set of conditions, the COD value was 0.236 mm (0.00929 inches), using the equations in Appendix F. Assuming that the leak rate is proportional to the crack-opening area, for the same 19 lpm (5 gpm) prescribed leak rate, the postulated leakage crack length would be 65 degrees for the elbow case versus 90 degrees for the straight pipe case, i.e., approximately a 25 to 30 percent reduction.

In Test Case 4b, the effect of the difference in the J-solutions between the straight-pipe solution and the elbow solution was assessed. For this case, the same pipe geometry (16-inch diameter by 37.0 mm [1.455 inches] thick), crack size (θ = 45 degrees), pressure loading (15.5 MPa [2,250 psi]), and material data were used as in Test Case 4a. The same conditions were used for both the straight-pipe and elbow solutions. The only difference was that the applied moment value assumed in both the straight pipe and elbow analysis was 388 kN-m (3,440 in-kips). This was the crack initiation moment value for the straight-pipe case using the GE/EPRI J-estimation scheme when using a lower bound J-R curve for a stainless steel shielded-metal-arc weld (SMAW) from Reference 3.5. For the straight-pipe case, the applied J value was found to be 195 kJ/m^2 (1.111 in-kips/inch^2). For the elbow case, the applied J value was calculated to be 244 kJ/m^2 (1.394 in-kips/inch^2) when using the equations and influence functions in Appendix F. This represents a 25 percent increase in applied J, which would result in a reduction in the load-carrying capacity of a cracked pipe or a corresponding reduction in the critical crack size to be used in a LBB assessment.

3.1.5 Effect of Weld Residual Stresses on the Postulated Leakage Crack Size for a Leak-Before-Break Assessment

The final set of test cases considered applicable to LBB assessments is Test Case 5 (Table 3.5) in which the effect of weld residual stresses on the postulated leakage crack size is assessed. In this set of test cases, the same input data were used as in Test Case 1. For Test Case 5, the critical crack size analysis is based on including the thermal expansion stresses at normal operating conditions in the applied stress term, much like it is currently assumed for a draft SRP 3.6.3 LBB analysis. The only difference between Test Cases 5a and 5b is that Test Case 5a ignores the effect of weld residual stresses on the crack-opening-displacements (and resultant postulated leakage through-wall crack size) while Test Case 5b includes the effect of weld residual stresses on COD and postulated leakage crack size. For Test Case 5a (no residual stresses), the postulated leakage crack size was found to be 189 mm (7.45 inches) from a SQUIRT4 analysis while for Test Case 5b (where residual stresses are considered), the postulated leakage crack size was found to be 212 mm (8.36 inches). Knowing from Test Case 1a that the critical crack size for this test case was 394 mm (15.53 inches), the margin on crack size was 2.08 for the case where residual stresses were ignored and 1.86 for the case where residual stresses were considered. Thus, considering weld residual stresses in the postulated leakage crack size analysis resulted in about a 10 percent reduction in margin on crack size in this example. In this particular case, the required margin of 2.0 on crack size is satisfied for the case where residual stresses

Table 3.5 Example problem illustrating the effect of weld residual stresses on LBB

Purpose or Objective of Test Case	Input Parameters	Results and Conclusions
	Test Case 5 – Effect of Weld Residual Stresses on LBB	
Test Case 5a – Baseline case where weld residual stresses are ignored in postulated leakage TWC analysis	Same as Test Case 1a Critical crack size based on including thermal stresses in stability analysis (existing draft SRP 3.6.3 method)	Postulated leakage crack size = 189 mm (7.45 inches) Critical crack size = 394 mm (15.53 inches) Margin on crack size = 2.08
Test Case 5b – Case where weld residual stresses are included in postulated leakage TWC analysis	Same as Test Case 1a Critical crack size based on including thermal stresses in stability analysis (existing draft SRP 3.6.3 method)	Postulated leakage crack size = 212 mm (8.36 inches) Critical crack size = 394 mm (15.53 inches) Margin on crack size = 1.86

are ignored, but it is not when the effect of weld residual stresses on COD, and thus the postulated leakage crack length, are considered.

3.2 Example Test Cases Illustrating the Effects of the Key Results from this Program on In-Service Flaw Evaluations

Tables 3.6 and 3.7 summarize two example test cases that illustrate the effects of the key results from this program on in-service flaw evaluations. Included in these tables are the purpose or objective of each test case, the input parameters invoked, and the key findings from each test case. As was the case for the LBB illustrations, each test case is a series of multiple example problems whereby the key findings are gleamed by comparing the results from these individual problems.

3.2.1 Role of Secondary Stresses on In-Service Flaw Evaluation Criteria

In Test Case 6 (Table 3.6) the role of secondary stresses on in-service flaw evaluation criteria were examined. Data for this test case was gathered from an actual LBB submittal for a 14-inch diameter surge line. For Test Case 6a, the thermal expansion stresses (i.e., secondary stresses) were included in the applied stress term, but with a safety factor of 1.0, while the applied safety factor for the primary membrane and bending stress terms was 1.39. This is the approach currently followed in the ASME Section XI Appendix C criteria for cracks in austenitic flux welds, such as SAW and SMAW. For Test Case 6b, the thermal expansion stresses were again included in the applied stress term, but with a full safety factor of 1.39.

In both cases, the length of the surface crack was assumed to be 50 percent of the pipe circumference. For Test Case 6a, where the thermal expansion stresses were included with a safety factor of 1.0, the allowable crack depth was calculated to be 69 percent of the pipe wall thickness. For Test Case 6b, where the thermal expansion stresses were included with a safety factor of 1.39, the allowable crack depth was calculated to be 58 percent of the pipe wall thickness, i.e., 15 percent reduction in allowable crack depth.

3.2.2 Effect of Actual Margins on In-Service Flaw Evaluation Criteria

In Test Case 7 (Table 3.7), the effect of actual margins on in-service flaw evaluations was considered. For this test case, the same input data as used in Test Case 2a were used except a surface flaw (versus a through-wall crack) in a stainless steel SMAW was evaluated. The surface crack was 25 percent of the pipe circumference long and 30 percent of the pipe wall thickness deep. Using the equations in ASME Section XI Appendix C, the allowable bending moment at emergency and faulted conditions was first calculated. The allowable bending moment was found to be 497 kN-m (4,400 in-kips). An elastic uncracked analysis was then conducted until the moment at the assumed crack section in the IPIRG pipe loop reached this value. The time necessary to reach this moment value in this elastic analysis was 2.41 seconds. Next, a nonlinear uncracked analysis was conducted, using the same forcing function as in the elastic analysis, out to this time of 2.41 seconds. The maximum moment value achieved in this 2.41 seconds in the nonlinear analysis was 426 kN-m (3,769 in-kips). Finally, the allowable crack depth for the same 25 percent long crack using the procedures in ASME Section XI Appendix C was calculated for this moment value. The allowable crack depth, accounting for the nonlinear behavior of the pipe,

Table 3.6 Example problem illustrating the role of secondary stresses on in-service flaw evaluation criteria

Purpose or Objective of Test Case	Input Parameters	Results and Conclusions
	Test Case 6 – Role of Secondary Stresses on In-Service Flaw Evaluations	
Case 6a – Include thermal expansion (P_e) stresses along with primary membrane (P_m) and primary bending (P_b) stresses for faulted (i.e., SSE) conditions in Section XI Appendix C flaw evaluation, with full safety factor of 1.39 for P_m and P_b, but safety factor = 1.0 for P_e (Current Section XI Appendix C method)	Source of data: Actual plant LBB application for 14-inch diameter surge line • OD = 14 inches • t = 31.6 mm (1.246 inches) • Crack location in a TP316 stainless steel SMAW • P = 16.0 MPa (2,327 psi) • T = 285°C (545°F) Flow stress = $3S_m$ for critical flaw size analysis (S_m = 121 MPa [17.5 ksi] for TP316 at 288 C [550 F]) Algebraic sum of dead-weight and SSE moments used to calculated primary bending moments components; components combined using square root of sum of squares • Dead weight: M_y =-2.34 kN-m (-1,729 ft-lbs), M_z = 14.1 kN-m (10,360 ft-lbs) • Seismic: M_y = 17.4 kN-m (12,814 ft-lbs), M_z = 12.2 kN-m (8,969 ft-lbs) • Dead weight plus seismic: M_y = 15.0 kN-m (11,085 ft-lbs), M_z = 26.2 kN-m (19,329 ft-lbs) • Combined dead-weight and seismic bending moment = 30.2 kN-m (267.4 in-kips) Thermal moments combined by square root sum of squares • M_y = 219 kN-m (161,404 ft-lbs), M_z = 64.6 kN-m (47,651 ft-lbs) Combined thermal expansion moment = 228 kN-m (2,019 in-kips)	For a surface crack half the pipe circumference in length, the allowable flaw depth was 69 percent of the pipe wall thickness (a/t=0.69)
Case 6b – Same as for 6a except thermal expansion stresses (P_e) included with full safety factor of 1.39 (same safety factor for P_e as for P_m and P_b)	Same as above, except safety factor on thermal expansion stress = 1.39, the same as for the primary membrane and primary bending stresses	For a surface crack half the pipe circumference in length, the allowable flaw depth was 58 percent of the pipe wall thickness (a/t=0.58)

Table 3.7 Example problem illustrating the effect of actual margins on in-service flaw evaluation criteria

Purpose or Objective of Test Case	Input Parameters	Results and Conclusions
	Test Case 7 – Effect of Actual Margins on In-Service Flaw Evaluations	
Case 7 – Additional margin in flaw evaluation criteria due to using elastic analysis to analyze a nonlinear problem (uncracked pipe analysis)	Same as for Test Case 2a except considering a surface crack in a stainless steel SMAW.	Crack size for elastic uncracked analysis = 25 percent of pipe circumference long and 30 percent of pipe wall thickness deep M_{max} based on ASME Section XI Appendix C analysis for such a crack in a stainless steel SMAW at Emergency and Faulted conditions = 497 kN-m (4,400 in-kips) Time at M_{max} (elastic uncracked analysis) = 2.41 seconds M_{max} (nonlinear uncracked analysis) at time = 2.41 seconds = 426 kN-m (3,769 in-kips) Allowable crack depth for 25% long cracks for M_{max} (elastic analysis; 497 kN-m [4,400 in-kips]) = 0.3t Allowable crack depth for 25% long crack for M_{max} (nonlinear analysis; 426 kN-m [3,769 in-kips]) = 0.5t

was 50 percent of the pipe wall thickness. Thus, by accounting for the nonlinearities in the pipe due to pipe yielding, the allowable crack depth for the same 25 percent long crack increased from 30 percent of the pipe wall thickness (when using elastic analysis) to 50 percent of the pipe wall thickness (when using nonlinear analysis), a 60 percent increase. In other words, using the results from elastic stress analysis in an ASME Section XI in-service flaw evaluation, as is typically done, can introduce a significant unaccounted for margin in the flaw assessment.

3.3 Example Test Cases Illustrating the Application of the Newly Developed Flaw Evaluation Criteria for Class 2, 3, and Balance of Plant (BOP) Piping Systems

To examine the impact of the newly developed flaw evaluation criteria for Class 2, 3, and BOP piping, a third set of sample problems was considered.

3.3.1 Differences Between the Existing ASME Section XI Appendix H F-functions and the F-functions Developed in the BINP Program

To examine the differences between the existing Appendix H F-functions and the F-functions developed as part of this program, the example problem in Table 3.8 was considered. A comparison of the results from Cases 8a and 8b shows that the values of F from the Appendix H equations are in fairly close agreement with the values of F (i.e., the elastic crack-driving force) calculated using the newly-developed equations for the R/t = 10 case. However, for the higher R/t ratio case (R/t = 40), the Appendix H equations (which are independent of R/t) significantly underpredict (25 to 35 percent) the value of F (the elastic crack-driving force) for both the tension and bending load cases, regardless whether the 15 percent conservative or best-fit coefficients were used with the newly developed equations. Consequently, the existing ASME Section XI Appendix H F-function equations are probably not adequate for certain Class 2, 3, and Balance of Plant (BOP) piping systems which are fabricated from very large R/t ratio pipes. For such piping systems, one is going to need to use equations such as those developed in this program in order to calculate F, and thus K.

One limitation associated with this newly-developed method for calculating F is that it is limited to relatively short flaws, especially for the high R/t ratio pipes. The finite element results to which these equations were fit were limited to flaw aspect ratios (c/a, that is, half crack lengths/crack depths) of 32 or less and flaw depths of 80 percent of the pipe wall thickness or less. From Equation 3.1, which relates the flaw length (θ/π) to the flaw aspect ratio (c/a), one can see that for a flaw half way through the wall thickness (a/t = 0.5), the maximum flaw length (θ/π) for which the methodology is valid is only 6.4 percent of the pipe circumference for a pipe with an R/t ratio of 40. For shallower flaws, or pipes with higher R/t ratios, this maximum valid flaw length is even less. Thus, to make this methodology generally applicable to a wider range of Class 2, 3, and BOP applications, one would need to do additional finite element analyses, for flaws with higher aspect ratios, and then check these newly-developed curve fit expressions for F to these finite element results.

$$\frac{\theta}{\pi} = \left[\pi \frac{R}{t}\right]^{-1} \left(\frac{a}{t}\right)\left(\frac{c}{a}\right) \qquad (3.1)$$

Table 3.8 Example problem illustrating the differences between the existing F-functions from ASME Section XI Appendix H and the newly-developed F-functions from the BINP program

Purpose or Objective of Test Case	Input Parameters	Results and Conclusions
	Test Case 8 – Differences in F-functions	
Case 8a – Calculate values of F-function using existing equations in ASME Section XI Appendix H for pipes with different R/t ratios	Internal surface crack loaded in bending and tension $\theta/\pi = 0.0625$ $a/t = 0.5$ $R/t = 10$ and 40	ASME Appendix H • $F_T = 1.376$ • $F_B = 1.359$
Case 8b – Calculate values of F-functions using newly-developed equations from BINP program for pipes with different R/t ratios	Internal surface crack loaded in bending and tension $\theta/\pi = 0.0625$ $a/t = 0.5$ $R/t = 10$ and 40	Newly-developed F-functions ($R/t = 10$) (using 15% conservative coefficients) • $F_T = 1.357$ • $F_B = 1.203$ (using best-fit coefficients) • $F_T = 1.18$ • $F_B = 1.046$ Newly-developed F-functions ($R/t = 40$) (using 15% conservative coefficients) • $F_T = 2.110$ • $F_B = 2.011$ (using best-fit coefficients) • $F_T = 1.855$ • $F_B = 1.748$

3.3.2 Effect of R/t ratio on Elastic-Plastic J-Estimation Scheme (SC.TNP) Analyses

The analyses in Table 3.9 were conducted to examine the effect of R/t ratio on elastic-plastic J-estimation schemes, such as SC.TNP. For the first case (Case 9a) the existing SC.TNP1 analysis was used to calculate the maximum moment capacity. For SC.TNP1, the length parameter (Lw) is set to the pipe wall thickness. For the second case (Case 9b), the revised SC.TNP analysis was used to calculate the maximum moment capacity. For this case, the length parameter (Lw) is set to the pipe wall thickness (t) multiplied by a correction factor C1 (i.e., Lw = C1*t). The correction factor C1 is a function of the pipe R/t ratio, the flaw depth, flaw length, and loading condition (bending versus pressure and bending).

Two sets of analyses were run for each test case. For each set, the pipe diameter was 24-inch. For one set, the pipe wall thickness was equal to Schedule 120 pipe (46.0 mm [1.812 inches]). For the second set, the pipe wall thickness was 6.35 mm (0.25 inch), which is more representative of Class 2, 3, and BOP piping. For each case, the flaw depth was a third of the pipe wall thickness and the flaw length was a fourth of the pipe circumference. This flaw depth was selected for analysis in that it allowed the C1 correction factor for the Schedule 120 pipe case to be nearly equal to 1.0. In that way the maximum moment carrying capacity for both the SC.TNP1 (Lw = t) and revised SC.TNP analyses (Lw = C1*t) would be nearly the same since C1 equals 1.0. For both sets of analyses, the pipe pressure was set equal to a value necessary to achieve a pressure induced membrane stress of $0.5S_m$ for Type 304 stainless steel at 288°C (550°F).

From Table 3.9 it can be seen that the maximum moment-carrying capacity for the Schedule 120 pipe (t = 46.0 mm [1.812 inches]) was approximately 2,550 kN-m (22,600 in-kips) for both analysis methods. This is as expected since the input parameters were chosen such that the value of C1 would be close to 1.0. On the other hand, for the thinner pipe (t = 6.35 mm [0.25 inch]), which is more representative of Class 2, 3, and BOP piping, the existing SC.TNP1 analysis (Lw = t) overpredicts (non-conservatively predicts) the moment-carrying capacity of the cracked pipe by about 15 to 20 percent when compared with the revised SC.TNP analysis (Lw = C1*t). Since the revised SC.TNP analysis is based on curve fitting finite element results for the case of larger R/t ratio pipes, it appears that the use of the SC.TNP1 analysis, which was developed for pipes with R/t ratios between 5 and 20, would result in an overprediction of the moment-carrying capacity of cracked pipe for pipes with larger R/t ratios. Thus, for Class 2, 3, and BOP applications, one should probably use the revised SC.TNP analysis in an in-service flaw assessment.

3.3.3 Effect of Transition Temperature on Fracture Initiation Behavior of Ferritic Class 2, 3, and BOP Piping

One last illustrative example to consider is the effect of transition temperature on the fracture initiation behavior of ferritic Class 2, 3, and BOP piping. In this test case, a 24-inch diameter pipe with a 9.5 mm (0.375 inch) wall thickness (standard weight) operating near 4°C (40°F) during the winter was considered. The question is, does this pipe risk having a crack initiate in a brittle manner, or can we rest assured that a crack in this pipe will always initiate in a ductile manner? For this case we looked at the data provided in Appendix E. If the pipe is A106 Grade B and its Charpy 85 percent

Table 3.9 Example problem illustrating the differences in maximum moment-carrying capacity between the SC.TNP1 analysis (Lw = t) and revised SC.TNP analysis (Lw = C1*t) for different R/t ratios

Purpose or Objective of Test Case	Input Parameters	Results and Conclusions
	Test Case 9 – Effect of R/t Ratio on J-Estimation Scheme (SC.TNP) Analyses	
Case 9a - Predict maximum moment using SC.TNP1 analyses; Lw = t (pipe wall thickness)	24-inch diameter a/t = 0.333 $\theta/\pi = 0.25$ t = 46.0 mm (1.812 inch, Schedule 120) and t = 6.35 mm (0.25 inch); R/t = 6.12 and 47.5, respectively Pressure-induced membrane stress = $0.5S_m$ for Type 304 stainless at 550F • 17.7 MPa (2,560 psi), Schedule 120 pipe • 2.43 MPa (353 psi), 0.25 inch thick pipe Yield = 165 MPa (24 ksi) Ultimate = 455 MPa (66 ksi) E = 176 GPa (25,500 ksi) $\alpha = 4$ n = 5 Lower bound stainless steel SMAW J-R curve (WHIPJETW.jdr)	M_{max} = 2,550 kN-m (22,616 in-kips), R/t = 6.12 M_{max} = 505 kN-m (4,467 in-kips), R/t = 47.5
Case 9b - Predict maximum moment using revised SC.TNP analyses; Lw = C1*t	Same as above Lw = 46.3 mm (1.823 inch), (t = 46 mm [1.812 inch]); C1 = 1.006 (R/t = 6.12) Lw = 28.5 mm (1.124 inch), (t = 6.35 mm [0.25 inch]); C1 = 4.496 (R/t = 47.5)	M_{max} = 2,550 kN-m (22,589 in-kips), R/t = 6.12 M_{max} = 430 kN-m (3,805 in-kips), R/t = 47.5

shear area transition temperature is near the upper bound in Figure 3.1, then the Charpy 85 percent shear area transition temperature is approximately 77°C (170°F). This Charpy data can be related to a full-thickness fracture propagation transition temperature (FPTT) through the bottom curve in Figure 3.2. From Figure 3.2, for a 9.5 mm (0.375 inch) thick pipe, the FPTT is found to be approximately 16°C (30°F) less than the Charpy 85 percent shear area transition temperature of 77°C (170°F). Thus, the FPTT for the 9.5 mm (0.375 inch) thick pipe is 60°C (140°F).

Next, the fracture initiation transition temperature (FITT) for a through-wall cracked (TWC) pipe can be estimated from the data shown in Figures 3.3 and 3.4. From these two figures, the FITT for the TWC pipe is 33 to 50°C (60 to 90°F) less than the FPTT from a full-sized drop-weight-tear test (DWTT) specimen test. Assuming a worse case scenario, the FITT is 33°C (60°F) less than the FPTT of 60°C (140°F), i.e., the FITT for the TWC pipe would be 27°C (80°F).

Finally, from Figure 3.5 one can estimate the difference between the FITT for a surface crack and a through-wall crack. From the top figure in Figure 3.5, one can see that for a flaw 50 percent of the pipe wall thickness or greater, the FITT for a surface crack is approximately 33°C (60°F) less than the FITT for a through-wall cracked pipe. For shallower flaws, the difference in transition temperature between the surface crack and through-wall crack is even greater. Thus, for a 50 percent deep surface crack in a 9.5 mm (0.375 inch) thick pipe, the worst case fracture initiation transition temperature is approximately -7°C (20°F).

Thus, for a 9.5 mm (0.375 inch) thick A106 Grade B pipe with these near worst case transition temperature properties (Charpy 85 percent shear area temperature equal to 77 C [170 F]), the upper-bound transition temperature for a 50 percent deep surface crack in a pipe to initiate in a brittle manner is approximately -7°C (20°F). For this piping system, operating at a minimum temperature of 4°C (40°F) in the winter, a crack in the pipe should not initiate in a brittle manner.

Cracks in thicker pipes are more likely to initiate in a brittle manner. If the pipe were 25.4 mm (1.0 inches) thick (versus 9.5 mm [0.375 inches] thick), then the difference between the FPTT and the Charpy 85 percent shear area transition temperature would be +13°C (+23°F) instead of -16°C (-30°F); the resultant upper bound FITT for the surface-cracked pipe would be 23°C (73°F), versus -7°C (20°F); and the likelihood that such a surface crack would initiate in a brittle manner would be much greater. However, it is not clear how many Class 2, 3, and BOP piping systems are this thick. If there are no Class 2, 3 and BOP piping systems this thick, operating at this low temperature, then the likelihood of a surface crack initiating in a brittle manner may be remote.

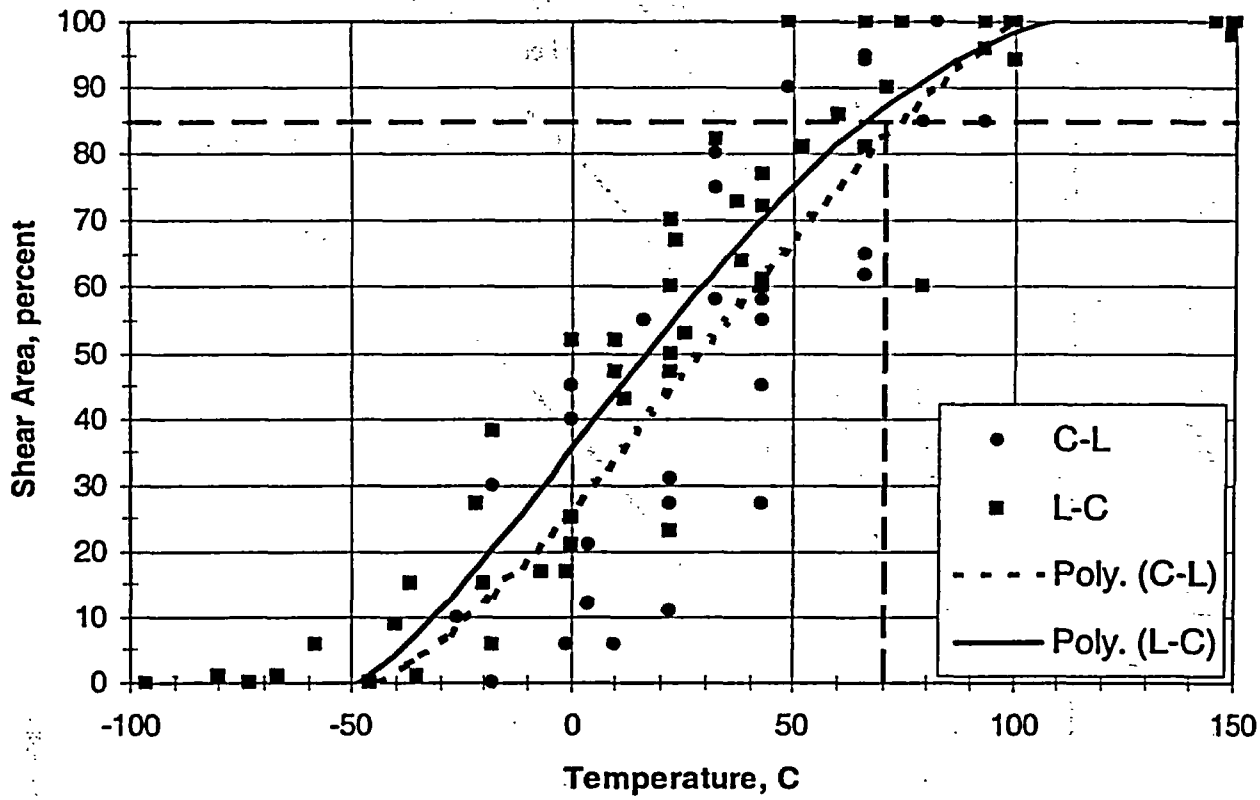

Figure 3.1 Shear area versus temperature from full-thickness Charpy test data for A106B pipe taken from PIFRAC database

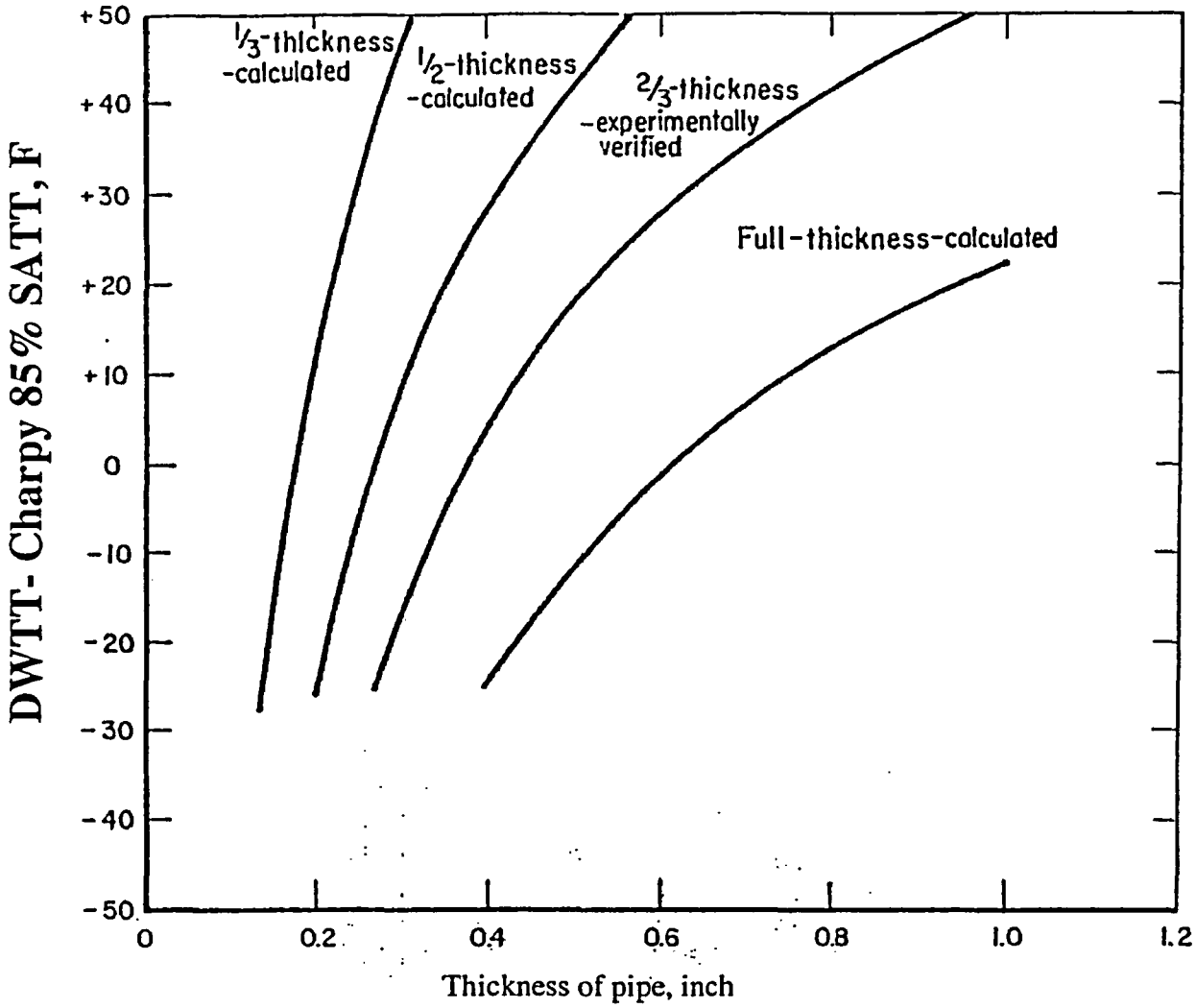

Figure 3.2 Relationship between DWTT and Charpy 85% shear area transition temperatures (SATT) as function of Charpy specimen thickness

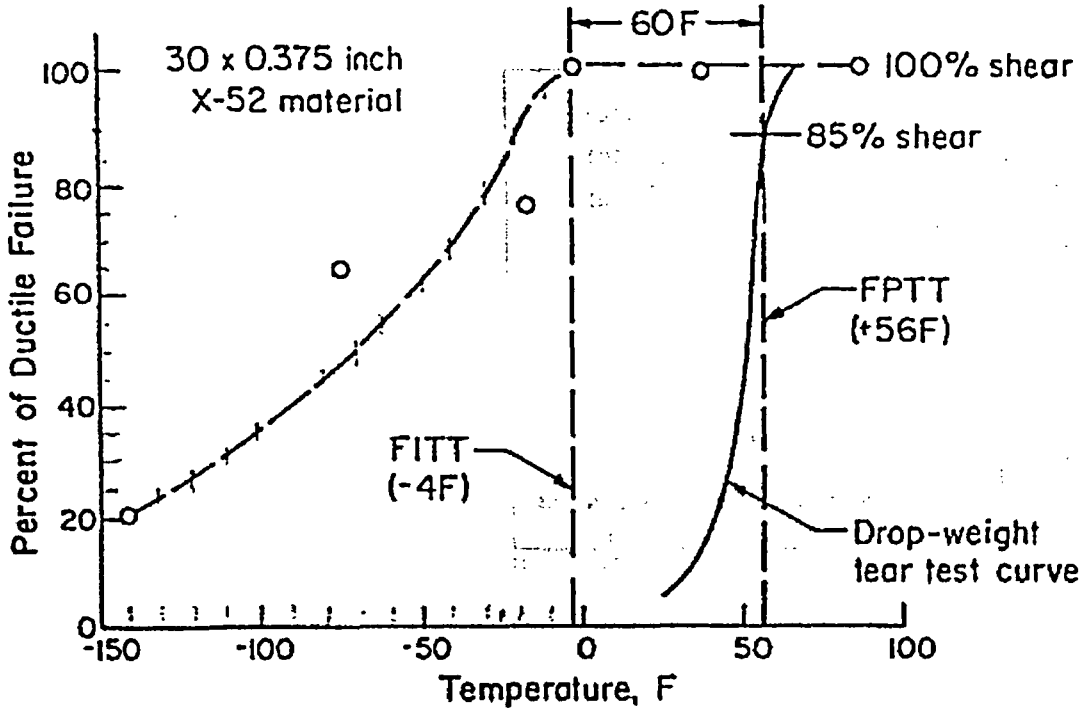

Figure 3.3 Axial through-wall-cracked pipe and DWTT data showing the temperature shift from the FITT to the FPTT for linepipe steel

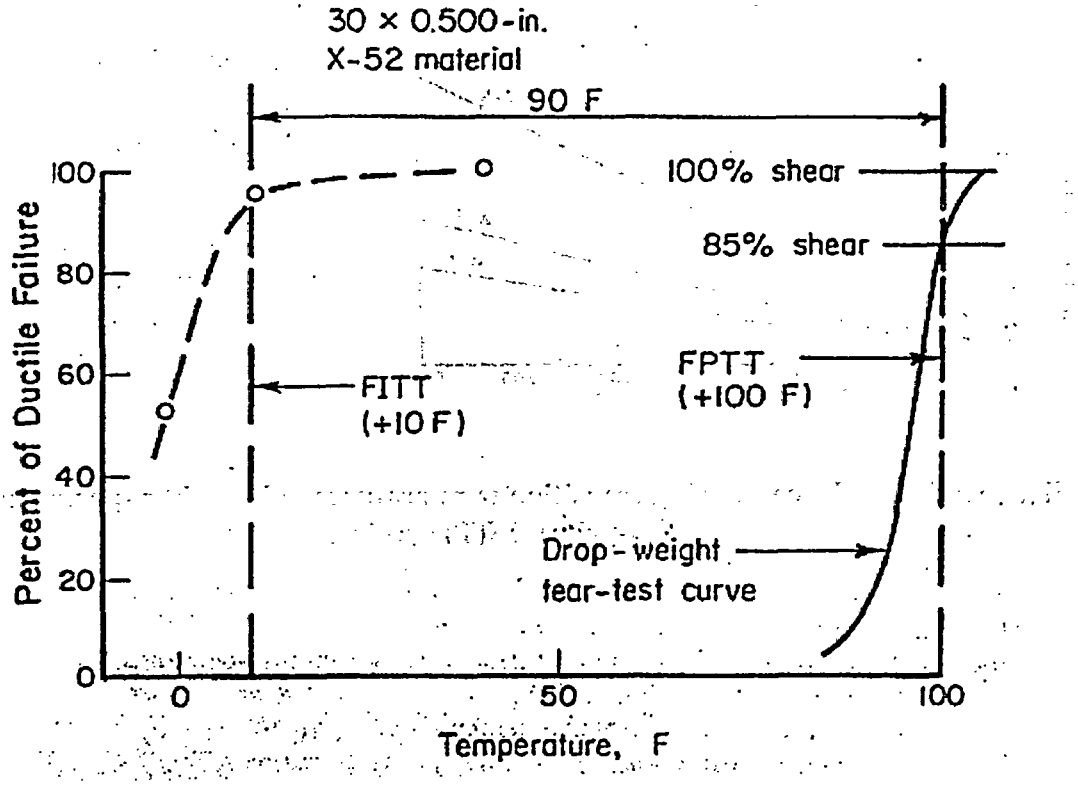

Figure 3.4 Axial through-wall-cracked pipe and DWTT data showing the temperature shift from the $FITT_{(TWC)}$ to the FPTT for linepipe steel

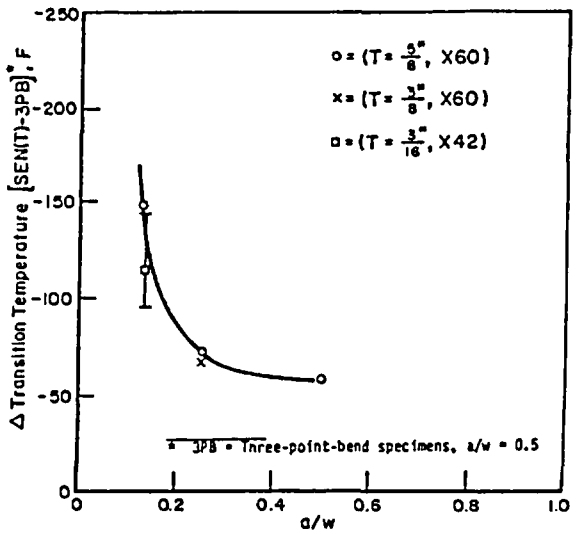

a) Transition temperature shifts

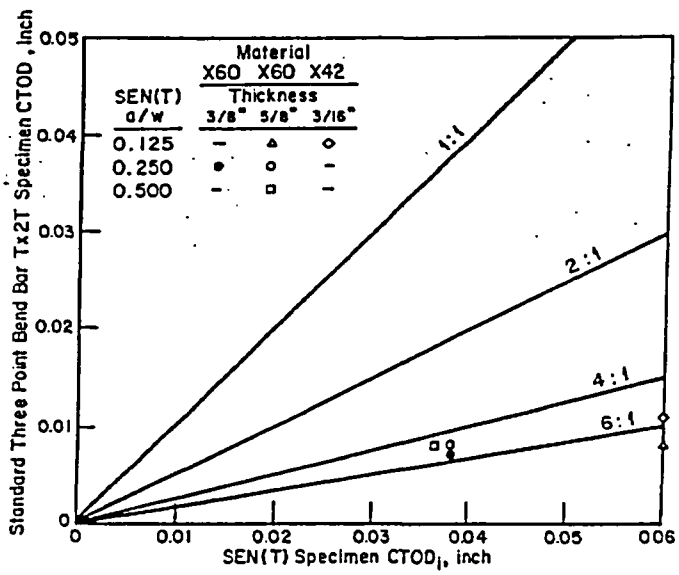

b) Upper shelf CTOD values

Figure 3.5 Results comparing transition temperatures of bend-bar specimens and fixed-grip SEN(T) specimen

3.4 References

3.1 "Leak-Before-Break Evaluation Procedures," USNRC draft Standard Review Plan 3.6.3, August 1987.

3.2 ASME Boiler and Pressure Vessel Code, 1995 Edition.

3.3 Rahman, S., and others, "Probabilistic Pipe Fracture Evaluations for Leak-Rate-Detection Applications," NUREG/CR-6004, April 1995.

3.4 Rudland, D. L., Wilkowski, G., and Scott, P., "Effects of Crack Morphology Parameters on Leak-Rate Calculations in LBB Evaluations," *International Journal of Pressure Vessels and Piping*, Vol. 79, pp. 99-102, 2002.

3.5 "Whipjet Program Final Report," for Beaver Valley Power Station, Unit Number 2, prepared for Duquesne Light Company, January 1987.

4. CONCLUSIONS AND RECOMMENDATIONS FROM THE BINP PROGRAM

The objective of the Battelle Integrity of Nuclear Piping (BINP) program was to address some of the remaining key issues in the technology of nuclear piping integrity. The program was structured as a series of independent tasks, each aimed at addressing one of these issues. Priorities were set based on each issue's potential impact on LBB or in-service flaw evaluation criteria. The conclusions and recommendations from this program are presented next.

4.1 Conclusions

The main conclusions for the various tasks are:

4.1.1 Task 1: Secondary Stresses

In this context, the term secondary stresses refers to the global thermal expansion or seismic anchor motion type displacement-controlled stresses, not the localized through-thickness weld residual stresses. As a result of the Task 1 experiment and related experiments from the IPIRG programs (Refs. 4.1 and 4.2), it was concluded that:

- Secondary stresses contribute just as much to the fracture process as do the primary membrane and primary bending stresses whenever the ratio of the failure stress in the uncracked pipe to the yield stress ($\sigma_{failure}/\sigma_{yield}$) is less than 1.0. If $\sigma_{failure}/\sigma_{yield}$ is greater than 1.0, then secondary stresses become less important, probably in some nonlinear fashion. However, this nonlinear relationship is not defined at this time, and limited data currently exist from which this relationship may be defined.
- The existing criteria in draft Standard Review Plan (SRP) 3.6.3 for LBB (Ref. 4.3) for addressing secondary stresses in LBB evaluations are conservative, at least for the case where the piping system under consideration is fabricated using lower toughness shielded-metal-arc or submerge-arc welds. For those cases, the secondary stresses are considered equally with the primary membrane and primary bending stresses. For piping systems fabricated with higher toughness tungsten-inert gas (TIG) welds, the draft SRP procedures do not include the secondary stresses. However, for these higher toughness situations, the failure stresses may be high enough that yielding remote from the crack location may be prevalent. In such applications, it has been argued that the contribution of secondary stresses may not be as significant. In those cases, an as yet undefined nonlinear correction to the secondary stress contribution has been suggested to be needed. In addition, as applicants are seeking LBB relief for smaller and smaller diameter piping systems, the potential exists that the postulated leakage crack size (as a function of pipe circumference) may be large enough that the failure stress may be less than the yield strength, even for the case of postulated cracks in higher toughness TIG welds. In that case, the secondary stresses may need to be considered with the primary membrane and bending stresses, contrary to the existing criteria.
- The existing flaw evaluation criteria in ASME Section XI for austenitic submerge-arc and shielded-metal-arc welds are adequate.

4.1.2 Task 2: Alternative Seismic Load History

As a result of the analysis of the alternative seismic load history pipe-system experiment conducted as part of Task 2, the following was concluded:

- The combined effect of cyclic history and material composition (sulfur content) resulted in a 25 percent reduction in load-carrying capacity when compared with the results from the first simulated seismic experiment conducted in IPIRG-2 (Ref. 4.2). Of this, about half (10 to 15%) was attributed to the more damaging cyclic history associated with the BINP Task 2 experiment and about half (10 to 15%) was attributed to the fact that the crack in the BINP Task 2 experiment was in a higher sulfur, lower toughness heat of wrought stainless steel pipe (DP2-A8II) while the crack in the IPIRG-2 Experiment 1-1 was in a lower sulfur, higher toughness heat of wrought stainless steel pipe (DP2-A8I). This conclusion is based on data for a relatively high toughness material (stainless steel base metal) for which limit-load conditions should prevail. Preliminary analysis conducted as part of this program indicated that for the case of a lower toughness material (cracks in carbon steels or stainless steel flux welds), in possibly a larger diameter pipe, where EPFM conditions probably prevail, and where the effect of toughness on the load-carry capacity is more significant, the more damaging cyclic history may result in as much as a 30- to 40-percent reduction in load-carrying capacity. Even though this is one of the more significant effects on the load-carrying capacity of all the conditions considered, in light of the effect of actual margins discussed next, this is still probably a second order effect if the crack is small enough that the failure stress is above the yield strength of the uncracked pipe.

4.1.3 Task 3: Actual Margins

During the IPIRG programs (Refs. 4.1 and 4.2) it was hypothesized that there may be some previously unaccounted-for margin in the LBB and in-service flaw evaluation criteria as a result of conducting elastic analysis to quantify a nonlinear problem. It was thought that plasticity in the piping system (remote from the crack section) and plasticity associated with the crack might absorb energy that would otherwise go into driving the crack. As part of this task, it was shown that this additional unaccounted-for margin due to nonlinear behavior, either from remote plasticity or the presence of the crack, could have a potentially significant effect on either an LBB or in-service flaw evaluation assessment. Specifically, it was shown as part of this effort that:

- This effect had potentially the largest impact on either LBB or in-service flaw evaluations of any of the effects formally considered as part of this program, especially if the stresses in any part of the uncracked piping system would be above yield when the crack reached its maximum load-carrying capacity.
- The magnitude of this effect depends on a number of factors, including the magnitude of the load history, the stiffness and/or flexibility of the piping system and its associated boundary conditions, and the potential crack location along the piping system under consideration. To illustrate the potential magnitude of this effect, the additional margin observed at certain locations along the surge line at 1 safe shutdown earthquake (SSE) loading was on the order of a factor of 10 or more. This margin was due solely to the remote plasticity, and

not plasticity from the presence of the crack.

- The nonlinearities associated with pipe yielding, remote from the crack, tended to have a more pronounced effect on the margins than the nonlinearities associated with the crack.
- For LBB assessments, if one fails to demonstrate LBB using the more typical Level 2 type assessment, one may be able to demonstrate LBB by conducting a nonlinear analysis as part of a Level 3 assessment, as suggested in NUREG/CR-6765 for a future LBB Regulatory Guide.

4.1.4 Task 4: Restraint of Pressure-Induced Bending

Near the end of the Second IPIRG program, an uncertainty analysis was conducted to identify the key issues, yet to be resolved, in the area of piping integrity (Ref. 4.4). This uncertainty analysis, along with a series of piping review meetings sponsored by the US NRC, formed much of the basis for the conduct of the BINP program. The most significant issue with regards to LBB analysis that was identified in this uncertainty analysis was that of restraint of induced bending that occurs during axial membrane loading in the presence of a circumferential crack. This was initially termed "restraint" of pressure-induced bending; but the restraint of the bending is for any axial stress component. As part of Reference 4.4, it was concluded that for small diameter pipe (on the order of 4-inch nominal diameter), the margin on LBB may be over a factor of ten less than anticipated when using traditional LBB analysis in which this effect is not considered. It was thought that this effect might be a key factor in future LBB applications, especially for small and intermediate-diameter pipe. However, as a result of the analyses conducted in Task 4, this was found not to be the case. The conclusions drawn as a result of Task 4 are:

- Restraint of pressure-induced bending has a minor effect on LBB. The only time it could possibly play a significant role is for small-diameter pipe, possibly operating at low operating stresses, for which the leakage crack length is a large percent of the pipe circumference (approaching 50 percent of the pipe circumference).
- In addition to large crack lengths (expressed as a percent of pipe circumference), a condition of high restraint (which is more pronounced in larger diameter pipes) is needed for this effect to be significant.

4.1.5 Task 7: Development of a Flaw Evaluation Criteria for Class 2, 3, and Balance-of-Plant (BOP) Piping

The flaw-evaluation criteria that currently exist in ASME Section XI for austenitic (Appendix C) and ferritic (Appendix H) piping are for Class 1 piping systems. No such criteria currently exist in the ASME code for Class 2, 3, and BOP piping. However, as inspection requirements for these piping systems increase, the need for such criteria is becoming more pressing.

There are two main differences between Class 1 piping and Class 2, 3, and BOP piping. The first is that Class 1 piping typically operates at higher pressures, and as such is typically fabricated from pipes with lower R/t ratios. The criteria in Section XI were typically developed for pipes with R/t ratios of 20 or less. Class 2, 3, and BOP piping can be fabricated from pipes with R/t ratios that approach 80. (Some service water systems have R/t ratios that may exceed 80.) The second difference is that Class 2, 3, and BOP piping, which is

typically fabricated from ferritic pipe, oftentimes operates at temperatures where there is a concern for transition temperature effects. Activities associated with this task were aimed at addressing each of these differences. The main conclusions reached as a result of this task are:

4.1.5.1 Effect of R/t Ratio

- As part of this effort, a series of influence functions was developed by curve fitting published finite element results of K-solutions and the associated F-functions (Refs. 4.6 and 4.7). It was found that there is a rather significant effect of R/t ratio on the elastic F-functions for higher R/t ratio pipes (i.e., there was a significant difference between the ASME Section XI Appendix H equations and the new F-function equations for the higher R/t ratios.) The Appendix H solutions are supposedly only applicable to pipes with R/t ratios of 5 to 20. The agreement between the Appendix H equations and the new equations was fairly good in this regime, but as would be expected, the solutions diverged at higher R/t ratios.
- A major limitation associated with the new equations is that the FEA solutions which were used in the curve fitting process were limited to c/a values (half crack length divided by crack depth) of 32 or less. This limits the applicability of these new equations to relatively short flaws, especially for the higher R/t ratio pipes where these equations are most needed. For a pipe with an R/t ratio of 50, the limit on flaw length for a 50 percent deep flaw is about 10 percent of the pipe circumference, i.e., $2\theta = 36$ degrees.
- A second major activity associated with this task was the extension of one of the EPFM J-estimation schemes for surface-cracked pipe to pipes with larger R/t ratios. The existing estimation schemes (e.g., SC.TNP1) were developed for pipes with R/t ratios of approximately 5 to 15. As part of this effort, the SC.TNP analysis was modified to make it more applicable to pipes with higher R/t ratios. The modification was made by adjusting the Lw term, which is the term which defines the distance from the crack plane at which the stress in the pipe approaches the uniform remote bending stress, i.e., the effect of the crack on the stress field diminishes. For the modified SC.TNP analysis, the Lw term was defined in terms of the pipe wall thickness as $Lw = C1*t$. The modified solution for J agrees much better with results from finite element analyses. However, the solutions developed as part of this program have only been developed for a single strain-hardening exponent ($n = 5$). The methodology is currently being extended for different strain-hardening exponents as part of another US NRC program.

4.1.5.2 Transition Temperature Effects

A methodology for predicting the brittle fracture initiation transition temperature (FITT) of a surface crack in a ferritic pipe was developed. This methodology is based on several starting points. The most accurate would be to use a fixed-grip, SEN(T) specimen in the L-R orientation to get the proper constraint and anisotropy for a surface-crack in a pipe. Correlations were also established for obtaining the transition temperature from a C(T) specimen (higher constraint than surface-crack pipe) and obtaining the transition temperature from Charpy V-notch specimens. Predicting the surface-cracked pipe brittle-to-ductile quasi-static transition temperature from the Charpy test requires knowing, or being able to estimate, the 85 percent shear area transition temperature from a set of Charpy

specimens. Based on this analysis, and the existing database of Charpy data for nuclear grade ferritic pipe, it appears that the risk of initiating a brittle fracture from a surface crack in a Class 2, 3 or BOP piping system may be minimal. To illustrate, consider the potential worst case scenario from a brittle fracture initiation viewpoint as:

- Assume an upper bound for the 85 percent shear area transition temperature from Charpy specimens to be +77°C (+170°F),
- For pipe wall thicknesses typical of Class 2, 3, and BOP applications (less than 15 mm [0.6 inch] thick), the worse case ΔT between the full-size DWTT specimen, which is routinely used to measure the fracture propagation transition temperature (FPTT) for full thickness line pipe steels, and Charpy specimen transition temperature curves is approximately -1°C (-2°F)[7],
- The difference between the fracture propagation transition temperature (FPTT) determined from a DWTT specimen and the fracture initiation transition temperature (FITT) from a C(T) specimen, bend bar, or through-wall-cracked (TWC) pipe is -33 to -50°C (-60 to -90°F); assuming a worst case shift in transition temperature of -33°C (-60°F) means that the FITT for through-wall cracked pipe would be approximately 42°C (108°F),
- The difference between the FITT for a through-wall crack in a pipe and a surface crack in a pipe is approximately -31°C (-55°F) for a surface crack 50 percent of the pipe wall thickness in depth (or greater),
- Thus, assuming a worst case scenario throughout from a transition temperature perspective, the FITT for a surface crack in this pipe would be approximately 12°C (53°F). While clearly there are applications in the winter where one of these Class 2, 3, or BOP piping systems may operate at a temperature less than 12°C (53°F), all of the worst case conditions had to be aligned for a flaw in the piping system to initiate in a brittle manner. Even though the likelihood is remote, one should still consider the possibility in a flaw evaluation criterion, and the methodology developed as part of this effort provides the tools for doing so.
- The analysis developed as part of this effort was validated with experimental data developed as part of this program. Laboratory specimen tests [Charpy, dynamic tear test (DTT), C(T) and SEN(T) tests] plus full-scale A106B pipe tests were conducted. The pipe fracture tests were all tests with the crack in the base metal. To further develop this flaw evaluation criterion would require additional tests to be conducted with the surface crack in a weld to account for the effect of weld residual stress effects and potential constraint effects.

4.1.6 Task 8a: Development of Fracture Criteria for Through-Wall Cracks in Elbows

As part of this effort an analysis methodology for predicting the applied J and the crack-opening displacements (COD) for both an axial and circumferential through-wall crack in an elbow was developed. This

[7] If the wall thickness were greater than 15 mm (0.6 inch), then the shift in transition temperature would be more positive and the bottom line fracture initiation transition temperature (FITT) for a surface crack for this worst case scenario would be higher.

methodology was developed in support of the US NRC's initiative to formalize their LBB procedures through the publication of a new Regulatory Guide on LBB.

The main conclusion drawn from this effort was that this new analysis methodology for through-wall-cracked elbows was not actually needed. The use of straight-pipe solutions to predict the behavior of circumferential through-wall cracks in elbows is probably adequate, at least for elbows with lower R/t ratios. The differences in J and COD predictions between the new elbow through-wall crack analysis and existing straight pipe solutions (GE/EPRI) are minimal (less than 15 percent). As such, one can probably use straight-pipe solutions to predict the behavior of through-wall cracks in elbows.

4.1.7 Task 8b: Analysis of the V. C. Summer Bimetal Weld Case for Primary Water Stress Corrosion Cracking (PWSCC)

An assessment was made, using the finite element method, of the weld residual stresses in the vicinity of the hot leg to reactor pressure vessel (RPV) nozzle bimetallic weld. The entire history of fabrication of the weld was included in the analysis, including the Inconel buttering, post-weld heat treatment (PWHT), weld deposition, weld grind-out and repair, hydro-testing, service temperature heat-up, and finally service loads. The purpose of this assessment was to examine the effect of different weld repair procedures on the resultant weld residual stresses and their potential impact on primary water stress corrosion cracking (PWSCC). The key findings from this effort were:

- The as-fabricated *axial weld residual stresses* alternate sign as one proceeds from the inside to the outside surface of the pipe near the weld region. Tension to compression to tension and back to compression axial residual stresses develop in the as-fabricated pipe weld. The tensile residual stresses at the inside surface were higher when the outside weld repair was deposited first followed by inside welding, as compared with the opposite case. Thus, to reduce the effect of circumferential PWSCC after weld repairs, inside welding followed by outside welding is preferred.
- The final hoop residual stresses after complete fabrication are mostly tensile in the weld region. For the case of outside welding followed by inside welding after the bridge repair, high tensile residual stresses are produced everywhere. For the case of inside welding followed by outside welding, a small zone of compressive hoop residual stresses develops near the pipe inside surface in the weld. This again supports the preference to make the repairs using the inside welding followed by outside welding process to get more favorable stresses on the inside surface.
- Hydrostatic testing did not significantly alter the fabrication residual stresses.
- Heating the hot-leg pipe system up to the operating temperature of 324°C (615°F) reduces the axial fabrication stresses to mainly compressive values due to the rigid constraint provided by the vessel and steam generator. Hoop residual stresses are unaffected by heating up to operating temperatures.
- Since as-fabricated axial residual stresses are low at operating temperature, circumferential PWSCC is not expected due solely to fabrication stresses. Service loads dominate circumferential PWSCC in this application.
- Axial crack growth is dominated by the fabrication residual stresses.
- Based on the PWSCC crack growth law from Reference 4.8 and the analysis

results here, axial cracking should be confined to the weld region. Starting from a crack 5 mm (0.2 inch) in depth, the axial crack should break through the pipe wall within two years. The crack nucleation time should be studied in more detail.

- Circumferential cracks should take about twice as long to become through wall cracks as axial cracks. Circumferential cracks will tend to grow longer than axial cracks. However, since service loads dominate circumferential cracks, they will slow their growth in the circumferential direction as they grow toward the compressive bending stress region of the pipe. The service loads consist of thermal expansion mismatch, tension caused by 'end cap' pressure, and bending.
- Weld repairs alter pipe residual stress fields near the start/stop regions of the repairs. This may help slow down the growth of a growing stress corrosion crack.
- Grinding of welds may lead to scratches, which in turn may provide crack initiation sites. Grinding should be performed carefully. It is of use to study the effect of grinding on both residual stresses (caused by grinding) and crack initiation sites. Numerical models of the grinding process can be developed.

4.1.8 Task 9: Weld Residual Stress Effects on COD Predictions for LBB Analyses

Preliminary analysis conducted as part of the uncertainty study conducted at the end of the Second IPIRG program indicated that weld residual stress effects could have a potentially significant effect on the predicted crack-opening displacements (COD) needed for an LBB assessment (Ref. 4.4). This effect was especially pronounced for thin-wall pipe operating at low stress levels. This preliminary analysis suggested that the through-wall residual stress field in welded pipe could cause the crack faces of a through-wall crack to rotate closed on the outside surface, thus restricting the flow of fluid through the crack much more so than what might be predicted based on existing crack-opening displacement analyses, such as the GE/EPRI method (Ref. 4.9). This restriction in flow would in turn cause the postulated leakage crack to be longer than anticipated (when using the conventional GE/EPRI analysis) for a prescribed leakage detection capability. Obviously, the longer than anticipated postulated leakage crack length would be detrimental to LBB. As part of this effort a series of corrections to the GE/EPRI method was made. The key findings from this development effort were:

- As originally predicted, it was shown that the crack faces tend to rotate so that the crack on the outside surface opens less than on the inside surface. Furthermore, it was shown that there was a critical stress level that must be applied in order to overcome the crack closure on the outside surface, and thus open the crack. However, for most practical applications, the effect of weld residual stresses on the crack-opening displacements was not a major contributing factor for LBB analyses, i.e., less than a 15 to 20 percent effect on COD, and thus also on crack length.
- The effect of the weld start/stop locations on the predicted crack-opening displacements can be ignored in LBB analysis. The crack tends to be more opened in the start/stop region than away from the start/stop location. As a result, the postulated crack length away from start/stop location, where this analysis of the effects of weld residual stresses on CODs is valid, would be longer than in region of the start/stop, so it would be

conservative to ignore the effect of the start/stops when using this revised weld residual stress COD analysis.

- Corrected coefficients for GE/EPRI method have been incorporated as an option in the newly revised version of SQUIRT, Windows® Version 1.1.
- To generalize this methodology would require a look at more pipe diameters and more wall thicknesses.

4.2 Recommendations

The ultimate objective of this program was to develop the technical basis for implementing changes in the codes and standards and rule-making process for nuclear piping applications. Some recommended areas where these codes and standards could be impacted are:

4.2.1 Potential Recommendations with Respect to Leak-Before-Break Procedures

Potential changes/recommendations to the existing LBB procedures that may be warranted as a result of the efforts conducted as part of the BINP program are:

- Leave the criteria in the existing draft SRP 3.6.3 regarding the handling of secondary stresses as is when writing the new Regulatory Guide for LBB, especially for the case where one is evaluating a piping system fabricated with shielded-metal-arc or submerge-arc welds. For those applications, the secondary stresses are considered equally with the primary membrane and primary bending stresses in the draft SRP procedures. For piping systems fabricated with higher toughness tungsten-inert gas (TIG) welds, as well as the stainless steel base metal case, the draft SRP procedures do not consider the secondary stresses. However, in most cases for these higher toughness situations, the failure stresses should probably be high enough that yielding remote from the crack location should be prevalent. In such applications, it has been argued that the contribution of secondary stresses may not be as significant. In those cases, an as yet undefined nonlinear correction to the secondary stress contribution has been suggested. Furthermore, as applicants are seeking LBB relief for smaller and smaller diameter piping systems, the potential exists that the postulated leakage crack size (as a function of pipe circumference) may be large enough that the failure stress may be less than the yield strength even for the higher toughness TIG welds. In that case, the secondary stresses may need to be considered with the primary membrane and bending stresses, contrary to the existing criteria.
- Allow the applicants, if they so chose, to use nonlinear stress analysis (instead of elastic analysis) to define the applied stresses in those cases where LBB cannot be demonstrated using the more conventional Level 2 type LBB assessment. This Level 3 type analysis offers the applicant the potential of realizing a significant increase in margin due to the nonlinear behavior in the piping system.
- Incorporate statistically-based crack morphology parameters for each of the relevant cracking mechanisms into the new Regulatory Guide for LBB. Furthermore, unless technical justification can be demonstrated to do otherwise, specify their usage in all new LBB submittals.
- Use the existing straight-pipe solutions for J and COD (e.g., GE/EPRI method) in the analysis of postulated through-wall cracks in elbows.
- Ignore the effect of restraint of pressure induced bending in the majority of future LBB applications. The only time it may

prove to be an issue is for small diameter piping (where the postulated leakage crack size is a large percentage of the pipe circumference) that is highly restrained by the surrounding pipe and boundary conditions.

- Even though the effect of weld residual stresses on the crack-opening displacement analyses for LBB considerations is small, the effect is easy enough to consider, especially since an option already exists in the latest version of SQUIRT (Version 1.1) to account for it. As such, unless a valid justification can be presented to ignore this effect (i.e., the welds have been stress relieved), this effect should be considered in future LBB applications, and wording to that effect should be included in the new Regulatory Guide for LBB.

4.2.2 Potential Recommendations with Regards to In-Service Flaw Evaluation Criteria

Some potential changes/recommendations to the existing in-service flaw evaluation procedures that may be warranted as a result of the efforts conducted as part of the BINP program are:

- Incorporate the F-functions developed as part of this program into a new section of the code for Class 2, 3, and BOP piping flaw evaluations. However, before actually incorporating these new F-functions into the code, the equations and associated correlation coefficients should be modified to handle longer flaws.
- Develop a new code criterion for elastic-plastic fracture mechanics (EPFM) for Class 2, 3, and BOP piping using the modified SC.TNP analysis as the technical basis.
- Implement a criterion into the Class 2, 3, and BOP flaw evaluation procedures whereby if the 85 percent shear area transition temperature from Charpy specimens is less than 65°C (150°F), then there is no need to consider the impact of brittle fracture initiation. If the Charpy 85 percent shear area transition temperature is greater than 65°C (150°F), then the methodology developed as part of this effort can be built into the code structure. Alternatively, there may be some thickness limit criteria, whereby if the pipe thickness is greater than some predetermined value, then one would be forced to use the Class 1 EPFM criteria in Section XI. Note, this recommendation is only currently valid for cracks in ferritic base metals subjected to quasi-static loading conditions. For cracks in welds and cracks subjected to dynamic loadings, additional work is required.

4.2.3 Recommendations for Future Work

While the efforts undertaken as part of this effort furthered the technical basis for a number of piping integrity issues, a few areas remain where additional related work could further enhance this basis. Probably the most important areas of future work would be:

- Extending the F-function equations to a wider range of crack lengths. This would involve finite element analyses for cases of high R/t ratios and long cracks.
- Conducting additional transition temperature pipe experiments where the crack is located in a weld so that an assessment of effect of weld residual stresses and constraint on the transition temperature can be made. Also, a study looking at the effects of dynamic loading on the transition temperature behavior is also probably needed.

- Conducting a study aimed at quantifying the crack nucleation time and the effect of surface grinding marks on the crack initiation behavior of primary water stress corrosion cracking.

Other possible areas of future work include:

- Extending the modified SC.TNP analysis for a wider range of strain hardening exponents (n). This effort is currently being undertaken as part of the US NRC Large Break Loss-of-Coolant Accident (LB LOCA) frequency distribution redefinition program.
- Extending the restraint of pressure-induced bending solution for the asymmetric support case to more R/t values. Currently, the solution equations are only truly applicable to pipes with R/t ratios of 10. As a first step, the equations should be extended to the case of R/t = 5, which is more typical of PWR piping systems.
- Expanding the solutions for the effect of weld residual stresses on the crack opening displacements to more pipe diameters and wall thicknesses.

4.3 References

4.1 Scott, P., and others, "Crack Stability in a Representative Piping System Under Combined Inertial and Seismic/Dynamic Displacement-Controlled Stress," Subtask 1.3 Final Report, NUREG/CR-6233, Vol. 3, June 1997.

4.2 Scott, P., and others, "IPIRG-2 Task 1 – Pipe System Experiments with Circumferential Cracks in Straight-Pipe Locations," NUREG/CR-6389, February 1997.

4.3 "Leak-Before-Break Evaluation Procedures," USNRC draft Standard Review Plan 3.6.3, August 1987.

4.4 Ghadiali, N., and others, "Deterministic and Probabilistic Evaluations for Uncertainty in Pipe Fracture Parameters in Leak-Before-Break and In-Service Flaw Evaluations," NUREG/CR-6443, June 1996.

4.5 Rahman, S., and others, "Probabilistic Pipe Fracture Evaluations for Leak-Rate Detection Applications," NUREG/CR-6004, April 1995.

4.6 Anderson, T. L., "Stress Intensity Solutions for Surface Cracks and Buried Cracks in Cylinders, Spheres, and Flat Plates," prepared for The Materials Property Council, Inc., March 2000.

4.7 Chapuliot S., and Lacire, M. H., "Stress Intensity Factors for External Circumferential Cracks in Tubes Over a Wide Range of Radius Over Thickness Ratios," PVP Vol. 388, 1999.

4.8 Westinghouse Electric Co., "Integrity Evaluation for Future Operation Virgil C. Summer Nuclear Plant: Reactor Vessel Nozzle to Pipe Weld Regions," WCAP-15615, December 2000.

4.9 Kumar, V., and others, "An Engineering Approach for Elastic-Plastic Fracture Analysis," EPRI Report NP-1931, July 1981.

NRC FORM 335
(2-89)
NRCM 1102,
3201, 3202

U.S. NUCLEAR REGULATORY COMMISSION

BIBLIOGRAPHIC DATA SHEET

(See instructions on the reverse)

1. REPORT NUMBER
(Assigned by NRC, Add Vol., Supp., Rev., and Addendum Numbers, if any.)

NUREG/CR-6837, Volume 1

2. TITLE AND SUBTITLE

The Batelle Integrity of Nuclear Piping (BINP) Program Final Report

Volume 1: Summary and Implications of Results

3. DATE REPORT PUBLISHED

MONTH	YEAR
June	2005

4. FIN OR GRANT NUMBER
W6775

5. AUTHOR(S)

P. Scott (1), R. Olson (1), J. Bockbrader (1), M. Wilson (1), B. Gruen (1), R. Morbitzer (1), Y.Yang (1), C. Williams (1), F. Brust (1), L. Fredette (1), N. Ghadiali (1), G. Wilkowski (2), D. Rudland (2), Z. Feng (2), R. Wolterman (2)

6. TYPE OF REPORT
Technical

7. PERIOD COVERED *(Inclusive Dates)*
Nov. 1997 - Sept. 2003

8. PERFORMING ORGANIZATION - NAME AND ADDRESS *(If NRC, provide Division, Office or Region, U.S. Nuclear Regulatory Commission, and mailing address; if contractor, provide name and mailing address.)*

(1) Batelle
505 King Avenue
Columbus, OH 43201

(2) Engineering Mechanics Corporation of Columbus
3518 Riverside Drive, Suite 202
Columbus, OH 43221

9. SPONSORING ORGANIZATION - NAME AND ADDRESS *(If NRC, type "Same as above"; if contractor, provide NRC Division, Office or Region, U.S. Nuclear Regulatory Commission, and mailing address.)*

Division of Engineering Technology
Office of Nuclear Regulatory Research
U.S. Nuclear Regulatory Commission
Washington, DC 20555-0001

10. SUPPLEMENTARY NOTES
C.A. Greene, NRC Project Manager

11. ABSTRACT *(200 words or less)*

Over the past 15 to 20 years, significant research has been conducted aimed at furthering the understanding of the fracture behavior of piping systems in commercial nuclear power plants. While the results from these prior programs have advanced the state-of-the-art understanding, there remained a number of key technical issues still to be resolved.

The BINP program was developed to address what was perceived to be the most critical of these unresolved issues. The program was structured as a series of independent tasks, each focused on one of these issues. After the research was completed, it was found that many of these issues did not have as significant an effect on leak-before-break (LBB) or in-service flaw evaluation criteria as was originally thought. However, one of the areas where significant benefit can be realized for both LBB and in-service flaw evaluations is by using nonlinear stress analysis instead of elastic analysis in the flaw assessments. The additional margin gained by accounting for the energy dissipated by plastic deformation can be significant. Another important advance was the preliminary development of the technical basis for flaw evaluation criteria for Class 2, 3, and balance-of-plant piping.

12. KEY WORDS/DESCRIPTORS *(List words or phrases that will assist researchers in locating the report.)*

Pipe
Fracture Mechanics
Leak-Before-Break
Flaw Evaluation

13. AVAILABILITY STATEMENT
unlimited

14. SECURITY CLASSIFICATION
(This Page)
unclassified
(This Report)
unclassified

15. NUMBER OF PAGES

16. PRICE

NRC FORM 335 (2-89)

Printed
on recycled
paper

Federal Recycling Program

UNITED STATES
NUCLEAR REGULATORY COMMISSION
WASHINGTON, DC 20555-0001

OFFICIAL BUSINESS